A Strategic Approach to Battery Sizing and Selection in Hybrid Vessels Operations

Master Sustainable Energy Technology
Elissa Bitar

TUDelft

Jan De Nul GROUP

A Strategic Approach to Battery Sizing and Selection in Hybrid Vessels Operations

by

Elissa Bitar

Student Name	Student Number
Elissa Bitar	5749441

TU Supervisor:	Dr.ir. H. Polinder
TU Supervisor:	Dr. E. M. Kelder
Company Supervisor:	Mr. Christof Lamproye
Company Supervisor:	Mr. Eben Heyneman
Daily Supervisor:	Mr. Sankarshan Durgaprasad
Project Duration:	December, 2023 - August, 2024
Faculty:	Electrical Engineering, Mathematics and Computer Science, Delft

TUDelft

Preface

Summary

As climate change concerns increase, the maritime industry faces an urgent need to reduce emissions and adopt sustainable practices. The integration of hybrid systems, particularly those incorporating Battery Energy Storage Systems (BESS), has emerged as a promising solution to enhance energy efficiency and lower the environmental impact. This Master Thesis focuses on developing a methodology for determining the most suitable battery size and type for existing vessels to be hybridized, balancing effectiveness and cost-efficiency. This thesis was conducted in collaboration with Jan De Nul Group, a leading global firm in environmental services, engineering, marine construction, and dredging.

The primary goal of this research is to design a methodology that compares different control strategies for sizing battery systems and selecting appropriate chemistries. A case study based on a trailing suction hopper dredger vessel was explored.

Three control strategies were evaluated using numerical modeling: optimal operation of the current scenario without batteries, load smoothing using a moving average approach, and optimal range operation of generators. To optimise the number of running generators and reduce maintenance costs, an automatic start-stop logic is implemented as a model initialisation. The optimal operation of the current scenario without batteries highlights the need for battery integration to compensate for the high supply deficit. In addition, the load smoothing strategy creates a more stable demand curve, allowing generators to operate more efficiently, while the optimal range strategy keeps generators near their rated power, maximizing efficiency and minimizing fuel consumption.

The study assesses battery performance under two scenarios: continuous full cycling throughout the year and calendar aging specifically during harbour operations. Battery power is calculated based on demand and generator output, considering state-of-charge constraints. Three types of lithium-ion batteries were evaluated for their suitability in ocean-going hybrid vessels: Lithium Nickel Cobalt Manganese Oxide (NMC), Lithium Iron Phosphate (LFP), and Lithium Titanate Oxide (LTO).

A total of 648 parameter combinations under the load smoothing strategy and 216 under the optimal range strategy were assessed. Using four key criteria, the selection of battery options was narrowed down. Given the limitations of the model used in this research, findings suggest that batteries affected primarily by calendar aging have shorter lifespans, making cycling behaviour preferable for achieving longer battery lifetime and higher Return On Investment (ROI). The optimal range strategy leads to higher fuel savings compared to load smoothing, while load smoothing results in a longer battery lifespan due to fewer equivalent cycles. In summary, selecting the best battery solution hinges on whether the priority is immediate ROI or long-term operational efficiency. This thesis offers a comprehensive methodology for integrating BESS, contributing valuable insights to the advancement of sustainable energy solutions in the maritime sector.

Contents

List of Figures

List of Tables

Nomenclature

Abbreviations

Abbreviation	Definition
AC	Alternating current
AHP	Analytic Hierarchy Process
ANP	Analytic Network Process
BESS	Battery energy storage system
CAPEX	Capital expenditures
$Cd(OH)_2$	Cadmium hydroxide
CO_2	Carbon dioxide
CPE	Constant Phase Element
DC	Direct current
DE	Diesel engine
DG	Diesel generator
DoD	Depth of discharge
ECM	Equivalent Circuit Model
ESS	Energy storage system
GHGs	Greenhouse gases
KO	Potassium hydroxide
LCA	Life cycle assessment
LCCA	Life cycle cost assessment
$LCO/LiCoO_2$	Lithium cobalt oxide
Li	Lithium
LIB	Lithium-ion battery
$LFP/LiFePO_2$	Lithium iron phosphate

Abbreviation	Definition
LMO/LiMn$_2$O$_4$	Lithium manganese oxide
LTO/Li$_2$TiO$_3$	Lithium titanate oxide
MILP	Mixed-integer linear programming
MINLP	Mixed-integer non-linear programming
MnO$_2$	Manganese oxide
Na	Sodium
NaOH	Sodium hydroxide
NaNiCl$_2$	Sodium nickel chloride (ZEBRA)
Na$^+$	Sodium ions
NCA/LiNiCoAlO$_2$	Lithium nickel cobalt aluminum oxide
Ni	Nickel
Ni-Cd	Nickel cadmium
Ni-Fe	Nickel iron
Ni-H	Nickel hydrogen
Ni-MH	Nickel metal hydride
Ni-OOH	Nickel oxide hydroxide
Ni-Zn	Nickel zinc
NIS	Negative ideal solution
NO$_x$	Nitrogen oxide
NMC/LiNiMnCoO$_2$	Lithium Nickel Cobalt Manganese Oxide
NSGA-II	Non-dominated sorting genetic algorithm
OCV	Open-circuit voltage
OPEX	Operating expenses
PbO$_2$	Lead-acid batteries
PIS	Positive ideal solution
PSB	Polysulphide bromine
RT	Room temperature

Abbreviation	Definition
SEI	Solid electrolyte interphase
SFOC	Specific Fuel Oil Consumption
SoC	State-of-charge
TOPSIS	Technique for Order Preference by Similarity to Ideal Solution
TSHD	Trailing suction hopper dredger
VRFB	Vanadium redox flow battery
VRLA	Valve-regulated lead-acid
Zn	Zinc
Zn^{2+}	Zinc ions
Zn-Br	Zinc bromine
ZnO	Zinc oxide

Symbols

Symbol	Definition	Unit
C-rate	The amount of energy discharged in one hour	$[h^{-1}]$
E	Energy	kWh
f	Frequency	[Hz]
I	Current [A]	
N	Synchronous speed	[RPM]
p	Number of poles in the motor	[-]
P	The power	[W]
R	Resistance	$[\Omega]$
r	The fuel consumption rate	[g/s]
SoC	State of Charge	[-]
T	Temperature	[K]
V	Voltage	[V]

Symbol	Definition	Unit
τ	The torque produced by the engine	[Nm]
ω	The angular speed	[rad/s]
η	The efficiency	[-]
Δt	Time step	[hours]
FC	Fuel consumption	tonnes
MC	Maintenance costs	euros

1

Introduction

1.1. Background

Maritime transportation plays a vital role in the worldwide economy. However, it contributes significantly and steadily to the emissions of greenhouse gases (GHGs) worldwide. Global shipping contributed 1,076 million tonnes of CO_2 emissions in 2018, which is roughly 2.9% of all emissions caused by human activity worldwide. Without intervention, shipping emissions are predicted to increase to 130% above 2008 levels by 2050. The objectives of the Paris Agreement, which seeks to prevent dangerous climate change by keeping global temperature rises well below 2°C and ideally below 1.5°C, would be seriously jeopardized by such an increase [1].

Maritime transportation accounts for 3 to 4% of all CO_2 emissions in the European Union [2]. Addressing the challenge of decreasing GHGs emissions from international maritime activities requires global action. The International Maritime Organization committed in July 2023 to set new GHGs emission reduction goals and to finalize a comprehensive set of measures by 2025 to meet these targets, which is an important step towards achieving this objective. The particular actions that will be taken to fulfill these promises and meet the goals of the Paris Agreement will become clear in the years to come [1].

As concerns about climate change continue to increase, the maritime industry faces a significant point where reform is needed. This urgency highlights the paramount importance for businesses to adopt eco-friendly practices and reduce hazardous emissions. Consequently, the maritime sector is increasingly recognizing the importance of embracing efficient and clean energy sources. Integration of hybrid systems featuring Battery Energy Storage Systems proactively helps decrease emissions by storing excess renewable energy and supplying it when needed, thereby decreasing reliance on fossil fuel-based power generation, meeting the demand for sustainable energy within the maritime industry. This significant shift results from the industry's collective acknowledgment of the pivotal role that environmentally responsible actions play in leading us toward a more sustainable future. An integral aspect of this transition involves the integration of batteries where the sizing and selection of specific chemistries is a crucial decision that affects the practical application of these developing technologies for existing vessels.

1.1.1. Jan De Nul Group

Jan De Nul Group is a leading global firm with expertise in environmental services, engineering, marine construction, and dredging. Since its founding in Belgium in 1938, the company has expanded to become a major player in the development and upkeep of marine infrastructure, offering its services to both public and private clients globally. Dredging, which entails the extraction, removal, and transportation of submerged sediments, is the primary occupation of Jan De Nul. This service is crucial for creating and maintaining navigable waterways, constructing ports and harbors, and land reclamation projects.

Jan De Nul has participated in some of the largest dredging projects in history, advancing both the growth of global trade and the economic development of coastal areas. Apart from its core business of dredging, Jan De Nul Group has expanded to offer offshore services like installing offshore wind farms, burying and laying underwater cables and pipelines, and providing services for oil and gas companies. The company's expertise in marine engineering enables it to handle complex offshore construction projects, commonly in severe environmental conditions.

Environmental sustainability is another crucial aspect of Jan De Nul's operations. The company provides solutions for environmental dredging and soil remediation, aiming to lessen the environmental effects of its projects and promote the restoration of ecosystems. By using cutting-edge techniques and instruments, Jan De Nul works to ensure that its activities support sustainable development. With a contemporary fleet that includes strong dredgers and specialized vessels, Jan De Nul Group is able to undertake ambitious and complex projects all over the world. As a major player in the development of the environment and marine infrastructure, the company is dedicated to safety, quality, and environmental care. Its projects support economic growth and global trade while aiming to protect and improve nature.

1.2. Research Question

This master's thesis aims to answer the following question,

What battery size and type best aligns with well-defined operational requirements of hybrid vessels, and which methodology is suitable for determining this?

Hence the **primary research question** that this thesis will address is:

What is a methodology that can be employed for determining the most suitable battery size and type, balancing effectiveness and cost efficiency, for existing vessels to be hybridized?

For the purpose of helping in addressing the main research question, the following sub-questions have been formulated:

Sub-question 1: What are the different battery technologies used in hybrid vessels, and what are the most suitable battery types for ocean going hybrid vessels?

Sub-question 2: What methodologies are commonly utilized in the maritime industry to assess the efficiency, performance, and sizing of batteries, considering variables like energy density, lifespan, and environmental impact?

Sub-question 3: What specific cost factors influence the selection of batteries for maritime vessels, and how do these factors impact the overall cost-effectiveness?

Sub-question 4: As an example, what methodology will be employed to select the optimal battery

technology for Jan de Nul's existing trailing suction hopper dredger vessel, comparing the impact of two different control strategies on the BESS requirements, taking sub-question 1-3 into account?

1.3. Report Structure

The format of this report is as follows:

- **Chapter 2:** Gives an overview of the recent trends and the literature. This Chapter outlines the framework of the review, from power systems analysis to different battery technologies, and highlights the significance of careful battery sizing and selection in the maritime industry.
- **Chapter 3:** Discusses the vessel system under consideration.
- **Chapter 4:** Formulates the numerical modeling of the system, covering the optimal operation of the current system, and the hybrid system possibilities.
- **Chapter 5:** Provides the numerical results of the optimal scenario and the load smoothing and optimal range scenarios, answering the research questions stated.
- **Chapter 6:** Provides a summary of the conclusions and offers recommendations for future research.

1.4. Methodology

The methodology employed in this thesis is depicted in Figure 1.1. The research evaluates three strategies based on the vessel's load profile: optimal operation of the current scenario without batteries, load smoothing, and the optimal range of the generators. An automatic start-stop logic is applied across all strategies, optimizing the number of running generators at each time step based on power demand, which leads to maintenance savings. The control strategy determines the power profile of the generators, directly influencing fuel savings. The battery power is then calculated as the difference between the power demand and the generators' output, following various state-of-charge (SoC) control logics. These calculations take into account the battery constraints, including rated power, C-rate, minimum and maximum state of charge, and initial state of charge, ensuring that the battery operates within its optimal parameters. Static and dynamic losses within the system and the battery are also considered, which are crucial for determining the battery's power profile and overall lifetime. The return on investment is then evaluated through a cost analysis that includes maintenance savings, fuel savings, and battery lifetime. This analysis eventually determines the most suitable battery solution.
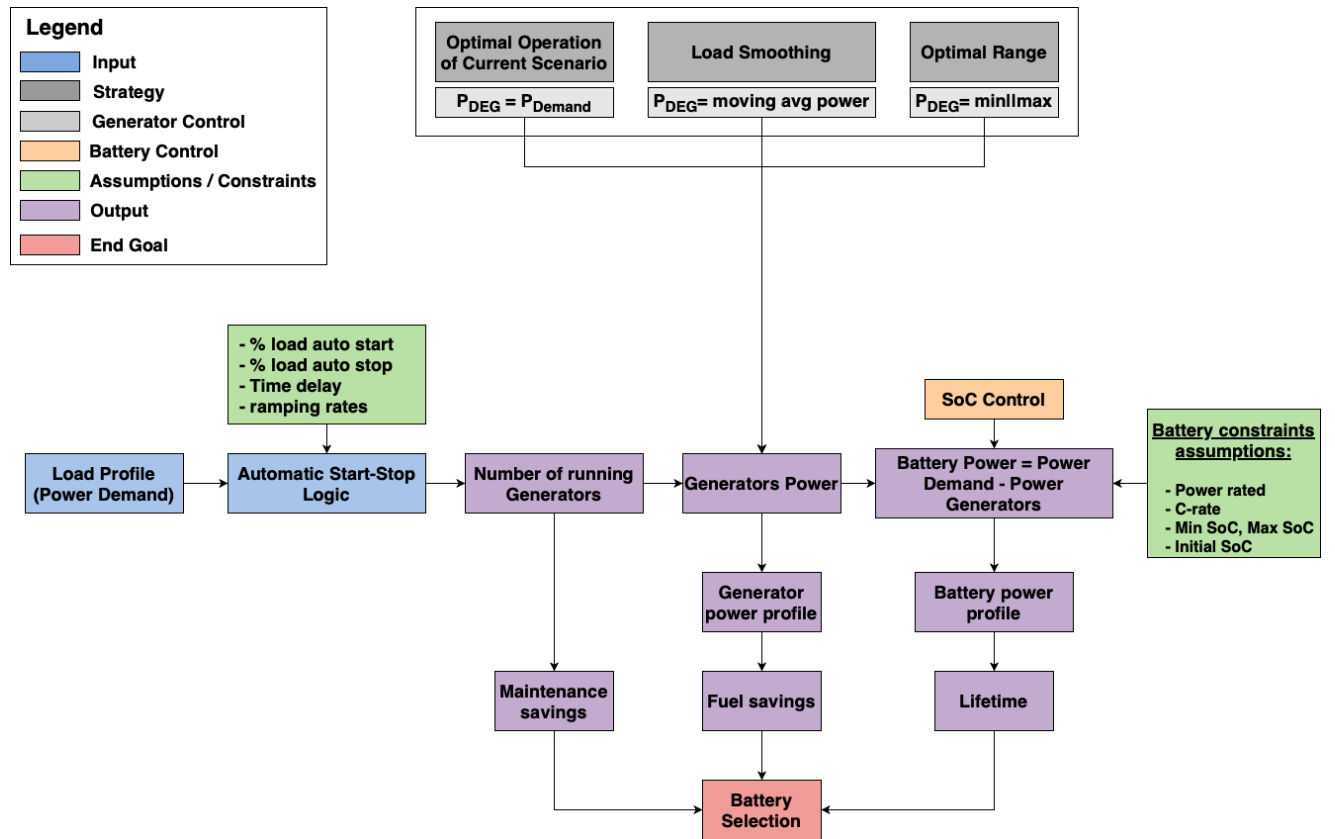
Figure 1.1: Methodology Overview

2

Literature Review

The objective of this thesis literature review is to outline the different battery technologies relevant to the hybrid system vessels, describing the different methods for sizing, selecting, and utilizing ship batteries. By analyzing existing research and methodologies, this review seeks to provide comprehensive insights into effective methods for developing energy solutions in hybrid ocean-going vessel applications. The literature review will be presented in the following structure. First, Section 2.1 delves into the different power systems in maritime vessels, highlighting the hybrid system. Section 2.2 shows the variable energy storage systems technologies focusing in Section 2.3 on battery systems in the maritime applications underlying the specific types under scrutiny in this study. In Section 2.4, a detailed analysis of lithium-ion batteries will highlights their characteristics and compare them. Battery aging, sizing and modeling techniques are also discussed. Finally, Section 2.5 will cover the existing methodologies for battery selection in maritime applications.

2.1. Power System in Maritime Vessels

In the dynamic and demanding environment of maritime operations, the choice of power system plays a crucial role in determining a vessel's performance, efficiency and environmental impact. Mechanical, electrical, and hybrid propulsion systems are various propulsion systems and each system has unique benefits and challenges ranging from the direct energy transfer of mechanical propulsion to the adaptable and effective electrical and hybrid systems. The main propulsion engine types include electric, gas turbine, diesel, steam turbine, and various combinations of these [3]. Maritime vessels primarily utilize two distinct types of power systems: Alternating Current (AC) and Direct Current (DC). Each of these systems has specific applications, with power and voltage ranges varying depending on the type and size of the vessel, as well as the requirements. AC power systems work at different voltage ranges. Low voltage typically at 110V, 220V, 380V, 440V, or 690V, where medium voltage systems usually operate between 1kV and 11kV with common values being 3.3kV, 6.6kV, and 11kV [4]. The power ranges from kilowatts (kW) to tens of megawatts (MW), depending on the size and type of vessel [5]. On the other hand, DC systems operate at voltage ranges of low voltage of 12V, 24V, or 48V common in smaller boats and for auxiliary systems in larger vessels, and high voltage systems that range from 200V to 1000V or more used for propulsion and other high-power applications, having power ranges ranging from a few hundred kilowatts (kW) to MW [6]. In [7], the authors evaluate fuel savings, emissions, reliability, system weight and volume, of an analytic comparisons between Low Voltage AC and Low Voltage DC (LVDC) systems for a diesel-electric propelled application, where superior performance is shown by LVDC systems.

Mechanical propulsion systems offer a range of benefits, including reduced nitrogen oxide (NOx) emissions during efficient operation, and low conversion losses [8]. These systems maximize performance for ships on regular routes operating most efficiently at a vessel's design speed, yet, certain obstacles persist, including increased maintenance requirements resulting from high engine loading and inefficient fuel usage [9]. Below are the different propulsion systems in a vessel, replicated from [8].
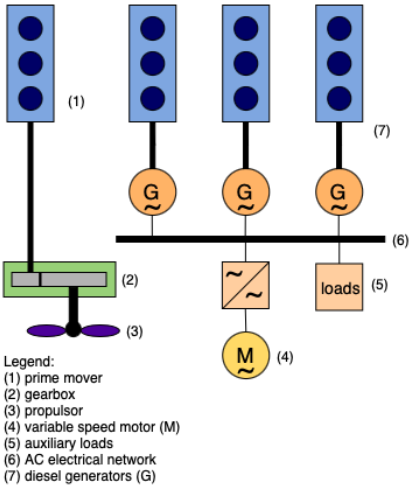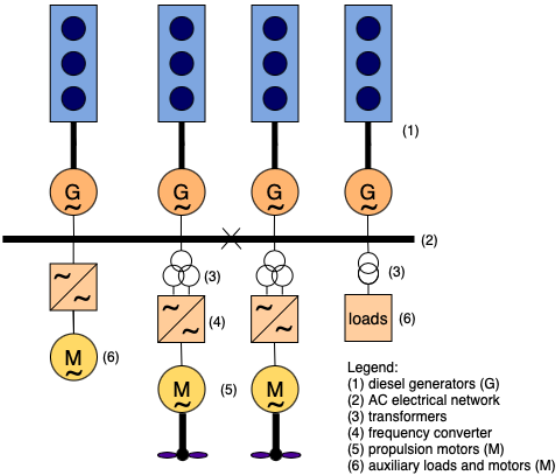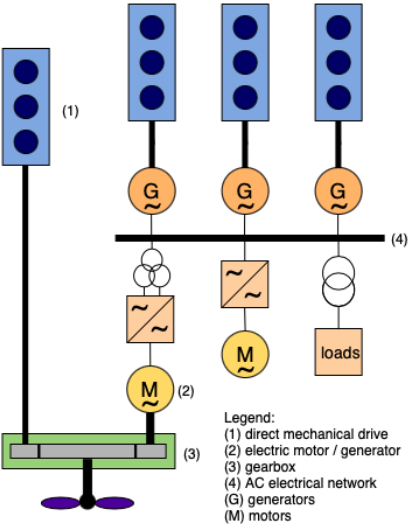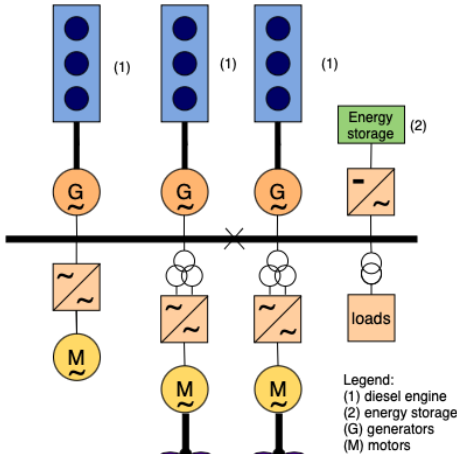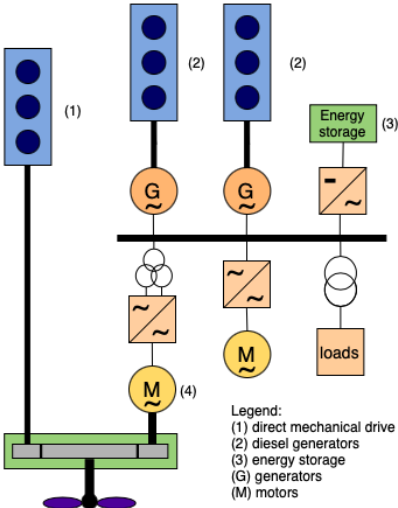
Figure 2.1: Various propulsion systems

An electrical propulsion system offer significant benefits for maritime operations. These systems perform exceptionally well in handling heavy hotel loads and power management across a range of operating profiles, guaranteeing maximum fuel efficiency [8]. The distributed nature of electrical propulsion allows multiple engines to operate closer to their design points at higher speeds, effectively sharing the power load. Additionally, by sharing engines for auxiliary and propulsion loads, the maintenance load is reduced and operational efficiency is increased [8].

These systems do not, however, come without difficulties. The increased specific fuel consumption near top speed is caused by multiple conversion stages (chemical to thermal energy, thermal to mechanical energy, mechanical to electrical energy) because system goes under several transformations stages (diesel engine, generator and electric motors). Low part load operation of redundant engines can result in high emissions and inefficient fuel consumption. Moreover, fluctuations in voltage and frequency can occur in electrical systems when load demand changes from its rated conditions or when there are issues in power management and synchronization between sources, potentially reducing their dependability and availability [10]. A large number of variable speed drives may result in unstable power loads, which would present more operational difficulties. This demonstrates the complex relationships between the operational efficiency, environmental impact, and technical challenges of electrical propulsion systems. It serves as an example of how carefully thought out designs and applications must be made in order to maximize benefits and minimize drawbacks, especially when it comes to achieving sustainable maritime operation. However, hybrid propulsion systems offer a superior maritime propulsion solution by combining the best features of electrical and mechanical propulsion technologies in an inventive way. Hybrid propulsion increases fuel efficiency, reduces emissions, and increases operational flexibility by combining the advantages of both systems [10].

In this project, an electrical propulsion system equipped with a hybrid power supply is used, see figure 2.1. This system employs electrical power from two sources: a diesel generator, which generates electrical power using diesel engines, and energy storage systems. The propulsion is then driven by motors, which use the electrical power produced from both the diesel-powered generators and the energy storage system, providing a smooth and effective propulsion system.

2.1.1. Hybrid Marine Diesel Electric Power System

A. Diesel Generator Set

The term "vessel electric propulsion system" refers to the use of an electric motor, typically an AC motor, to drive the ship's propeller as opposed to utilizing the prime mover directly. A typical arrangement of the main components in a modern diesel-electric propulsion system, are the generator sets, switchboard, bus tie, converter, motor, and thruster, for an AC system.

A.1. Diesel Engine

Four-stroke engines now make up the majority of Diesel Engines (DE) [11]. Because they are smaller and less expensive, diesel engines are typically driven at a medium speed in a diesel-electric propulsion system. Figure 2.2 represents the normalized Specific Fuel Oil Consumption (SFOC) of a fixed speed generation where its optimum operating range lies between 60% to 100% of the power. It demonstrates that at 60% of the power rating, the diesel engine uses less than 200g of fuel per kWh.
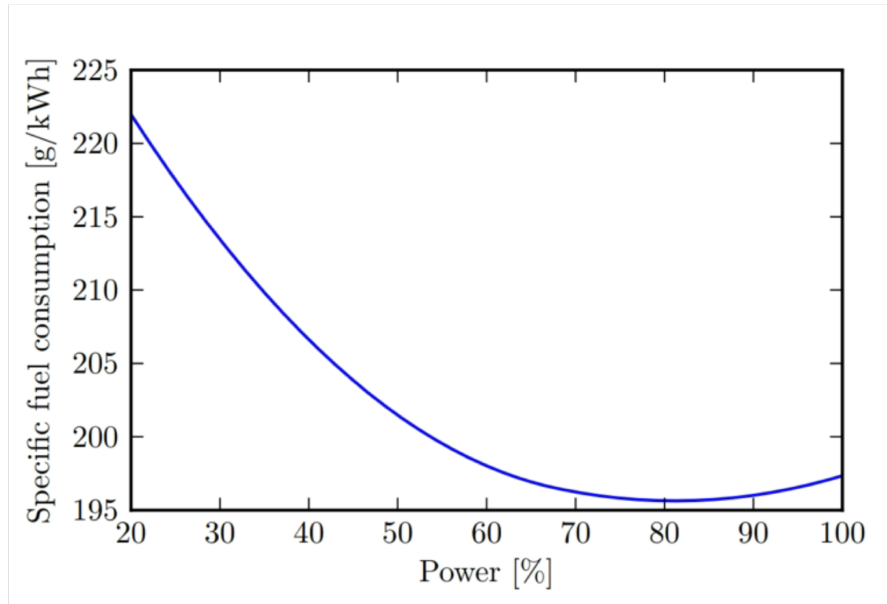
Figure 2.2: Normalized specific fuel oil consumption of a fixed speed generation
[12]

A.2. Generator

According to Faraday's laws, generators are electrical devices that use electromagnetic induction to convert mechanical energy, typically produced by a diesel engine, into electrical energy. These devices come in AC forms. The rotor, a moving component, and the stator, a stationary component, are two essential components of a generator's design.

Synchronous generators operate by providing direct current to the rotor in order to create an electromagnet. They are particularly common in high-load maritime applications. The diesel engine, or prime mover, turns this rotor, creating a magnetic field that interacts with the stator. This interaction causes an alternating current in the stator windings [13]. However, Permanent Magnet Synchronous Motors also do exist and use permanent magnets in the rotor to generate a constant magnetic field, removing the need for a DC supply [14]. The term "Synchronous" indicates the alignment between the induced frequency voltage and the rotational speed of the rotor. There is a fixed relation between the motor speed and the electric frequency represented by:

$$N = 120 \times \frac{f}{p} \tag{2.1}$$

Where N is synchronous speed in RPM, f is frequency in Hz and p is the number of poles in the motor [15].

Asynchronous generators, also known as induction generators, operate on the principle of electromagnetic induction. In these generators, the rotor is driven by an external mechanical source such as hydro turbines or wind. When the rotor speed exceeds the synchronous speed, it causes an electromotive force in the stator windings, resulting in the generation of alternating current power [16]. The efficiency of diesel generators varies depending on their design, size, and operating conditions, but it typically ranges from 30% to 50% [17].

A.3. Genset Efficiency

A diesel engine's specific fuel oil consumption, can be used to express the engine's energy production efficiency [18].

$$\text{SFOC} = \frac{r}{P} \tag{2.2}$$

where:

- r is the fuel consumption rate in grams per second (g/s),
- P is the mechanical output power produced in watts (W).

The engine's power output can be calculated in the following way:

$$P = \tau \cdot \omega \tag{2.3}$$

where:

- τ is the torque produced by the engine in newton-meters (Nm),
- ω is the angular speed in radians per second (rad/s).

Therefore, SFOC is measured in grams per joule (g/J), however it is commonly expressed as grams per kilowatt-hour (g/kWh). At low loads, the fuel efficiency is low because the specific fuel consumption is higher leading to more fuel consumption to produce each unit of power. On the other hand, at high loads, the fuel efficiency is higher due to a lower specific fuel consumption [19].

A.4. Genset Sizing

A crucial part of designing the powerplant system is choosing the number and size of gensets. By operating a suitable combination of gensets that meet constraints, electric propulsion can increase efficiency [18]. From an optimisation point of view we would like to keep the running gensets close to an optimal operating point. Determining the ideal genset size may be difficult if the power requirements are highly variable. One may consider having many gensets to be able to accommodate various loads at a high efficiency, but in reality this will not be cost effective. In order to meet fluctuating power requirements, gensets must have some spare capacity in order to start and stop. Secondly, the costs of gensets are not directly correlated with their power generation capacity. Equal or unequal genset sizes might be an ideal choice, depending on power usage profiles. An unequal size of gensets may result in an increase in spare part costs, but if the same supplier is chosen, many spare parts will be identical between engines of different sizes [18]. Larger diesel engines generally exhibit higher efficiency. Redundancy requirements largely determine the number of generators employed; if one generator fails, the others must be able to continue providing the required power supply [20].

B. Switchboard and Bus tie

A switchboard is an electrical device that distributes electrical power from one or more sources to various loads. It has circuit breakers, fuses, and electrical switches that are used to isolate, preserve, and regulate electrical equipment [21]. Where as a bus tie is an electrical component used in power distribution systems to connect two or more busbars. The busbars are metallic bars that conduct electricity within a switchboard [22].

C. Power Electronic Converters

Power electronic converters play an important role in hybrid vessels by managing the conversion and distribution of electrical power from multiple sources, such as diesel engines, batteries, and renewable energy systems. The power electronic converters that are relevant in this thesis research are described below.

1. **DC-DC Converters**: They convert a source of direct current from one voltage level to another. Three types can be found: the buck converters that step down the voltage, the boost converters that step up to voltage, and the buck-boost converters that can step the voltage up or down. Efficiency varies widely based on the design and load conditions. A range of 85-98% can be found, where for example ABB has a DC-DC converter efficiency of 98% [23].

2. **AC/DC Bidirectional Converters (Rectifiers)**: These converters work in both direction converting the alternation current to direct current and vice versa. It has high efficiency, typically in the range of 95% to 98% [24].

3. **DC-AC Inverters (Unidirectional)**: The converters are unidirectional converting direct current to alternating current. They are critical for devices that run on AC power and have a typical efficiency of 97% [25].

4. **Transformers**: Transfer electrical energy between circuits through electromagnetic induction, changing AC voltage levels. It can increase the voltage, decrease the voltage, and provide electrical isolation without changing the voltage levels. They are critical for power distribution and safety in electrical systems. They do have a high efficiency up to 99% [26].

D. Electric Propulsion Motors

The motor is typically the destination to which energy flows. This is done by converting the electrical energy back into mechanical energy, which results in the moving of the thruster, thus the vessel. [27]. Electric motor come in different types that have various sizes and control characteristics. These are the DC (commutator) motors, induction motors, synchronous motors, doubly fed machines, and superconducting motors [28].

E. Other Systems

Beyond propulsion systems, maritime vessels are equipped with different other essential systems that consume significant amounts of energy. Navigation systems, including radars, GPS, and electronic chart display and information systems, are important for safe and precise navigation. Communication systems ensure continuous contact with shore stations and other vessels, incorporating radios, satellite communication, and internal networks. Heating, Ventilation, and Air Conditioning systems known as HVAC maintain a suitable environment for crew and passengers by controlling temperature and air quality. Lighting systems ensure safety and visibility. Safety systems, such as fire suppression, emergency lighting, and lifeboats, are vital for emergency situations. Deck machinery, including winches, cranes, and capstans, supports cargo handling and anchoring operations. Pumps are essential for various functions, such as ballast water management, bilge water removal, and cooling. In addition, air compressors supply power for pneumatic tools and starting engines. Auxiliary power systems, including generators and energy storage, support these different operations, ensuring that vessels remain operational and efficient across all maritime activities [29].

F. Energy Storage Integration Topologies

Energy storage systems (ESS) can be integrated into a vessel's power system through several ways, depending on the primary distribution bus's voltage level. Depending on their voltage levels, AC systems can take on different topologies. For low voltage AC systems (≤ 690V), the ESS can be connected to the primary distribution bus via a DC/AC converter [30]. When a Diesel Engine Generator is present, it can be directly linked to the AC bus, thereby regulating the bus voltage. Medium voltage AC systems necessitate the integration of the BESS through an AC/DC converter coupled with a transformer. Elevating the distribution voltage leads to a reduction in system current, which, in turn, diminishes the system's weight, cost, and the expense associated with protection devices. However, the inclusion of transformers contributes to an increase in system weight. On the other side, an Energy Storage System can be connected to a DC bus in a multi-drive setup, by means of a DC-DC converter to manage power flow and ensure efficient charging and discharging processes [31].

2.2. Energy Storage Systems in Maritime application

In the maritime industry, energy storage has gained popularity as a way to improve ship efficiency and reduce environmental impact. An energy storage device, power conversion, and control are the components of an energy storage system. Rechargeable batteries, flywheels, and capacitors/supercapacitors

are among the energy storage devices relevant to the maritime applications. The life cycle, energy and power density, efficiency, charge and discharge rates, and other characteristics of these devices vary from one another. According to the kind of energy stored, they are typically divided into three groups: electrochemical, mechanical, and electrical as illustrated in Figure 2.3.
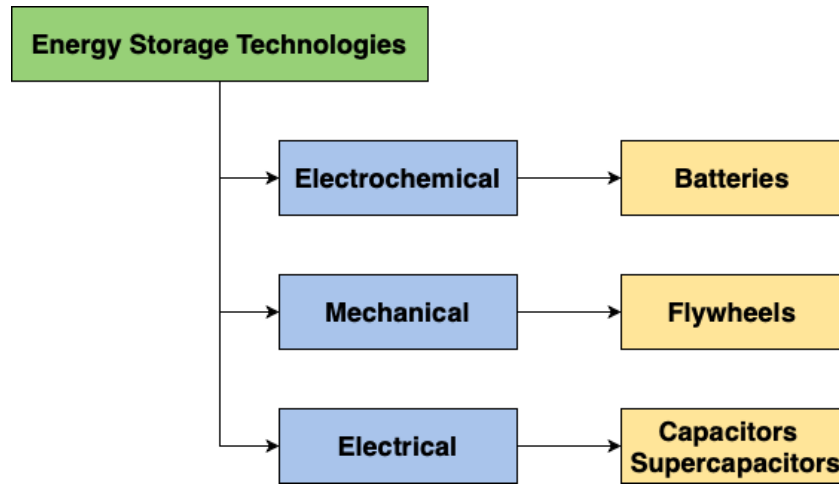
Figure 2.3: Energy Storage Technologies

An overview of the energy storage technologies relevant to the maritime industry, starting with the electrochemical storage technique, which is represented by batteries that store energy in chemical formed cells [10], then there are the mechanical storage technique represented by flywheel that stores energy in the form of rotational kinetic energy [32], and finally the electric storage technique represented by capacitors or supercapacitors that stores the electricity in a type of field that is located in between two plates separated by electrolyte [33]. In [34], a broad range of power requirements can be satisfied by combining different energy storage technologies. For high-power applications, for instance, combining batteries and supercapacitors is advantageous. On the other hand, combining batteries and flywheels improves the integrated energy storage system's capabilities by taking advantage of both the high-power output of the batteries and the energy storage capacity of the flywheels. The latter are beneficial at storing and releasing energy over a long periods of time.

Higher energy and power technologies are two categories into which maritime ESS technologies can be divided. Although they have a lower power, higher energy devices like batteries, can provide energy for extended periods of time. However, higher power devices can only provide very high power for a limited amount of time. Examples of these devices are flywheels, capacitors/supercapacitors, and higher power batteries. Battery technology's broad characteristic range allows it to be used in both categories [35]. The operational dynamics of energy storage systems are defined by the terms "slow response" and "fast response," which emphasize how quickly these systems can meet energy demands. High energy capacity devices have a slower response time and are designed for long-term applications. They are also made for prolonged output and energy storage. High-power devices, on the other hand, are made to deliver and absorb power quickly. They have a fast response time, making them perfect for applications that require fast adjustments to power fluctuations or sudden energy bursts. Table 2.1 summarized the response time of the ESS relevant to the maritime.

Higher energy devices (Slow response)	Higher power devices (Fast response)
Battery (s-min) [36]	Flywheels (ms-s) [34]
	Capacitor/Supercapacitor (ms) [34]
	Battery (ms-s) [34]

Table 2.1: Classification of high energy and high power energy-storage systems
,

In the Figure 2.4 below, a comparison between the specific energy and specific power of the energy storage systems is shown [37]. Superconducting Magnetic Energy Storage systems represented in the Figure, while highly efficient and capable of delivering rapid bursts of power, are expensive and require complex cryogenic cooling systems required to maintain the superconducting state. Additionally, the technology is still in the early stages of development for large-scale applications, making it less practical compared to other energy storage solutions like batteries [34].
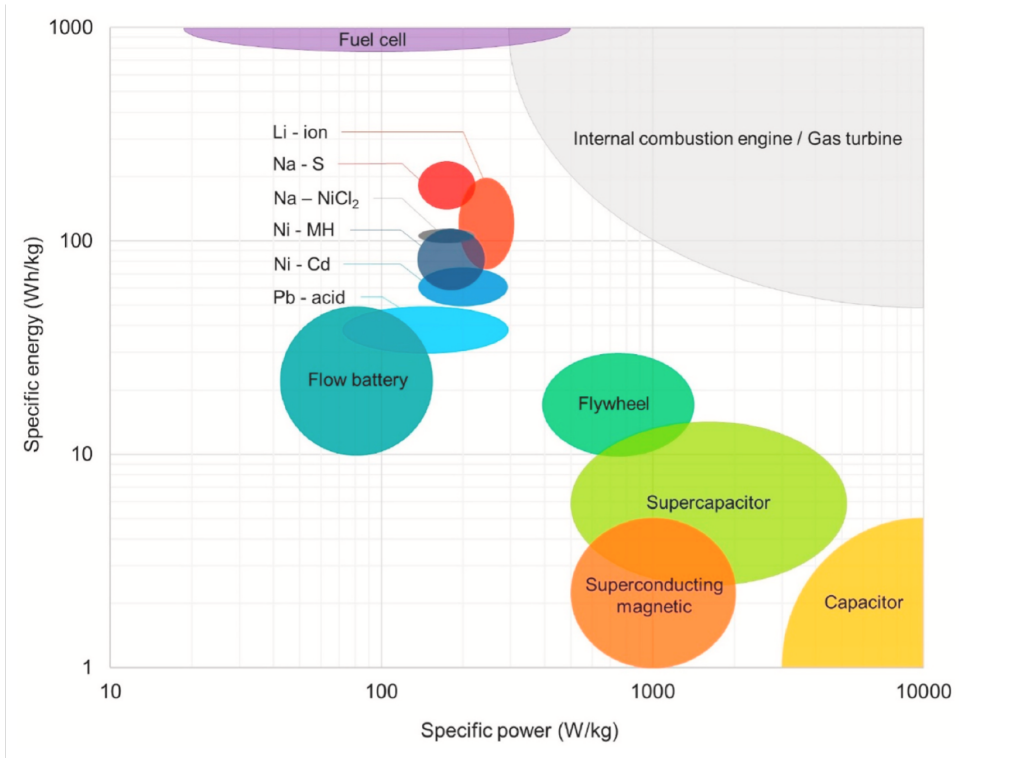
Figure 2.4: Comparison of power and energy density for energy storage media

As previously mentioned, the focus of this thesis is on oceangoing vessels that are being retrofitted to incorporate an electrical power system that is backed by a hybrid power source. The main means of energy storage in this system is through the use of batteries, which is a crucial component that will be covered in detail in the next Sections.

2.2.1. Implications of ESS integration

Design Impact

Integrating an energy storage system in hybrid vessels, aligns with design modifications that has an impact on the vessel architecture, weight distribution, and overall efficiency. These upgrades are es-

sential for advancing vessel performance and ensuring it meets the standards regulations.

Weight and Space Allocation

ESS introduce extra weight and space allocation in the vessel, thus affecting stability that makes the designer more aware regarding centralizing equipment throughout the vessel, to ensure safe and efficient operation. Energy storage system setups often demand structural additional supports to bear the extra load. Battery rooms should be included, including the installing of the vibration damping and the thermal installation, as it is essential to protect the batteries from hazards [38].

Safety Considerations

Integrating ESS in hybrid vessels, incur multiple safety challenges that must be mentioned through detailed planning and operational guidelines. These considerations are important to prevent accidents and ensure safety.

1. **Thermal Management:** Lithium-ion batteries, are more subjected to thermal issues, where overheat leads to chemical reactions in the battery cells. A thermal management system is important to eliminate this risk.

   - **Cooling Systems:** To control the ESS's temperature limits, it is important to use developed cooling solutions like liquid cooling or forced air system [39].

   - **Heat Dissipation:** To prevent overheating, heat sinks and ventilations should be implemented and accounted for in the design [39].

2. **Vibration and Shock Protection:** Hybrid vessels face significant challenges due to the wave movements and storms. The design of the energy storage system must incorporate these factors to prevent damage that could affect the system's lifespan. To protect the ESS, secure and robust mounting solutions are employed, which protect the system from vibrations and impacts, thus eliminating the risk of damage from such external forces. These mounting systems ensure that the ESS remains intact and functional even in harsh marine environments [40].

Fire Systems

Fire systems are crucial in hybrid vessels. The risk of battery explosion, requires the installation of advanced fire detection and fire suppression systems.

1. **Fire Detection:** To insure safety and prevent fires, early fire detection should be taken place at the moment when a spark shows up.

   - **Smoke and Heat Detectors:** Installing smoke and heat detectors in ESS compartments can provide early warnings of potential fires, enabling quick intervention [41].
   - **Gas Detection Systems:** to monitor the gases that might be released from the batteries [42].

2. **Fire Suppression:** Effective fire suppression systems are essential to control and extinguish fires in battery compartments, where conventional methods might not be sufficient.

   - **Fixed Fire Suppression Systems:** Employing fixed systems such as water mist, foam, or inert gas-based solutions (e.g., FM-200, CO2) is recommended for ESS compartments. These systems should be capable of rapid deployment to minimize fire spread [43].

   - **Automatic Sprinkler Systems:** Integrating automatic sprinkler systems can provide immediate response to fire incidents, ensuring quick control and minimizing damage [43].

2.3. Battery Systems in Maritime Applications

Battery systems offer the flexibility to store and generate electrical energy, using it optimally for system operation. This advantage has been demonstrated in hybrid electric vehicles on land. For instance, in a hybrid car, batteries assist in balancing the engine's load. Some battery systems are engineered to deliver high power quickly, enabling the engine to operate more efficiently and steadily. When the vehicle slows down or operates below peak efficiency, the battery charges, storing energy for later use.

These advantages apply to maritime propulsion systems, where various vessels possess specific operational characteristics, requiring batteries to meet varying energy and power requirements while also accounting for the intended lifespan of the battery. While batteries have the capability to solely power a vessel for short distances or durations, the main goal is usually to improve the vessel's overall performance and efficiency. BESS aboard a vessel serve various purposes. These different functions directly influence the system required characteristics and capabilities [44]. By optimizing loading between generator sets, these batteries lessen ramping and increase the fuel efficiency of the system. They reduce numbers of operating hours results in reduction of maintenance. Furthermore, batteries improve the system by acting as standby power sources without using fuel. As a result, battery systems strengthen system reliability in addition to increasing system efficiency. On the other hand, there are some disadvantages like the high investment expenses that result from the substantial initial costs [45], even though prices are progressively going down as technology advances [46]. In addition, batteries have a limited lifespan and their storage capacity degrades over time. These parameters are compared in Section 2.3.1 and 2.4.1. Both the capacity and efficiency of a battery decrease with repeated charge-discharge cycles, leading to a lower performance and consequently needing replacement [47]. The author's standard definitions for this research are specified below for the various functions related to oceangoing hybrid vessels.

1. **Spinning reserve:** Larger vessels run multiple generators on board to provide redundancy. Batteries acting as a spinning reserve ensure that fewer generators need to be connected. When necessary, the battery energy storage system serves as a backup in case the generator fails and can handle additional loads when needed. Advantages of spinning reserve is the reduction in fuel consumption and decreases of the carbon footprint of the ship. Nevertheless, disadvantages include high replacement and initial costs.

2. **Peak shaving:** Peak shaving is a technique that uses batteries to reduce power demand spikes, easing the burden on generators and smoothing out fluctuations in power demand. A benefit of the peak shaving function is the reduction of the number of generators with a decrease in the strain on them. On the other hand, it requires accurate prediction of energy peaks, which can be difficult to predict. Inaccurate result can lead to insufficient power supply or unnecessary battery cycling, which could shorten their lifespan.

3. **Optimise load:** In order to ensure that the generators run as efficiently as possible, optimizing the load means precisely adjusting the power supply to match the vessel's current energy requirements. When demand exceeds the generator's capacity, the battery supplies the excess power, and when there is excess power coming from the generators running at optimal, the excess will be stored in the battery. This is done in order to keep the generators running within their optimal power range. A benefit is the lower running costs due to reduced fuel consumption. However, risk of inefficiencies could result from the battery system's inability to react appropriately to sudden variations in load.

4. **Load smoothing:** The power supplied by the generator is derived from the smoothed power demand. When the generators cannot keep up with the varying power demand, the battery provides the power. The mechanism ensures that there will always be enough power and energy to support such a function.

5. **Ramp support:** Ramp support is where batteries offer instantaneous power support, assisting generators during periods of sudden high demand. This quick response is vital in maintaining

power quality and avoiding generator lag's, such as interruptions or power dips. Such systems require batteries with high power capabilities, which can be expensive. A disadvantage is the frequent high-power charges and discharges that can shorten the lifespan of the system by accelerating battery degradation.

6. **Harvest energy:** Energy harvesting involves capturing and storing energy from various operations and natural resources, like regenerative braking from cranes for example. This stored energy can be used to power the vessel's systems, which lessens the need for conventional generators.

7. **Backup power:** The backup power function works similarly to an uninterruptible power supply, where the battery system supplies emergency power in case of a main power failure. This can be a localised system for critical loads and it can guarantees that these critical systems will remain operational, preserving safety and operational integrity during unforeseen power outages. On the other hand, these systems must be designed to cover all crucial loads for the duration of potential outages, which can be challenging to anticipate and expensive to accommodate.

As an example, on the Thialf vessel and in order to secure the power supply during a DE fault and replace the one operating DE in each engine room, the author of [48] employed the spinning reserve function. Power peaks and valleys were also absorbed, and DE operation was made smoother, by using an enhanced dynamic performance function (peak shaving).

In [44], the authors offer ESS, specifically batteries, as practical and efficient ways to provide peak shaving and primary reserve in small isolated power systems. It has be proven that integrating ESS into these systems substantially increase frequency stability, manage peak demand, and decrease the reliance on traditional generation methods, thus improving the operational efficiency and system stability. In addition, the economic benefits of the ESS are assessed using a mathematical model through Mixed Integer Linear Programming (MILP) approach.

2.3.1. Types of Rechargeable Batteries for Hybrid Vessels

The process and classification of a battery are covered in Appendix A. This study centers on rechargeable batteries as they prove the most fitting choice for hybrid vessels.

This literature review comprehensively assesses diverse rechargeable batteries for ocean-going hybrid vessels, covering lithium-based (Li-based) [49], nickel-based (Ni-based), sodium-based (Na-based) [50], lead-acid batteries [51], and flow batteries [47]. Multiple types within each category are examined providing crucial insights into widely used battery technologies. Furthermore, a summary of possible future batteries will offer insights into emerging solutions that could further enhance the efficiency and sustainability of maritime hybrid systems. The analysis aims to outline the fundamental aspects, performance variations, and characteristics of these batteries, enabling a comparative examination for suitability in the context of ocean-going hybrid vessels. A thorough examination of each battery type, covering its technical details, benefits, drawbacks, and possible uses is discussed below.

Lithium-ion batteries

Lithium-based batteries, known for their high energy capacity, lightweight design, and high cell voltage, are extensively utilized in portable gadgets like mobile phones and electric vehicles [52]. Their popularity expands beyond portability, finding frequent use in stationary applications as well [53]. These batteries vary based on their electrode materials and electrolyte where the electrolyte may consist of liquid or polymer materials [53]. The performance of a Li-ion battery is determined by the electrode materials employed. Typically, the positive electrode contains Li-containing transition metal oxides, while the negative counterpart often comprises carbon-based materials like graphite or hard carbons [54].The battery's electrolyte usually consists of a Li salt dissolved in an organic solution [53]. However, the organic electrolyte's interface with the electrodes results in the formation of a solid electrolyte interphase

(SEI) during initial charge-discharge cycles at the anode. The anode is protected from direct contact with the electrolyte by this SEI. However, its gradual formation may result in Li loss, a reduction in capacity, and an increase in resistance. Li-ion batteries hold promise for stationary storage systems due to their high specific energy and power, coupled with relatively low capital costs [55], [54]. They exhibit an energy efficiency ranging from approximately 85-95 percent, endure numerous charge-discharge cycles, boast a lifespan of around 10 years. As previously mentioned, the positive electrode comprises Li-containing metal oxides, with various structures determined by specific materials. These diverse structures exhibit distinct performance parameters, which are further detailed below [53].

A. Lithium iron phosphate

Li-ion batteries employing lithium iron phosphate ($LiFePO_4$) as the positive electrode are known as LFP batteries. These batteries have high safety measures and have extended cycle life at a moderate expense. The LFP electrode not only offers robust security but also demonstrates substantial power output and packing density, making it suitable for a wide range of applications [54]. Furthermore, a comprehensive cycle life analysis has highlighted the remarkable stability of the LFP cathode in comparison to other Li-ion cathode materials. Furthermore, during discharge, the voltage curve of LFP batteries displays a characteristic plateau where about 80% of the stored energy is contained within this stable voltage range. Despite these factors, the combination of these qualities makes LFP batteries very attractive choices, especially when compared to other Li-ion batteries, for stationary applications.

B. Lithium cobalt oxide

Li-ion batteries utilizing lithium cobalt oxide ($LiCoO_2$) as the positive electrode are denoted as LCO. This electrode configuration has a high specific energy [56]. Nevertheless, significant concerns associated with this configuration are safety concerns and high-cost, mainly because of the cobalt dependency. The price volatility of cobalt and its possible toxic and environmental risks are important considerations [53].

C. Lithium manganese oxide

Li-ion batteries utilizing lithium manganese oxide ($LiMn_2O_4$) as the positive electrode are labeled as LMO batteries. These batteries showcase high specific power at a reasonable expense. However, they have a lack of electrolyte solution stability in this lattice configuration, which can result in capacity fade, thermal instability, and a shortened battery lifespan. [57].

D. Lithium nickel cobalt manganese oxide

Li-ion batteries using lithium nickel manganese cobalt oxide ($LiNiMnCoO_2$) in their positive electrodes are commonly known as NMC batteries. These batteries belong to the ternary Li-battery category, where the cathode material consists of three or more substances. The proportions of these materials can be modify to achieve specific cost levels, cell voltage requirements, and safety measures. Among various Li-ion batteries, NMC batteries stand out due to their remarkable safety standards, extended lifespan, and high energy density. They are also regarded as cost-competitive. However, challenges persist concerning the costs and the use of cobalt [58].

E. Lithium nickel cobalt aluminum oxide

Li-ion batteries utilizing lithium nickel cobalt aluminum oxide ($LiNiCoAlO_2$) in their positive electrodes are recognized as NCA batteries. These batteries are classified as ternary Li-ion batteries [59]. NCA batteries possess a notably high specific energy, approximately 250 Wh/kg, making them well-suited for integration into portable devices and electric vehicles [60]. However, the incorporation of cobalt escalates the initial costs considerably. In addition, NCA batteries have a shorter cycle life compared to other battery types. Safety concerns also arise with NCA batteries, which present a drawback. Both NCA and NMC cells demonstrate favorable traits for similar applications, leading to their usage in analogous Battery Energy Storage Systems [61].

F. Lithium titanate oxide

Batteries utilizing lithium titanate oxide (Li_2TiO_3) in their negative electrode, unlike conventional graphite-anode Li-ion batteries, demonstrate promise because of their remarkable power capacity and long cycle life. These LTO batteries, recognized for their rapid charging abilities, find suitability in high-power applications despite titanate's higher cost, which prevents its broader use in Li-ion batteries [62]. They have been available for some time, serving in high-power, high-cycle life applications like hybrid cars, and are proving to be very attractive for use in maritime applications because of their remarkable power and cycle life qualities. However, the natural low energy density resulting from LTO's low cell voltage necessitates a larger number of batteries, escalating costs significantly compared to comparable NMC batteries. Despite this disadvantage, the overall lifetime cost of LTO systems frequently turns out to be more economical when taking sizing and service life into account.

Nickel-based batteries

Nickel (Ni)-based batteries stand out for their high storage capacity, all at relatively low costs. With nickel being abundantly available as the fifth most common element on Earth, both in the Earth's crust and core, The nickel supply chain is still strong and regularly restocked. These batteries typically employ a $Ni(OH)_2$ cathode, while the choice of metal for the anode can vary. The electrolyte used is typically a concentrated solution of potassium hydroxide (KOH) or a combination of potassium hydroxide and sodium hydroxide [63].

A. Nickel-cadmium

Nickel-cadmium (Ni-Cd) batteries, the earliest form of Ni-based batteries, use metallic cadmium and nickel oxide hydroxide (NiOOH) as the anode and cathode, respectively [58]. These batteries have advantages like low maintenance costs and an extended cycle life because they use an alkaline potassium hydroxide solution as the electrolyte (around 2000-2500 cycles), and an efficiency level of approximately 75 percent. However, they suffer from drawbacks such as low energy density, high initial capital costs, and the toxicity of cadmium. Additionally, Ni-Cd batteries are susceptible to the memory effect, limiting their use to specific applications. To overcome these constraints, initiatives to improve the recycling procedures for Ni-Cd batteries have been in progress [63].

B. Nickel-iron

Nickel-iron (Ni-Fe) batteries were among the first commercially available Ni-based batteries, using metallic Fe and NiOOH electrodes. Despite their efficiency of approximately 60% and low energy density, they perform well in environments with vibrations due to their outstanding shock resistance [64]. They offer cost-effective manufacturing and good performance without environmental risks, but are nearly four times more expensive than lead-acid and Li-ion batteries. Also known as NiFe, these batteries use a NiOOH cathode, Fe anode, and a KOH electrolyte generating a 1.20 V cell voltage. However, limitations like low specific energy, poor low-temperature performance, and a high self-discharge rate, with substantial manufacturing costs, have prevented widespread adoption, maintaining the industry's preference for other batteries despite NiFe's durability and extended lifespan [65].

C. Nickel metal hydride

Nickel metal hydride (NiMH) employs a hydrogen-absorbing alloy and cadmium hydroxide ($Cd(OH)-2$) in the anode. It utilizes an aqueous solution of potassium hydroxide as its electrolyte. During the final stages of charging, hydrogen production occurs, needing good room ventilation to prevent potentially explosive hydrogen concentrations. NiMH batteries have become widely available for consumer use and share similar applications with NiCd. Offering a 40 percent higher specific energy than standard NiCd batteries, NiMH is considered favorable [63]. However, they are more delicate to charge compared to NiCd, prone to rapid rates of self-discharge, and devices with NiMH batteries can deplete within weeks when stored. The NiMH batteries have benefits such as low cost and non-flammable

electrodes and electrolytes, yet they suffer from drawbacks including low specific energy and energy density, hydrogen gas release during charging, resulting in the possibility of explosive environments, and high self-discharge rates.

D. Nickel-zinc

Nickel-zinc (Ni-Zn) batteries utilize a NiOOH positive electrode (cathode) and a zinc oxide negative electrode (anode), acknowledged for being non-toxic and environmentally friendly. However, challenges like separator penetration and electrode shape alterations limited their commercialization [64], [66]. While similar to nickel-cadmium in cathode material and alkaline electrolyte use, NiZn differentiates itself with a zinc (Zn) anode, leading to a voltage of 1.65V and a specific energy of 100 Wh/kg. Charging at a constant current to 1.9 volts per cell and unable to undergo flow charge, NiZn faces issues like high self-discharge and short cycle life due to dendrite growth, a topic that is constantly being researched. Despite presenting advantages such as low cost, high power output, and a favorable temperature operating range, they still fall behind lithium-ion batteries concerning specific energy and energy density [67].

E. Nickel-hydrogen

Ni-H_2 batteries, utilizing gaseous H_2 in a pressurized cell and featuring NiOOH as their positive electrode, show remarkable durability, lasting about 15 years at an 80 percent Depth of Discharge (DoD) and enduring approximately 30,000 cycles. Despite these advantages, their specific energy remains low, coupled with high self-discharge rates and significant costs associated with pressurized vessel requirements and platinum catalysts. As a result, Ni-H_2 batteries find primary application in aerospace, especially in satellites [68]. In contrast, Nickel Hydrogen (NiH) batteries, with a nominal cell voltage of 1.25V and specific energy ranging from 40 to 75 Wh/kg, offer a long life, low self-discharge, and good temperature performance (from –28°C to 54°C or –20°F to 130°F), rendering them ideal for satellite use. Efforts to apply NiH batteries terrestrially have been prevented by their high costs and low specific energy.

Sodium-based batteries

The abundance of sodium reserves on Earth is one of the many factors driving the development of sodium (Na)-based batteries for large-scale BESS. However, a noteworthy drawback is the limited operational temperature range of Na batteries, necessitating a thermal enclosure to maintain internal battery temperature and prevent damage. This enclosure, while important, prevents individual cell servicing. Moreover, regulating the operational temperature range requires an additional system, contributing to increased overall costs [69]. However, when the system runs on a regular basis, like once a day, the energy required for this regulation stays low. Despite these challenges, Na-based batteries offer advantages including low material costs, along with high energy density and efficiency.

A. Sodium-sulfur

Sodium-sulfur (Na-S) batteries use molten sodium and sulfur as electrodes, separated by a solid oxide electrolyte, demonstrating a distinct working temperature of about 300°C. This elevated temperature causes the electrodes' active materials to be liquid while maintaining other components in a solid state, demanding heat regulation to prevent damage. These batteries provide high specific energy and power, have a cycle life of up to 4500 cycles and a 15-year lifespan, ideal for high-specific-energy applications like load leveling [70]. Despite higher capital costs due to temperature-resistant components, they continue to be less expensive than Ni-Cd batteries. Safety concerns exist due to the high temperature, yet their low-cost and abundant raw materials make them environmentally friendly. Ongoing research on room temperature Na-S batteries aims for high theoretical energy density and low costs for large-scale energy storage, but challenges persevere concerning electroactivity, self-discharge, and cycle life. Efforts focus on improving cathode materials, electrolytes, separators, and anode protection to address these issues, although full resolution remains awaiting [71].

B. Sodium-nickel chloride

The ZEBRA batteries, also known as Sodium-nickel chloride batteries or $NaNiCl_2$ batteries, consist of molten sodium in the anode and make use of metal chlorides like $NiCl_2$ or $FeCl_2$ in the cathode, with solid beta alumina serving as the electrolyte. This configuration includes $NaAlCl_4$ within the cathode, reacting with sodium during full charging to enable tolerance against overcharge. These batteries have high voltage, minimal gassing in order to be safe, and overcharge resistance, yet they demand preheating to a high operating temperature of 300°C [72].

Lead-acid batteries

Lead-acid batteries feature a PbO_2 positive electrode paired with a Pb negative electrode, submerged in an H_2SO_4 electrolyte solution [58]. Despite being a mature and widely used technology, these batteries faces several challenges. Their disadvantages include a short cycle life of 500-1000 cycles, a relatively low specific energy around 33-42 Wh/kg due to the high density of Pb, and poor performance at low temperatures demanding thermal regulation. Despite these limitations, they have low capital and operational costs, leading to a good safety and exhibit good recyclability [73]. Among secondary batteries, it has the least environmental impact from cradle to gate. They show stable performance, yet overcharging can lead to water loss due to the evolution of H_2 and O_2. Their specific power reaches up to 180 W/kg, making them suitable for transportation like electric vehicles [70]. In stationary applications, valve-regulated lead-acid (VRLA) batteries are commonly used, though flooded batteries are also employed. VRLA batteries tend to have higher cost due to their increased complexity compared to flooded lead-acid batteries.

Flow batteries

Next to traditional batteries, flow batteries are another type of electrochemical energy storage devices playing a role in stationary energy storage applications. Vanadium redox, Polysulphide bromine, and Zinc bromine redox flow batteries are among the different types of flow batteries used as stationary energy storage devices. The technical characteristics of these batteries are provided in terms of ranges as indicated. The specific energy of flow batteries spans from 10 to 35 (Wh/kg), specific power of 100–166 (W/kg), round trip efficiency of 65–85 (%), service life of 15 (years), and self-discharge rate of 0. With these technical specifications, flow batteries are considered as an advantage in stationary storage applications with low self-discharge as well as high service life and quick response times [33].

Possible future batteries

A. Solid-state

Solid-state batteries represent a groundbreaking advancement in the maritime sector, offering substantial advantages such as increased safety, high energy density, and long service lives. These developments stand to redefine energy storage and use within maritime transportation, moving the industry towards a more eco-friendly and sustainable direction. Differing from conventional lithium-ion batteries, solid-state batteries use solid electrolytes rather than liquid ones, presenting several important advantages. With a cycle life over 10,000 cycles, these batteries can last three to four times longer than traditional batteries, decreasing the need for frequent replacements without increasing costs [74]. Because of their effective use of materials and initial energy input, solid-state batteries are more environmentally friendly. Safety is another area in which solid-state batteries excel. They can withstand high temperature (up to 160°C), and overheating without exploding, catching fire, or emitting smoke. With their ability to deliver a high energy density, these batteries provide sustained power over longer periods, a crucial requirement for the maritime industry known for its lengthy operational requirements. They are perfect for a variety of settings since they can function effectively in a wider temperature range—from 0°C to 35°C—without the need for cooling systems. While cooling may still be important in tropical climates, the overall dependency on bulky cooling systems is significantly decreased. Solid-state batteries offer a reliable, efficient, and safer alternative for the marine industry, promising to play a pivotal role in the sector's transition towards operational efficiency and sustainability [58].

B. Zinc-ion

These batteries use zinc ions (Zn^{2+}) as the main charge carriers through a water-based zinc chloride or ammonium chloride solution. They also incorporate a metallic zinc anode and investigate different cathode materials such as copper hexacyanoferrate, manganese oxide (MnO_2), α−, γ−, and δ− derivatives. This battery technology stands out for its affordable, safe, and environmentally use, offering high capacity and reversibility without the possibility of zinc dendrite formation. Although it has a specific capacity of 85 Wh/kg which is lower than the 240 Wh/kg of a typical lithium-ion batteries, it can achieve an energy density of 450 Wh/L. This is competitive in the lithium-ion market, even though some variations can achieve up to 650 Wh/L. This technology promises significant cost and safety benefits, specifically for applications where weight and space are important, such as in the maritime environment. However, the development of zinc-ion batteries requires further improvement in areas like cathode material behaviour, electrolyte efficiency, and production techniques to enhance performance and reliability [75].

C. Sodium-ion

Sodium-ion batteries, using sodium ions (Na^+) as charge carriers and an ion insertion material as the anode, show promising potential for large-scale energy storage systems due to sodium's availability and research interest resulting from its lower cost compared to lithium. However, challenges persist in identifying suitable materials capable of accommodating sodium efficiently due to its different size relative to lithium, having impact on the effectiveness of prior materials. Current research investigates various anode and cathode materials, including carbon-based compositions, metal alloys, and transition metal oxides for anodes and Na-containing oxides and salt systems for cathodes [76]. Despite these improvements, commercializing Na-ion batteries faces some challenges, demanding further research to overcome limitations concerning electrode stability, energy density, and commercial availability. Maintaining a solid-electrolyte interphase, controlling temperature, and addressing safety issues related to dendrite formation are still crucial components of this pursuit.

D. Lithium-sulfur

Due to their energy density, which is roughly five times greater than that of Li-ion batteries, Li-S batteries are being developed for specialized mobile applications such as aircraft, high-altitude satellites, and military electric vehicles. However, challenges inhibit their widespread commercial adoption, primarily associated with the failure mechanism. Unlike the gradual degradation seen in Li-ion batteries, Li-S batteries tend to experience more sudden degradation, limiting their reliability in applications that demand consistent battery performance. As a result, Li-S batteries are frequently disregarded for situations requiring consistent power because of these concerns [77].

E. Metal-air

Metal Air electrochemical batteries use pure electropositive metal as the anode material and ambient outside air as the cathode, usually with aqueous solutions as electrolyte, to generate electricity. The metal anode includes one of the alkali metals (Li, Na, K, Mg, Al), or transition metals (Fe, Zn); the nature of anode the determines which electrolytes are most effective. In order to facilitate electron exchange and maintain oxygen supply, the cathode must have an open porous structure. The biggest benefit of metal air batteries is its high theoretical energy density with low cost, which exceeds that of lithium ion batteries. However, metal air batteries also face serious challenges, such as low specific energy (<150 Wh/kg), short lifetime, and low efficiency [49].

Tables 2.2, 2.3, and 2.4 provide a summary of the performance parameters for each battery type. As can be seen, lithium-ion batteries have good performance metrics, including high specific energy and power, energy density, power density, and round-trip efficiency, making them suitable for a range of onboard systems. However, their high cost and environmental impact need to be carefully considered, particularly in environmentally sensitive marine ecosystems. Although they are less expensive than other options, lead-acid batteries have shorter cycle lives and lower specific energy. Flow batteries may have some limitations due to their moderate performance metrics and lower energy densities compared to other batteries but they possess no self-discharge. On the other hand, nickel-based batteries

demonstrate a moderate level of performance, with different sub-types exhibiting varying environmental and safety considerations. They also have low specific energy. Lastly, sodium-based batteries are costly due to their manufacturing process, insulation needs, and thermal management.

Performance parameters	Unit	Li-ion	Lead-acid	Flow batteries
Cell voltage	[V]	3.6 - 4.2 [78]	2 - 2.1 [78]	1.2 - 2.5 [60]
Specific energy	[Wh/kg]	150 - 250 [33]	30- 50 [37]	10 - 35 [79]
Specific power	[W/kg]	200 - 2000 [78]	75 - 300 [37]	100 - 166 [79]
Energy density	[Wh/L]	95 - 500 [78]	30 - 50 [34]	1 - 70 [80]
Power density	[W/L]	50 - 800 [78]	150 - 400 [78]	100 - 200 [79]
Lifetime	[years]	5 - 15 [33]	3 - 15 [34]	15 [60]
Cycle life	[-]	1000 - 10000+ [81]	500 - 1000 [37]	>12000 [37]
Round-trip efficiency	[%]	85 - 95 [37]	70 - 90 [37]	75 - 85 [60]
Self-discharge	[%/day]	0.1 - 0.3 [36]	0.1 - 0.3 [36]	$\sim$ 0 [36]
Environmental impact	[-]	sub-type dependent [60]	high [60]	moderate [60]
Safety	[-]	sub-type dependent [60]	high [60]	high [60]
Thermal stability	[-]	sub-type dependent [60]	moderate [60]	high [60]
Cost	[€/kWh]	sub-type dependent [60]	moderate [60]	high [60]

Table 2.2: Performance parameters of Li-ion, Lead-acid, and flow batteries

Nickel-based						
Performance parameters	Unit	Ni-Cd	Ni-Fe [60]	Ni-MH	Ni-Zn [60]	Ni-H$_2$ [60]
Cell voltage	[V]	1.29 [78]	1.37	1.35 [78]	1.6	1.55
Specific energy	[Wh/kg]	50 - 75 [33]	50	50 - 100 [60]	50 - 100	40 - 75
Specific power	[W/kg]	140 - 300 [33]	100	200 - 300 [78]	200	220
Energy density	[Wh/L]	50 - 150 [60]	30	170 - 240 [60]	280	60
Power density	[W/L]	150 - 400 [60]	20 - 50	10 - 600 [78]	100 - 200	50 - 100
Lifetime	[years]	10 - 20 [81]	20	5 - 15 [60]	5 - 15	20
Cycle life	[-]	1500 - 3000 [34]	10000	300 - 1800 [78]	500	30000
Round-trip efficiency	[%]	60 - 70 [33]	65	50 - 80 [78]	70	85
Self-discharge	[%/day]	0.03 - 0.6 [81]	0.03 - 0.1	0.3 - 0.6 [60]	0.6 - 1.0	0.03 - 0.1
Environmental impact	[-]	high [60]	moderate	moderate [60]	high	low
Safety	[-]	moderate [60]	high	high [60]	low	high
Thermal stability	[-]	moderate [60]	high	moderate [60]	low	high
Cost	[€/kWh]	680 - 1300 [78]	moderate	170 - 640 [78]	high	high

Table 2.3: Performance parameters of Nickel-based batteries

Sodium-based			
Performance parameters	Unit	Na-S	NaNiCl$_2$
Cell voltage	[V]	1.8 - 2.71 [78]	2.58 [82]
Specific energy	[Wh/kg]	120 - 240 [58]	100 - 120 [37]
Specific power	[W/kg]	150 - 230 [33]	150 - 200 [37]
Energy density	[Wh/L]	150 - 250 [34]	150 - 180 [60]
Power density	[W/L]	150 - 250 [35]	200 - 300 [60]
Lifetime	[years]	10 - 15 [34]	10 - 15 [83]
Cycle life	[-]	2500 - 4500 [81]	4500 [83]
Round-trip efficiency	[%]	70 - 90 [81]	85 - 95 [83]
Self-discharge	[%/day]	0.05 [33]	0.03 - 0.3 [60]
Environmental impact	[-]	low [60]	low [60]
Safety	[-]	moderate [60]	high [60]
Thermal stability	[-]	moderate [60]	moderate [60]
Cost	[€/kW]	high [60]	550 - 750 [83]

Table 2.4: Performance parameters of Sodium-based batteries

2.3.2. Battery Selection

Following a careful comparison between the various battery types previously discussed, lithium-ion batteries are the preferred choice in ocean-going hybrid vessels. This preference is attributed to their superior cell voltage of 3.6 V [50] where this can achieve higher power in a less space, and high energy density relative to other batteries. This is particularly important for maritime vessels where weight and space are critical factors. While safety concerns vary across lithium-ion sub-types, appropriate mitigation strategies make them feasible for hybrid vessel use. Their proven efficiency and long life cycle further highlights their suitability for meeting the energy demands within the sector [35], [84].

Among rechargeable technologies, lithium-ion batteries stand out for their extended lifespan, compactness, and lightweight nature. Additionally, their efficiency often exceeding 90%, low self-discharge rate, and minimal memory effect make them a viable option for various emerging applications. The term" memory effect" describes the phenomena where the battery, when repeatedly recharged after only being partially discharged, seems to remember its previous state of charge and loses capacity. The longevity of Lithium-ion, exhibiting a cycle life of more than a thousand cycles, is noteworthy [49]. However, the battery's performance is significantly affected by the operating conditions, particularly factors like temperature and power output (C-rate). Despite their higher comparative cost, especially with frequent use, their high energy density and long cycle life may compensate for the initial investment, proving beneficial for extended deployments. This characteristic holds particular significance in maritime settings where frequent replacement, installation, and maintenance incur substantial expenses [49], [85]. Several maritime organizations and shipping companies have already employed lithium-ion batteries in vessels, demonstrating their practical viability and advantages in real-world applications. Some example of hybrid vessels are: the "Viking Lady", which is an offshore supply vessel that was converted to a hybrid electric vessel with a 442kWh Li-ion battery resulting in significant improvements in fuel efficiency with a 10-15% savings in fuel consumption where the emissions where reduced by 55% [86]. "MF Ampere", known as the world's first large-size all-electric battery powered car ferry that operated with a 1090 kWh battery reducing the fuel consumption by 1000 m^3 annually and a maintenance cost reduction of 20-25% [87]. The "E-Kotug" hybrid tugboat that integrates lithium-ion batteries with diesel engines which allows for flexible and efficient operation in harbor environments with a reduction of 50% in emissions and 25% in fuel consumption [88]. A detailed overview of other hybrid vessels can be found in [89].

To conclude this Section, following a thorough comparison of various rechargeable battery technologies, this study will focus on lithium-ion batteries proved beneficial for ocean-going vessels, delving further into the exploration of the different lithium-ion technologies.

2.4. Lithium-ion Batteries

Lithium-ion battery systems stand as a significant contributor to emission reduction in the maritime industry, providing a special combination of power density and energy. The term "lithium-ion" encompasses a diverse array of specific electrode combinations or chemistries, each carrying distinct advantages in energy density, power density, cycle life, charge rates, and electrode stability. There isn't a one-size-fits-all lithium chemistry suitable for every marine application; engineering trade offs play an important role. Understanding the battery specifications for each application is essential to determine the most optimal chemistry. This study will delve into the details of various lithium-ion chemistries, including lithium iron phosphate (LFP), lithium cobalt oxide (LCO), lithium manganese oxide (LMO), lithium nickel cobalt manganese oxide (NMC), lithium nickel cobalt aluminum oxide (NCA), and lithium titanate oxide (LTO), analyzing their respective advantages and limitations in hybrid ocean-going vessels. The basic principles and components of a lithium-ion battery are explained in Appendix A.

2.4.1. Lithium-ion Comparison

The advantages and disadvantages of the six different types of lithium-ion batteries are thoroughly outlined in the Table below, along with an emphasis on their applications within the maritime industry.

Battery Technology	Advantages	Disadvantages	Applicable for Maritime	Ref.
LFP	- Long cycle life - Good thermal stability - Resistant to changes in temperature - Higher safety characteristics - High current capability - Moderate expense - Steady plateau in the voltage curve	- Low specific energy - Lower voltage - Lower power capabilities	Its good safety features and long lifespan make it attractive for maritime applications where safety is paramount.	[90] [58]
LCO	- High energy density - High specific energy - Low self-discharge rate	- Low power rate - Short cycle life - Impedance increases over time - Thermal runaway concerns - High cost - Security issues	High energy density but relatively shorter cycle life and low safety making it less attractive compared to other Li-ion chemistries in the maritime sector.	[91] [58]
LMO	- High thermal stability - High specific power - High charging rates - Low internal resistance	- Lower energy capacity - Shorter cycle life	Shorter cycle life makes it less attractive compared to other Li-ion chemistries.	[92] [58]
NMC	- Safe - Extended lifespan - High specific energy - Long cycle life - Cost competitive	- Important characteristics maintaining equilibrium for a stable lifespan could be challenging	Flexible design with respect to energy and power capabilities. The most used chemistry in marine applications at present due to its balanced properties.	[93] [58]
NCA	- High specific energy and energy density - Chemistry stability due to Aluminum	- Safety concerns - Short life compared to other - Higher cost	High energy density and good lifespan but concerns over safety limit its application in maritime.	[94] [58]
LTO	- Rapid charging ability - High power capacity - Long cycle life - Higher safety characteristics due to thermal stability	- Low energy density - Relatively low specific energy - Initial cost is high, but total lifetime cost might be cheaper - Low cell voltage	Suitable for applications that require fast charging, high power, or very large amounts of cycling.	[95] [58]

Table 2.5: Lithium-ion batteries comparison

The Table below showcases the performance parameters of the six different types of lithium-ion batteries.

Lithium-ion							
Performance parameters	**Unit**	**LFP**	**LCO**	**LMO**	**NMC**	**NCA**	**LTO**
Battery voltage	[V]	∼ 3.5 [96]	3.7 - 3.9 [56]	3.7 [56]	3.6 - 3.7 [56]	3.7 [96]	2.4 [97]
Specific energy	[Wh/kg]	80 - 120 [58]	150 - 240 [58]	100 - 160 [96]	150 - 220 [58]	200 - 260 [90]	50 - 80 [58]
Specific power	[W/kg]	high [60]	moderate [98]	moderate [98]	moderate [60]	high [98]	high [98]
Cycle life	[-]	>2000 [90]	500-1000 [90]	300-700 [60]	1000-2000 [90]	500-1000 [98]	6000-10000[98], 20000 [45]
Environmental impact	[-]	low [60]	high [60]	moderate [60]	moderate [60]	high [60]	moderate [99]
Safety	[-]	high [56]	low [56]	moderate [56]	moderate [56]	low [60]	high [51]
Thermal stability	[-]	high [60]	low [60]	moderate [60]	moderate [60]	low [60]	high [99]
Cost	[€/kWh]	moderate [51]	high [56]	low [51]	moderate [56]	high [60]	high [100]

Table 2.6: Performance parameters of Lithium-ion batteries

Three different types of lithium-ion batteries LFP, NMC, and LTO are the focus of this study due to their strong potential and applicability in maritime applications. LFP batteries are noticed for their high safety, thermal stability, and relatively long cycle life, making them ideal for marine environments where safety and reliability are important. NMC batteries offer a higher energy density, which is crucial for maximizing energy storage and reducing weight on the vessel, thus enhancing operational efficiency. LTO batteries are chosen for their exceptional durability, with a significantly longer cycle life and superior performance in extreme temperatures, making them well-suited for the variable demands of hybrid vessel systems.

2.4.2. Lithium-ion Battery Aging

Batteries have a limited lifespan due to the aging process, which causes a reduction in capacity. Calendar aging and cycle aging are the two different forms of battery aging [101].

Calendar aging, which is mainly dependent on the temperature and charge level of the batteries, is the gradual reduction in capacity over time while the battery is not being used. The internal chemical reactions of the battery, which can change the chemical and physical properties of the battery's components, are the primary cause of this aging process [102]. Research on calendar aging has become a significant focus within the electric vehicle field due to the fact that their batteries remain inactive for

more than 90% of the time as demonstrated in [103]. Batteries prefer temperatures around 20°C and a SoC around 50% [104]. A thorough analysis of calendar aging of Li-ion batteries at various ambient temperatures is given by [105]. An annual battery degradation that is normalized and expressed as a percentage of capacity is provided by the data that the authors summarize.

Cycle aging, which primarily depends on the DoD and C-rates, is the capacity loss that occurs with each cycle. Less capacity loss is generally the consequence of a lower DoD, though this depends on the type of battery. Generally speaking, capacity loss increases with higher C-rates [106]. Multiple studies have been conducted on modeling battery systems for NMC in [107], [108], LFP in [109], [110], and LTO batteries in [111], [112]. According to [113], the tests demonstrated that the cycle aging was independent of the cycle shape and solely dependent on the moved charge Q. As a result, the number of cycles or time (cycles per unit time) can be used to represent aging. But this suggests that each cycle is equivalent to the others. The relationship between the number of life cycles and the Depth of Discharge is depicted in Figure 2.5. It is evident that the DoD has a substantial impact on cycle life. The technical specifications of the average C-rate must be taken into consideration when selecting a battery to maximize the number of cycles at a specific depth of discharge. For example, a supplier offers 75,000 cycles of high-energy batteries with a 20% DoD, while it offers 80,000 cycles of high-power batteries with a 20% DoD.
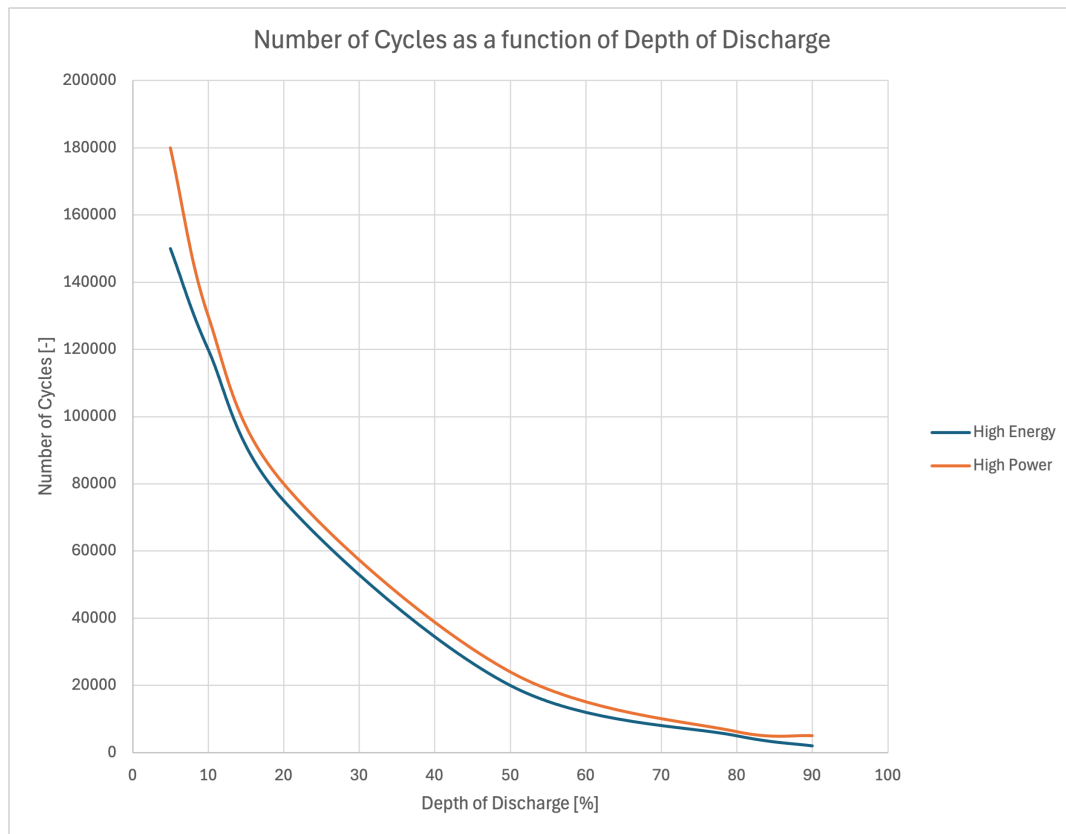
Figure 2.5: Number of cycles as a function of DoD [114]

It is acknowledged that distinct battery chemistries exhibit diverse degradation mechanisms, and the response to various abusive factors varies significantly across these chemistries. Furthermore, batteries with identical or comparable chemistries from various production lines can exhibit differences in degradation responses [115].

Table 2.7 has been created by combining different literature. It is evident that in NMC batteries, the C-rate plays a major role in capacity fading, while in LFP batteries, the C-rate plays a minor role. This implies that while LFP batteries are the better option for high-power applications, NMC batteries are

most suitable for high-energy applications. Compared to graphite-based batteries, LTO batteries have demonstrated less capacity fade.

Table 2.7: Cycle aging of LFP, NMC, and LTO batteries

Battery Chemistry	C-rates	Conclusion	Ref.
LFP (4500 cycles)	1C, 4C	Because the fast-charging method divided the charging into three stages, the cell was not overheated. As a result, the cell was better maintained. Internal resistance to discharge is larger than internal resistance to charge.	[116]
LFP (3 batteries)	1C, 4C	When used correctly with the right cell chemistry and design, fast charging has aging effects that are comparable to those of regular charging and does not impair cell performance over extended cycling.	[117]
NMC (12 batteries)	0.7C, 2C, 4C, 6C	Charging rates above 4C cause the battery to undergo chemical changes that shorten its lifespan and cause serious damage.	[118]
NMC (1000 cycles)	0.33C, 1C, 2C	The developed aging model has been shown to accurately predict the lifespan of NMC battery, with little variation from expected performance. This shows that the model can be used to asses the battery degredation in numerous applications.	[119]
LTO (4 batteries)	5C, 10C	For LTO batteries in high-rate applications at room T, the management of health should prioritize regulating the depth of discharge (DoD) over the C-rate.	[112]
LTO (43 cells)	1C, 3C	Due to LTO's distinctive calendar and cyclic lifetime behaviour, cathode degradation can be effectively monitored using LTO as a reference anode.	[120]

The Figure below illustrates a summary of crucial battery degradation mechanisms, including their causes and effects.
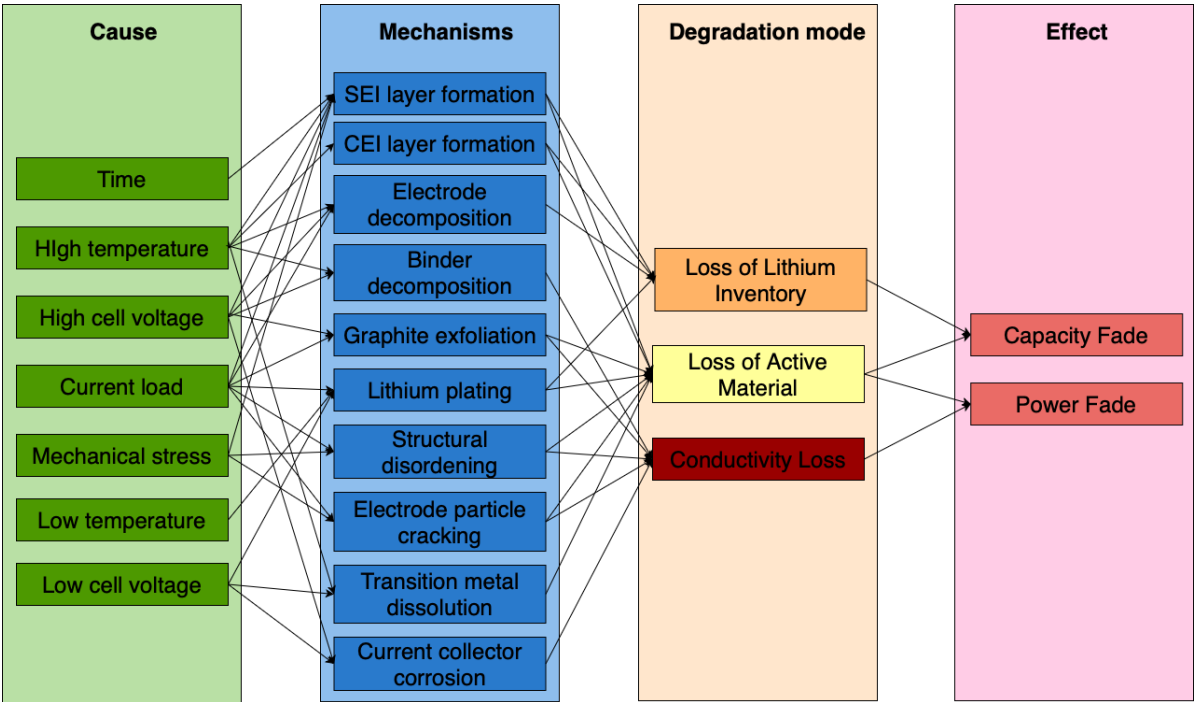
Figure 2.6: Summary of the relationship between operational stress factors, the corresponding aging mechanisms, aging modes, and their impact on the aging of lithium-ion batteries
[121]

In [121], the behaviour and empirical modeling of LIB aging were reviewed and the impact and interdependence of operational stress factors were highlighted. The review that has been presented comes to the conclusion that it is very challenging to generalize about aging behaviour in terms of how operational conditions affect it. Aging as a result is typically not caused by a single stress factor, but rather by a combination of stressors.

Different cycle aging calculation techniques can be found in literature. These are summarized in Table 2.8.

Aging Calculation Technique	Description	Ref.
Empirical Models	Simple models based on cycle count and empirical capacity fade relationships.	[122]
Semi-Empirical Models	Adapted models like Peukert's Law, integrating factors like DoD and rate of charge.	[119]
Physics-Based Models	Simulate electrochemical processes such as SEI growth and lithium plating.	[123]
Hybrid Models	Combine electrochemical/mechanical models with machine learning for more accuracy.	[124]
Thermal Models	Include the effect of temperature on aging using temperature-dependent parameters.	[125]
Fatigue Analysis Models	Use material fatigue concepts like damage accumulation and rainflow counting.	[126]
Stochastic Models	Probabilistic models that predict aging as a distribution rather than a fixed value.	[127]
Real-Time Monitoring Models	Onboard models that use real-time data to continually estimate aging.	[128]

Table 2.8: Summary of Cycle Aging Calculation Techniques

In this thesis study, the Rainflow Counting method was chosen, offering a comprehensive analysis of the complex and variable load profiles typical in real-world battery usage. Unlike simple cycle counting, which only accounts for full cycles, Rainflow Counting captures partial cycles and irregular usage patterns, providing a more realistic assessment of battery degradation. This method is particularly effective in estimating fatigue and damage accumulation, making it ideal for applications where life cycle prediction is critical. On the other hand, the authors of [129] evaluates three primary modeling techniques to predict the calendar aging of lithium-ion batteries. These are the Electrochemical Models (ECM), Semi-Empirical Models (SEM), and Data-Driven Models (DDM). Each technique is analyzed based on its accuracy, computational complexity, and ability to generalize across various conditions. While the ECM are computationally complex and extremely precise, they rely on fundamental principles for predicting aging mechanisms such as SEI layer development. Semi-Empirical Models are simpler and more efficient, using mathematical equations to relate aging to external conditions, but they may struggle to generalize across different scenarios. Data-Driven Models, such as those using Gaussian Process Regression, are good at capturing complex, non-linear data patterns, but rely heavily on high-quality training data. Because of its simplicity, the SEM model was selected for this thesis, and the calendar aging estimation will be evaluated based on [105].

2.4.3. Battery Sizing

Battery sizing is an important factor that needs to be taken into account in order to determine the optimal amount of energy storage and power required to meet demand.

Some of the key factors that influence the ideal battery sizing include unit commitment, investment costs, modeling techniques, maximum generator power, maximum C-rate, and ramp constraints.

1. **Unit Commitment:** This is the process of organizing power plant operations to meet energy demand while maintaining minimal costs. It requires determining the scheduling of the power generation units at any particular time in order to efficiently satisfy the load requirements.

2. **Investment Costs:** These include the costs associated with the battery itself, maintenance, safety installations, monitoring systems, and converters.

   - Battery Cost: The battery system's initial purchase cost.
   - Maintenance Costs: Ongoing expenses for regular maintenance and possible part replacements.
   - Safety Installations: Costs related to ensuring the battery installation meets safety regulations.
   - Monitoring: Costs associated with the systems that monitor and manage the battery's performance.
   - Converter Cost: Costs for inverters and power conversion systems needed for operating the battery.

3. **Modeling Techniques:** The methodologies and algorithms employed to determine the ideal battery size and operation strategy.

4. **Maximum Generator Power:** The maximum power output that the generator is capable of producing, which affects the size of the battery needed to control the load and store excess energy.

5. **Maximum C-Rate:** The maximum rate at which the battery can be charged or discharged, which influences its capacity to handle demand peaks.

6. **Ramp Constraints:** Limitations on the rate at which power output can increase or decrease, affecting the battery's role in balancing demand and supply.

7. **Battery Chemistry:** The different battery chemistry that have different characteristics.

The battery's cost significantly impacts the sizing procedure as it is directly related to the total cost of ownership. Therefore, careful consideration of these factors is important for determining the ideal battery size. In this thesis, only the battery cost is considered to understand the financial impact of the battery itself, as the analysis focuses on comparing three different battery technologies.

One of the modeling technique employed to size and select batteries is the optimization model. Table 2.9 summarizes some battery sizing optimization techniques that are found in literature.

Table 2.9: An overview of the input parameters of the battery sizing methods as found in literature

Optimization Method	Input Parameters	Ref.
Multi-Objective Double-Layer Optimization	- Operational profiles - Operational constraints - Component parameters - CAPEX and OPEX	[130]
Two-layered optimization approach	- Operational profile - SoC constraints - Discharge and charging rates - Energy demand - Cost	[131]
Mixed-integer linear programming	- Load demands - Minimum SoC - Maximum charging/discharging rates - Power rating - Energy capacity - Degradation factors - Replacement methods - Cost	[132]
Mixed-integer non linear programming	- Load demands - Costs of DG, batteries, and other system components - Operational constraints: SoC limits, safety margins, min and max power outputs - CAPEX, OPEX	[133]
Multi-objective particle swarm optimization	- Vessel operational profile (modes) - Max and min energy storage capacities - Power output constraints - Safety regulations - Cost parameters (initial investment costs, maintenance costs, potential savings) - Environmental objectives	[134]
Multi-objective genetic algorithm NSGA-II	- Ship operational demands - CAPEX, OPEX - Environmental constraints - System constraints: maximum power output, minimum operational efficiency needs, energy storage capacity - Component specifications	[135]

1. **Multi-Objective Double-Layer Optimization:** The methodology is adaptable to deal with a range of vessel types and takes into account differing operational profiles and emission reduction targets. It aims for environmentally friendly and affordable solutions while balancing the benefits to the economy and the environment. The method enables a complete optimization of both the energy management strategy and the sizing of the components. However, the solution cannot be generalized due to the difference in operational requirements and technologies. It can be complex to implement and computationally demanding. The accuracy of the input parameters is highly significant as is can affect the optimization results.

2. **Two-layered optimization approach:** This method allows for a precision in the battery sizing tailored to the operational requirements. It is capable of integrating multiple limitations to optimize expenses, efficiency, and mass. For accuracy, it utilizes real-world operational data. Nevertheless, extensive computational resources are needed due to the complexity of the model and it is sensitive to input data accuracy, particularly in dynamic maritime environments.

3. **Mixed-integer linear programming:** This technique allows of a detailed optimization taking into account a wide range of operational, and economic factors. It includes the CAPEX and OPEX along the degradation effects on replacement methods. It has a flexible model where the integration of different objectives and constraints makes it appropriate for complex systems designs. However, the integration of these various constraints and objectives leads to an increase in the computational requirements, where the optimization heavily depends on the precision of the input parameters which can be challenging and complex to estimate. Although strong, MILP may not fully capture the complexities of real-world situations since it requires linearizing non-linear aspects of battery degradation and operation.

4. **Mixed-integer non linear programming:** The MINLP allows for a precision in optimization leading to highly efficient system designs. It can model complex systems with different types of operational methods and components offering flexibility in system design and operation. On the other hand, the mixed-integer and nonlinear nature of the problem can lead to computational complexities, it also requires precise and comprehensive input data, which makes the process dependent on the availability and quality of the data. Due to the existence of local optima, finding global optimal solutions to MINLP problems can be difficult leading to the need of sophisticated optimization algorithms.

5. **Multi-objective particle swarm optimization:** MOPSO is particularly advantageous for problems with multiple objectives, such as cost minimization and environmental impact reduction, as it is good at finding the search space to find a set of optimal solutions. It is It is flexible enough to adapt to different operational and system design challenges and is well-suited for handling complex and nonlinear optimization problems. It offers a wide range of Pareto-optimal solutions, offering decision-makers a number of practical choices that provide a balance between trade-offs among various objectives. On the other hand, the performance of MOPSO can be extremely sensitive to the selection of algorithm parameters, such as particle size and coefficients, necessitating precise adjustment for best outcomes. Longer computation times may result from particle swarm optimization's iterative nature, particularly for large, complex systems with multiple objectives.

6. **Multi-objective genetic algorithm NSGA-II:** When faced with problems involving several different objectives, including decreasing emissions and maximizing performance at the same time, NSGA-II performs very well. It offer a wide range of Pareto-optimal solutions, enabling the decision-makers to choose the optimal solution. Nevertheless, the algorithm has a computational intensity specifically with a wide range of constraints and variables. It can take a lot of effort and specialized knowledge to fine-tune algorithm parameters to achieve the optimal performance.

On the other hand, a second common method employed currently in the industry to determine and size the energy storage system and power requirements from existing operational data, is the numerical approach. Numerical modeling is essential for battery sizing and selection in hybrid vessels due to its ability to simulate and evaluate various battery configurations under a range of operational conditions. By using numerical models, the performance and lifespan of different battery chemistries can be predicted. This method allows for the optimization of battery systems to meet specific energy and power requirements, ensuring that the selected batteries are both efficient and reliable. Moreover, numerical modeling helps in assessing the impact of different load scenarios and environmental factors, providing a comprehensive understanding of how batteries will perform in real-world maritime applications. This approach ultimately leads to better decision-making and more effective integration of batteries into hybrid vessel systems, as demonstrated in various studies focused on marine applications. This can be

modeled by determining first the energy storage system functionalities and control, taking into account other sources of power aboard the vessel. Some example of numerical modeling are discussed below. In [136], the author discuss the hybrid vessels that highlighted major improvements in power systems, pointing out the combination of energy storage systems. Studies insures different battery types like lithium-ion, nickel-metal hydride, lead acid etc. offers significant advantages in energy density and lifespan. Battery degradation remains a major problem, affected by factors including charge-discharge cycles, temperature, and operational conditions. As a result, comprehensive battery selection tech-nique has been promoted, including performance metrics, cost analysis, and lifecycle assessments to identify ideal solutions for specific marine purposes. Moreover, intelligent battery modeling methodolo-gies have developed, enabling exact simulations of battery behaviour under various scenarios, as a result assisting in the design and management of ESS for hybrid vessels. These innovations highlight the important role of advanced energy storage technologies in the development of life lasting maritime transport. In [137], LFP, NMC, and LTO batteries are studied for their suitability in different sizes of BESS for a hybrid electric marine vessel, focusing on the trade-offs between operational efficiency, fuel saving, and minimum BESS size needed for each chemistry. [138] explores the implementation of a hybrid power system in ships, specifically for crane operations, by incorporating lithium-ion batter-ies with traditional diesel generators. It models and simulates the ship's power system under different control strategies, comparing the hybrid system to a conventional system that relies only on diesel gen-erators. The study finds that the hybrid system can reduce emissions and fuel consumption by around 30%, leading to significant cost savings over time. In [139], the authors investigate a hybrid power distri-bution system for a 50,000 DWT tanker, focusing on fuel consumption and emission reductions. Using a numerical model, they compare battery configurations and charging strategies, including waste heat recovery systems (WHRS). The study finds that using WHRS for battery charging is the most effective strategy, saving up to 18.145% in fuel consumption and reducing emissions significantly over a period of five years.

On the other hand, the authors of [140] discuss an optimization procedure for the design and energy management of Hybrid Energy Storage Systems (HESS) used in full electric boats. The method is based on solving a calculus of variations problem using the Ritz Method, aiming to optimize the battery and super-capacitor sizes and manage their energy use efficiently. In [141], an analytical modeling method for designing and sizing Battery Energy Storage Systems in hybrid marine vessels was done. The study introduces models to evaluate the performance of BESS, including fuel savings, projected lifetime, and cost-benefit analysis, for a hybrid marine power system with diesel generators. Through different parameters, the study identifies the optimal BESS size to maximize fuel savings and minimize costs, focusing on two operational strategies: Strategic Loading and Spinning Reserve. The results demonstrate that considerable fuel savings can be obtained by a moderate-sized BESS with an energy capacity of around 2 MWh and a rated power of 2-3 MW, combined with optimized energy management strategies, achieving a positive cost-benefit ratio.

In this thesis research, a numerical modeling will be performed, focusing on sizing the battery system based on functionalities and operational requirements.

2.4.4. Battery Modeling Techniques

In the domain of battery model research, it is important to develop a battery model that accurately de-scribes the battery's external characteristics. The internal chemical reactions that batteries go through are complicated and non linear. However, polarization of a battery results from variations in the currents used for charging and discharging, leading to a nonlinear change in terminal voltage rather than merely resistive characteristics. This polarization causes an increase in the resistance that the charging and discharging currents experience as they pass through the battery [142].

Batteries experience aging-related problems over a long period of time, such as a decrease in ca-pacity and an increase in internal resistance. These elements play an essential role in the significant discrepancies between power batteries' stated and actual states of charge. Moreover, variations exist among individual cells within batteries, resulting in major attenuation of power performance from the cell level to the battery module and eventually to the battery pack. These complexities pose challenges

in constructing an accurate battery model that comprehensively includes all battery performance aspects. Therefore, current efforts are mainly focused on employing different methods to fully simulate the dynamic behaviour of the battery. Four different battery modeling technique can be summarized in Table 2.10 below, where the advantages and disadvantages are described.

Table 2.10: Comparative Analysis of Battery Modeling Methods

Model	Advantages	Disadvantages	Ref.
Data-Driven	Model-free, eliminates the need for challenging modeling processes, and enables rapid internal state evaluation.	Considerable sample size dependence and a slower rate of convergence.	[143]
Empirical/Semi-Empirical	Provides clarity and intuitive insights, forecasts aging using curve-fitting.	May oversimplify complex behavior and is limited to specific operational conditions.	[144]
Equivalent Circuit	Uses less complex components, simple structure, easily accessible parameters.	Not as accurate as electrochemical models in terms of estimation.	[143] [144]
Electrochemical	High estimation accuracy in describing internal chemical reactions.	Requires extensive computational work, long processing times.	[145]

A summary of some studies for battery modeling methods is shown in Table 2.11 below.

Battery Type	Battery Modeling	Ref.
LFP	Semi-empirical, amended equivalent circuit model	[115]
Li-ion	Empirical model	[121]
NMC	Equivalent circuit model	[146]
Li-ion	Data-driven	[147]
Li-ion	Electrochemical model	[148]
NCA	Electrochemical model	[149]

Table 2.11: An overview of battery modeling techniques
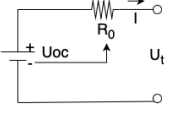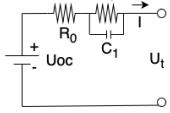
In this project, we will prioritize the use of the Equivalent Circuit Model, as it offers a balance between computational efficiency and model complexity, making it particularly suitable for real-time applications such as battery management systems in electric vehicles.

Equivalent Circuit Model

One of the battery modeling methods that are available in the literature, is the Equivalent Circuit Model, which is one of the most widely used battery modeling methods due to its simplicity, rapid execution time, and accurate open-circuit voltage (OCV) and SoC estimation under dynamic load and current conditions [150]. An in-depth knowledge of the battery's electrochemistry is not necessary to utilize the ECM,

but this model is still capable of offering insightful information about battery dynamics. It reflects the electrical characteristics of the battery by employing capacitors, resistors, current, and voltage sources.

Two popular equivalent circuit models are illustrated in Figure 2.7 with their expressions.

Model	Expression
Rint model	$U_t = U_{oc} - I \cdot R_0$ U_t is the terminal voltage, U_{oc} indicates the OCV. I is the discharging current and R_o is the Ohm resistance.
Thevenin model	$U_t = U_{oc} - U_1 - I \cdot R_0$ R_1 is the polarization resistance and C_1 is the polarization capacitance, U_1 is the voltage of the RC network.

Figure 2.7: The two common ECMs' expressions
[145]

The Rint model integrates a perfect voltage source U_{oc} in addition to the battery's DC internal resistance R_0 organized in series. Both parameters change with the SoC and temperature [145]. The equivalent circuit battery model, commonly referred to as the Thevenin model is shown in Figure 2.7. It consists of a series resistance R_0 to simulate the ohmic loss caused by the electrolyte and connection resistances. The $R_1 C_1$ parallel circuit models the charge transfer phenomenon within the cell and V_{oc} is the OCV across the cell which is a function of SoC. Article [151] presents an approach for the extraction of these battery parameters from the discharge experiments. This method uses system identification theory to derive each RC circuit in the Thevenin based ECM as a first order linear time invariant system. The test experiment was conducted using an LFP battery chemistry. The process shows a high degree of agreement between the experimental and simulated voltage [152].

In this thesis research, the Rint model will be utilized to model the battery dynamic behaviour. This is due to its simplicity in modeling battery characteristics. The model, includes a resistor and an ideal voltage source, providing a straightforward yet accurate representation of the battery's internal resistance and voltage dynamics. Its computational efficiency makes it ideal for real-time applications and control systems in hybrid vessels, where predicting battery performance quickly and accurately is essential to maximizing energy management and guaranteeing operational effectiveness. By using the Rint model, we can achieve a balanced trade-off between model accuracy and computational load, enabling efficient integration into the hybrid vessel's energy system.

2.5. Existing Methodologies for Battery Selection

This Section will cover the state-of-the-art methodologies related to battery technology selection, focusing on the assessment of different battery characteristics.

One of the most popular methods for choosing a battery for a hybrid vessel is the multi-criteria decision making, which evaluates various battery characteristics in relation to the operational needs of the particular ship. In [153], NMC battery was chosen based on the approach that prioritize energy density, efficiency, cycle life, and the operational requirements of the vessel, specifically the hybrid cruise vessel. This technique is likely to take into account the technical demands, environmental implications, and the economic viability of applying these battery systems on board of the ship, complying with the focus on optimizing the vessel performance and minimizing the environmental impact.

Another multi-criteria decision making method is the TOPSIS technique (Technique for Order of Preference by Similarity to Ideal Solution), which aim at determining the best option from a range of choices

based on the degree of closeness to the ideal solution. The method operates on the principle of choosing the solution that is the closest to the positive ideal solution (PIS) and furthest from the negative ideal solution (NIS). While the NIS achieves the opposite goal, the PIS is a theoretical solution that maximizes the benefit criteria and minimizes the cost criteria. This approach is examined in [154] and [155].

The author of [156], examined the battery selection criteria in full electric ships. The selection requirements encompass operational performance, safety, costs, and dimensions. Parameters such as power, capacity, longevity, safety, costs, and dimensions play crucial roles in this process. Capacity, depend on energy storage within electrodes and electrolyte structure, determine a battery's maximum usable energy. Power, which measures the charging and discharging abilities, necessitate an accurate balance between electrode thickness and chemistry for optimal functionality. Longevity, shaped by calendar and cycle life, heavily depends on electrode chemistry. Costs are primarily related to the electrode materials, terminals, and production of battery containers. All battery components are subject to safety considerations, with a focus on electrode and electrolyte chemistry. Finally, weight and dimensions are closely related to power and energy densities, and are significantly influenced by the design of the battery container and electrode chemistry.

The Analytic Hierarchy Process (AHP) and the Analytic Network Process (ANP) are two different selection criteria methods that can be applied across various fields. These can be used to choose batteries as well. In [157], the selection criteria for batteries focused on operational efficiency, energy density, recharge cycles, and cost effectiveness in order to support loading compensation for diesel engines and provide power during port operations. These criteria were used to compare the performance of two battery types: lithium-ion and ZEBRA ($NaNiCl_2$). The latter were selected due to their cost-effectiveness despite their greater volume and mass. This choice underscores the prioritization of the operational cost reductions and the suitability of the ZEBRA battery for the specific requirements and port stays of the platform supply vessels. For an in-depth description of how these techniques operate, see [158].

[159] presents a thorough analysis to select the optimal battery systems for maritime applications, focusing on all-electric vessels. Both life cycle assessment (LCA) and life cycle cost assessment (LCCA) are applied in this selection process to evaluate possible battery technologies from an environmental and economic point of view. This study specifically contrasts lead-acid, nickel-metal hydride (Ni-MH), and lithium-ion (Li-ion) batteries while taking lifecycle, cost, efficiency, and energy density into account. The goal is the find a battery that satisfies the ro-ro passenger ships from the Croatian short-sea navigation power and operational requirements while also supporting the reduction of emissions and the operational expenses. The technique emphasizes how important it is to conduct a comprehensive analysis that takes into account the battery system's whole lifecycle, from manufacturing to disposal, in order to choose the most economical and environmentally friendly option for maritime applications. Research on battery selection process in hybrid vessels is limited. Important considerations need to be taken into account when analyzing the battery selection type. These criteria include the energy density, cycle life, safety, cost, and operational performance.

<div style="text-align: right; font-size: 4em;">3</div>

Case Study: Trailing Suction Hopper Dredger Vessel

In this chapter, an analysis of the Trailing Suction Hopper Dredger Vessel is performed. Section 3.1 will provide an examination of the load profile and the operating expenses (OPEX).

3.1. Current System

A simplified representation of the vessel's electrical power plant is illustrated in Figure 3.1. The system comprises three synchronous diesel generators, each with a rated power of 7,200 kW. The vessel is equipped with multiple switchboards operating at different voltages. The primary consumers, including the propulsion motors and dredging pumps, are depicted in the single line diagram below.
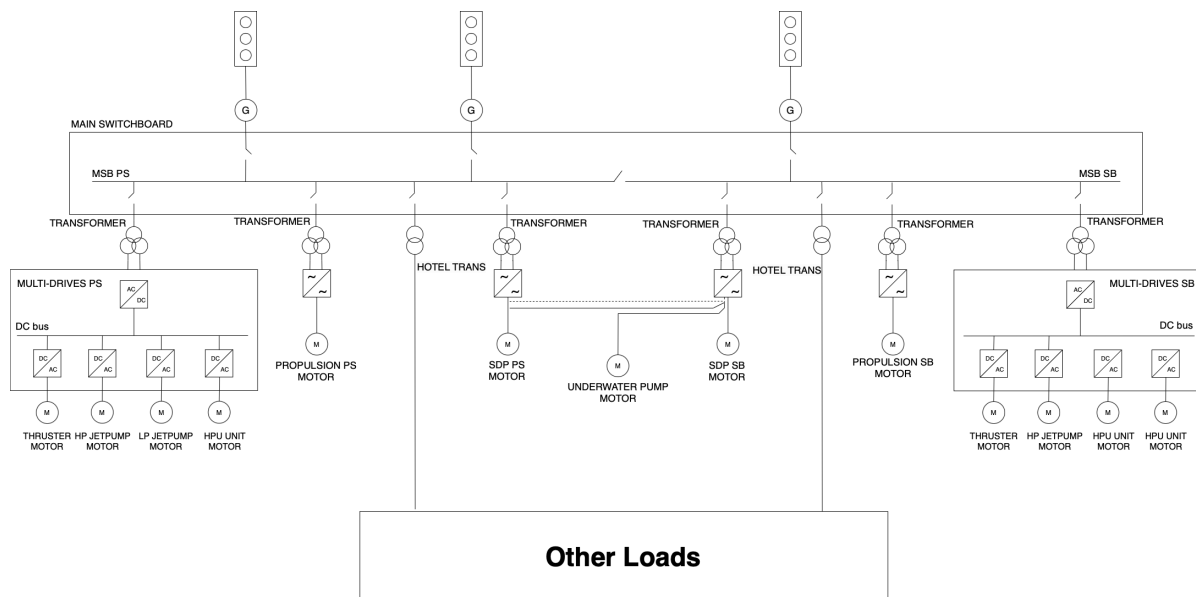
Figure 3.1: Single line diagram of the current system

3.1.1. Load Profile Analysis

For the efficient use of technology like energy management systems, and power production systems, reliable data of a vessel's load power profile is essential. The load power profile is largely influenced by the powerplant system, which can change greatly based on operational needs. Due to this, it is

difficult to forecast the load power profile for a given vessel. Therefore, it is critical to constantly track and gather data on a vessel's power usage. In order to gain a deeper understanding of the vessel's requirements, this part focuses on doing an event analysis of the load profile.

This Section details the analysis of the load profile for the trailing suction hopper dredger vessel across three distinct data scenarios. The data were collected with a sampling interval of three seconds. Figure 3.2 illustrates the power demand profiles as a percentage of time across the three operational scenarios: 12 consecutive days of normal dredging, 11 consecutive days of irregular dredging cycles, and 3 consecutive days of harbour operations. The power demand is categorized into three ranges: 0-7200 kW, 7200-14400 kW, and 14400-21600 kW.
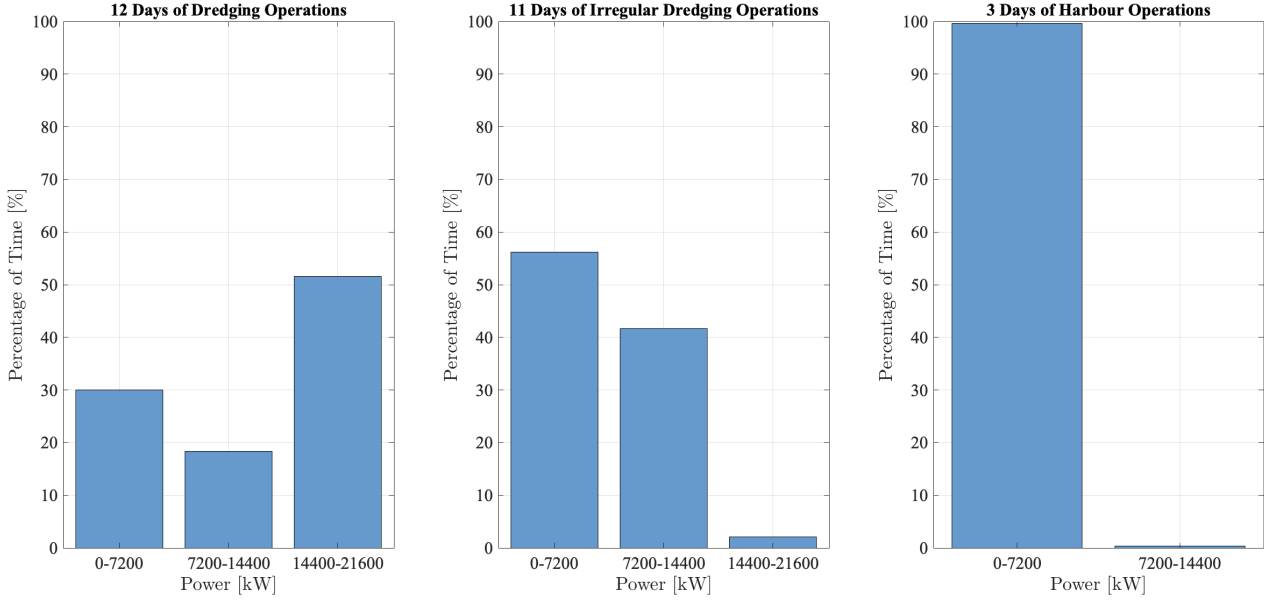
Figure 3.2: Comparison of frequency of power demand levels over different operational scenarios

Based on the distribution, it is evident that during dredging operations, the power demand typically requires all three generators to be operational. However, when the vessel is in the harbour, the power demand significantly decreases, allowing for operation primarily with just one generator, with occasional use of a second generator. Therefore, our approach will aim to explore the possibility of reducing the running time of the third generator while also decreasing the vessel's fuel consumption.

3.1.2. OPEX calculation

In this Section, the operational expenses are calculated, encompassing the fuel consumption and the maintenance costs as they offer an overview of the expenses incurred in operating the system in question.

Fuel Consumption

The total fuel consumption of each of the data was calculated based on the power supply of each generator at each time step. The Equations are as follow:

$$\text{Energy}(t) = \text{P}_{\text{Supply}}(t) \cdot \Delta t \tag{3.1}$$

Percentage of rated power for each generator at time Δt:

$$\text{\% of Rated Power}(t) = \left(\frac{\text{P}_{\text{Supply}}(t)}{\text{Rated Power of each generator}} \right) \cdot 100 \tag{3.2}$$

Based on the typical Specific Fuel Oil Consumption curve shown in Figure 3.3 for a diesel engine running on Marine Diesel Oil at steady state, and the percentage of rated power, the fuel consumption in g/kWh was calculated at each time step for each generator. This value is then multiplied by the energy at Δt to determine the fuel consumption in grams at each time step for each generator, converting it to tonnes. For engine loads below 25% of the rated power, the SFOC curve was extrapolated, and the author ensured that fuel consumption reaches zero at 0% of rated power.
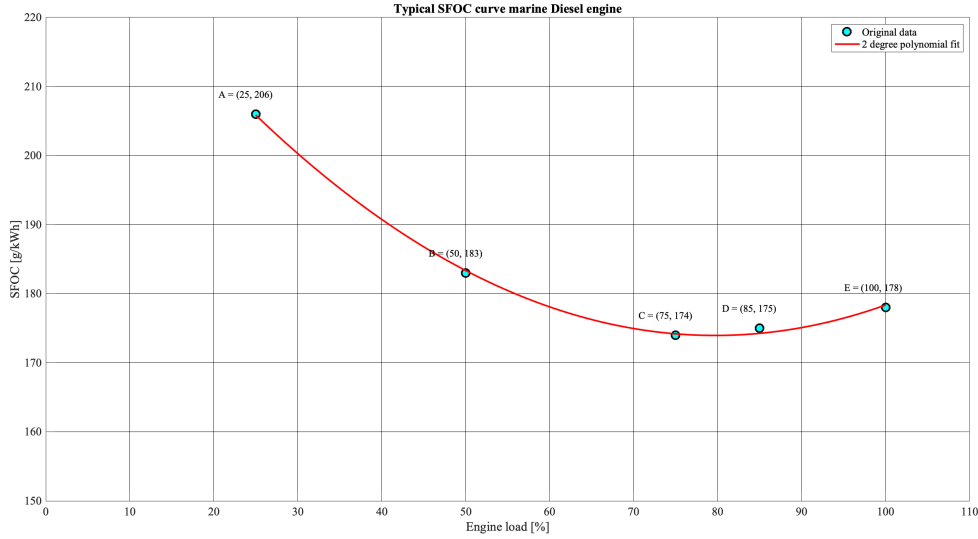
Figure 3.3: Specific Fuel Oil Consumption curve

The total fuel consumption in tonnes is calculated by:

$$\text{Total fuel consumption} = \frac{\sum \text{Total fuel consumption of each generator}}{10^6} \tag{3.3}$$

The fuel consumption was calculated to be 626.84 tonnes over 12 dredging days, 355.1 tonnes over 11 irregular dredging cycles, and 21.23 tonnes over 3 harbour days. These 26 days of data were analyzed and then extrapolated to estimate the vessel's behaviour over a full year, providing an estimate of the approximate yearly fuel based on different operational statuses. This was calculated to be equal to 14,083 tonnes/year. Where:

- Energy in kWh,
- P_{Supply} is the power supply of the generators in kW,
- Δt is the time step in hours,
- Fuel consumption in tonnes.

Maintenance Cost

The engine manufacturer's basic estimate indicates that the maintenance cost per running hour for a 7,200 kW engine is 40.4 euros. The operational time of the vessel in discussion is about 56% per year, while for 44% of the time, the vessel is considered in harbour operation. Maintenance costs (MC) can be calculated as follows:

$$\text{MC of each generator} = \left(\frac{\text{Percentage of Running Hours}}{100} \right) \cdot 24 \, \frac{\text{hours}}{\text{day}} \cdot \text{Number of Working Days} \cdot 40.4 \, \frac{\text{Euros}}{\text{hour}} \tag{3.4}$$

Summing up the maintenance costs of each generator, this amounted to 34,623 euros for 12 dredging days, 34,763 euros for 11 irregular dredging days, and 14,026 euros for 3 harbour days. Extrapolating the maintenance costs for 26 days results in an annual cost of €1,170,967.

<div align="right">

4

</div>

Numerical Modeling

Numerical modeling is a computational technique used to simulate and analyze real-world systems and events through mathematical models [160]. It represents an important tool for developing, designing, and evaluating the performance of hybrid marine power systems. By modeling the interactions between the battery, power sources, and energy management systems, this method has the potential to enhance efficiency, fuel savings, and emissions reduction, which could contribute to more sustainable and economical maritime operations. Section 4.1 introduces the auto start-stop logic, while Section 4.2 discusses the hybrid system and presents the two strategies employed in this thesis.

4.1. Optimal Operation of Current System

In practice, multiple generators supply power to meet demand at each time step, with a reduced frequency of switching ON and OFF. However, this distribution can lead to generators operating at low power levels, which is less fuel-efficient. To address this, an automatic start-stop logic has been implemented to optimise the number of running generators based on the power demand at any given time step. A simulation of the current scenario of each dataset was conducted using total power demand. The data was integrated into the automatic start-stop logic. The model is designed to optimise the number of running generators for the existing system, without accounting for the use of batteries. The system's logic is illustrated in Figure 4.1.
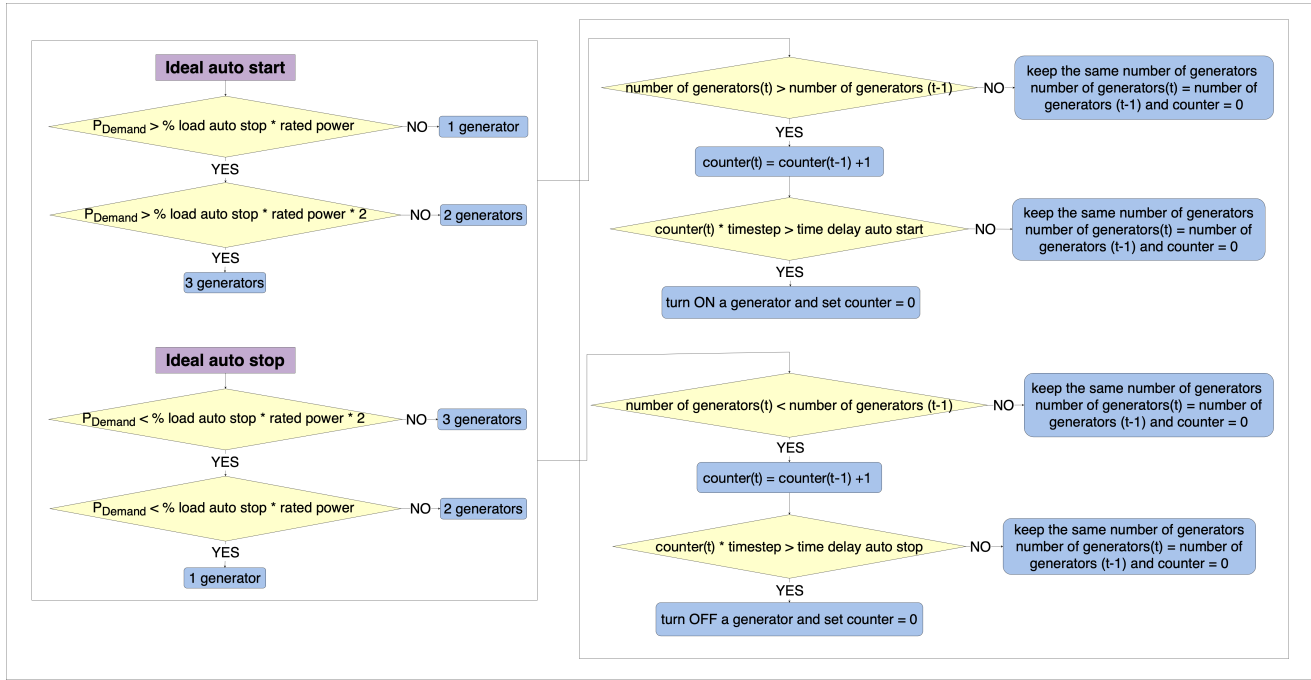
Figure 4.1: Automatic Start-Stop Logic for Generators

Depending on the load, the Power Management System will activate or deactivate a generator. This operation is influenced by four key factors: time delay auto start, time delay auto stop, percentage load auto start, and percentage load auto stop. To optimize this process, three distinct ranges for the percentage load auto start and auto stop were considered: [0.9 - 0.6], [0.8 - 0.5], and [0.6 - 0.3]. These ranges are crucial in defining the specific conditions under which varying numbers of generators are needed, as illustrated on the left side of Figure 4.1.

The selection of these specific percentage ranges was made to balance the system's responsiveness with the need to avoid unnecessary generator usage. For instance, a higher auto stop load percentage, such as 0.6, ensures the generator turns off sooner when the load decreases, thereby reducing unnecessary operation. Conversely, a higher auto start load percentage, like 0.9, delays the generator's activation until the load reaches a higher level, thereby preventing premature startups.

To further enhance efficiency, a time delay mechanism is implemented to minimize the frequency of switching between different numbers of generators. Three time delays—60, 120, and 300 seconds—were tested. Since a typical generator requires approximately 2 minutes to turn ON or OFF, shorter and longer duration were also examined to observe any differences in performance. During each time step, the system monitors changes in the number of active generators compared to the previous step. If an increase or decrease in the number of generators is detected, a counter is incremented, contributing to a decision on whether to maintain the current configuration or adjust the number of active generators.

$$\text{counter}(t) = \text{counter}(t-1) + 1 \tag{4.1}$$

If, for a specific duration, the counter exceeds the time delay based on the following Equation:

$$\text{counter}(t) \cdot \Delta t > \text{time delay} \tag{4.2}$$

then the number of generators will increase or decrease by one. This strategy helps determine the optimal number of running generators at each time step.

A ramping rate of 4% is considered, which represent a basic figure for starting a generator from 0 to full load in 25 seconds.

$$\text{Ramping up rate} = 0.04 \cdot 7200 \cdot \Delta t \tag{4.3}$$

To have a decent behaviour when turning off the generators, the ramping down rate is limited to three times the ramping up rate.

$$\text{Ramping down rate} = 3 \cdot 0.04 \cdot 7200 \cdot \Delta t \tag{4.4}$$

The following Equations provide a summary of the ramping rate process:

$$\frac{P_{\text{Demand}}(t)}{\text{number of generators}(t)} = \text{ideal } P_{\text{Gen i}}(t) \tag{4.5}$$

$$P_{\text{Gen i}}(t) = \begin{cases} \min\left(P_{\text{Gen i}}(t-1) + \text{ramping up rate}, \text{ideal } P_{\text{Gen i}}(t), 7200\right), & \text{if ideal } P_{\text{Gen i}}(t) > P_{\text{Gen i}}(t-1) \\ \max\left(P_{\text{Gen i}}(t-1) - \text{ramping down rate}, \text{ideal } P_{\text{Gen i}}(t), 0\right), & \text{if ideal } P_{\text{Gen i}}(t) < P_{\text{Gen i}}(t-1) \end{cases} \tag{4.6}$$

Where:

- $P_{\text{Demand}(t)}$ is the power demand at each time step in kW,
- $P_{\text{Gen i}(t)}$ is the power of one generator at each time step in kW.

In this model, the total power output is evenly distributed among the running generators at each time step.

4.2. Hybrid System

The owner of the vessel has requested an analysis to evaluate the installation of battery systems in order to increase the fuel efficiency and lower maintenance expenses while taking into account the investment cost that includes the battery cost. The main consumers of the vessel are the propulsion motors, and the dredging pumps.

Two suggested single-line diagrams are shown below with two distinct battery positions. In Figure 4.2, the BESS is connected to the AC bus bar by means of an inverter and a transformer.
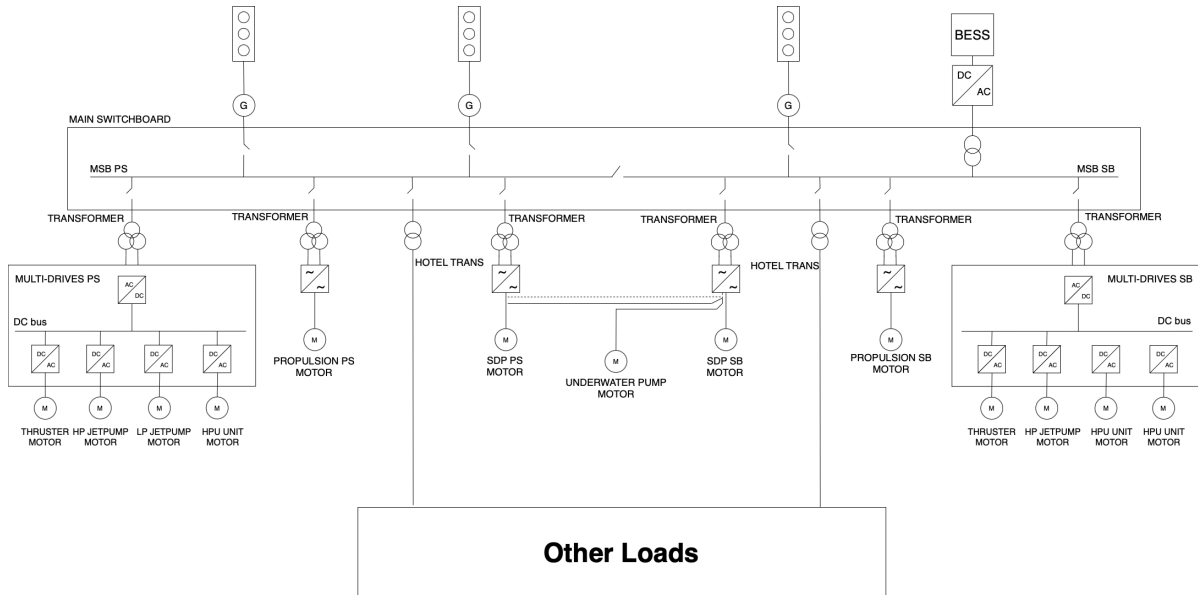
Figure 4.2: Single line diagram of the hybrid system - Generators side

Figure 4.3 illustrates the second battery position, where the BESS is connected to the vessel's multi-drive from both the Port Side and the Starboard Side. A DC-DC boost converter is used to connect the BESS to the DC bus. To provide bi-directional power exchange between AC and DC systems, the

AC/DC inverter needs to be upgraded to an active front end. It is assumed that the Active Front-End Converter has an efficiency of 0.98 [161] and the DC-DC converter an efficiency of 0.98 [162].
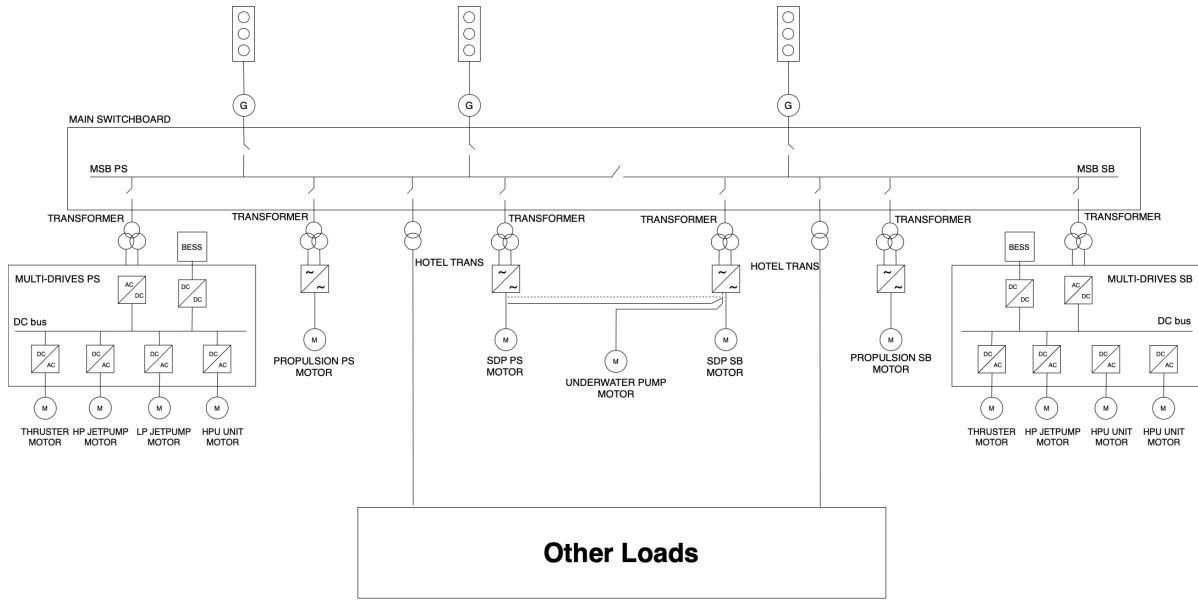
Figure 4.3: Single line diagram of the hybrid system - Multi drive side

As it has been mentioned, the main consumers of the vessels are the propulsion motors and the dredging pumps. For facilitating a power supply between the main consumers and the electrical system, the battery is connected on both sides of the multi-drive. The following table summarizes the efficiency assumptions for the components used in this analysis:

Table 4.1: Assumed efficiency of the transmission elements

Components	Efficiency
Active Front-End Converter	0.98 [161]
Converter	0.98 [162]
Transformer	0.99 [163]

To evaluate the cost-effectiveness of the battery integration aboard the vessel, the Return On Investment will be assessed offering a comprehensive analysis of the financial impact of the investment related to battery costs. It measures the overall profitability of the investment, comparing its financial effectiveness against other potential investments. The ROI is defined as the ratio of the net income to the initial investment. It is given by the Equation:

$$\text{ROI} = \frac{(\text{Yearly Savings} \times \text{Battery Lifetime}) - \text{Initial Investment}}{\text{Initial Investment}} \tag{4.7}$$

where:

$$\text{Yearly Savings} = \text{Fuel Savings} + \text{Maintenance Savings} \tag{4.8}$$

$$\text{Battery Lifetime} = \frac{\text{Total Number of Cycles}}{\text{Yearly Cycles} + \text{Calendar Aging}} \tag{4.9}$$

As outlined in Section 2.3, the batteries onboard a vessel perform multiple critical functions. This thesis focuses on two primary objectives: reducing the reliance on the third generator and lowering overall fuel consumption. To achieve these goals, the automatic start-stop logic was incorporated

within two specific battery functions: load smoothing using moving average, and optimal range of the generators. The selection of these functions is based on their complementary benefits. Load smoothing helps to balance and average the load, thereby enabling the generators to operate more steadily and efficiently. This reduces the strain on the generators, leading to smoother operation and improved fuel efficiency. Conversely, the optimal range method, which keeps the generators operating within their optimal range, ensures they operate closer to their rated power, thereby maximizing efficiency and minimizing fuel consumption. The following Section details the common system parameters and Equations used in the numerical modeling for both methodologies.

System Parameters	Units
Power rated	[kW]
C-rate	$[h^{-1}]$
SoC_{min}	[-]
SoC_{max}	[-]
converter efficiency	[%]
Active Front-End Converter efficiency	[%]
transformer efficiency	[%]

Table 4.2: System Parameters

To calculate the maximum energy capacity of the battery, the following Equation is used:

$$E_{capacity} = \frac{P_{rated}}{C\text{-rate}} \tag{4.10}$$

The initial usable energy of the battery is calculated from the total capacity and the initial state of charge of the battery:

$$\text{usable energy}(t = 0) = E_{capacity} \cdot SoC_0 \tag{4.11}$$

The power demand is represented by the combined output of the generators and the battery:

$$P_{Demand} = P_{Generators} + P_{Battery} \tag{4.12}$$

When the battery needs to be charged, conversion losses will occur, these are represented by:

$$P_{Battery,\,charging} = (P_{Demand} - P_{Generators}) \cdot (\eta_{transformer} \cdot \eta_{rectifier} \cdot \eta_{converter}) \tag{4.13}$$

Similarly, when the battery needs to discharge, conversion losses are represented by:

$$P_{Battery,\,discharging} = \frac{(P_{Demand} - P_{Generators})}{\eta_{inverter}} \tag{4.14}$$

The energy supplied by the battery at each time step is calculated by multiplying the battery's power supplied at that time step by the duration of the time step in hours:

$$E_{Supplied}(t) = P_{Supplied}(t) \cdot \Delta t \tag{4.15}$$

At each time step, the battery will have a new usable energy amount, calculated based on the previous usable energy and the new energy change. The relationship is given by the Equation:

$$\text{usable energy}(t) = \text{usable energy}(t - 1) - E_{battery}(t) \tag{4.16}$$

The state of charge of the battery, following charging or discharging, will correspond to the usable energy relative to the battery's maximum capacity, as determined by the following Equation:

$$\text{SoC}(t) = \left(\frac{\text{usable energy}(t)}{E_{\text{capacity}}} \right) \cdot 100 \tag{4.17}$$

It is crucial to ensure that the battery energy remains within a safe and efficient range. This can be expressed by:

$$E_{\text{capacity}} \cdot \text{SoC}_{\text{min}} \leq E_{\text{battery}}(t) \leq E_{\text{capacity}} \cdot \text{SoC}_{\text{max}} \tag{4.18}$$

Where:

- E_{capacity} is the maximum energy capacity in kWh,
- $P_{\text{maximum battery}}$ is the maximum power of the battery in kW,
- SoC_0 is the initial state of charge of the battery before usage,
- SoC_{min} is the minimum allowable state of charge limit,
- SoC_{max} is the maximum allowable state of charge limit.

In this study, the battery's initial state of charge was assumed to be 50%. According to [45], a specific C-rate for each battery chemistry was used, as each chemistry can withstand a different C-rate. The latter is the rate at which the battery can be charged or discharged relative to its capacity. For example, a 1C rate means the battery can be fully charged or discharged in one hour. A 0.5C rate means it takes two hours to charge or discharge the battery, while a 2C rate means it takes 30 minutes to charge or discharge the battery. To achieve the objective of reducing the operational time of generator 3, four different battery sizes were analyzed. These sizes were selected based on 25%, 50%, 100%, and 2*(rated power), of the rated power of generator 3, corresponding to 1800 kW, 3600 kW, 7200 kW, and 14,400 kW, respectively. A state of charge range of 20% to 80% was tested as this enhances battery longevity and performance [164]. The automatic start/stop logic is implemented as an initialization step in both strategies to determine the number of running generators at each time step. This evaluation considered three ranges of percentage load auto-start and auto-stop thresholds, along with the three time delays discussed in Section 4.1. Table 4.3 shows the different parameters values that were considered in this thesis study.

Parameter	Unit	Values Assumed
Power rated	[kW]	1800, 3600, 7200, 14400
C-rate	$[h^{-1}]$	NMC: 2.8C LFP: 0.7C LTO: 4.34C
SoC range	[-]	[0.2-0.8]
Percentage load start/stop ranges	[%]	[0.9-0.6], [0.8-0.5], [0.6-0.3]
Delay	[s]	60, 120, 300

Table 4.3: Values Assumed for Testing Combinations

4.2.1. Load Smoothing

This Section will discuss the load smoothing function for power distribution in hybrid vessel using the moving average.

As previously mentioned, the automatic start-stop logic is implemented as an initialization of the system, to determine the number of running generators at each time step. Moving average, is a control strategy that is derived from the power demand data, specific to the vessel in study. This control determines the running generator's power levels during ramp-up and ramp-down periods. The power supplied by the generators is evenly split among the running generators. The difference between the original power demand and the total generator's power, as set by the control, determines the battery power.

The moving average control was assessed using three different time windows: 1, 2, and 5 minutes. As the time window increases, the load is smoothed more effectively, reducing the frequency of sharp fluctuations and leading to a more stable operation of the system. This smoothing helps in minimizing the wear and tear on equipment, enhances efficiency by reducing the need for frequent adjustments, and can ultimately lead to lower operational costs and improved fuel efficiency. The generators operate according to control systems with specified ramping rate values. While diesel engines can accommodate a range of ramping rates, future developments are shifting towards ammonia-based systems as the primary power source, which are limited to handling only small ramping rates. In this analysis, ramping rates of 0.5% and 5% will be tested to represent both low and high ramping scenarios. These ramping rates are measured per second, while in our case scenario, data is recorded with a sampling rate of three seconds. The ramping rate calculation is as follows:

$$\text{Ramping limit} = \text{rated power} \times \text{number of running generators} \times \text{ramping rate} \times \text{sampling frequency} \tag{4.19}$$

Total generators power is determined based on the Equations below:

$$\text{P}_{\text{Generators}}(t) = \begin{cases} \text{P}_{\text{Demand}}(t) & \text{if } \text{P}_{\text{Demand}}(t) = \text{P}_{\text{Generators}}(t-1) \\ \min(\text{P}_{\text{Generators}}(t-1) + \text{ramping limit}, \text{P}_{\text{Demand}}(t)) & \text{if } \text{P}_{\text{Demand}}(t) > \text{P}_{\text{Generators}}(t-1) \\ \max(\text{P}_{\text{Generators}}(t-1) - \text{ramping limit}, \text{P}_{\text{Demand}}(t)) & \text{if } \text{P}_{\text{Demand}}(t) < \text{P}_{\text{Generators}}(t-1) \end{cases} \tag{4.20}$$

Battery power contribution is calculated as follows:

$$\text{P}_{\text{Battery}}(t) = \text{P}_{\text{Demand}}(t) - \text{P}_{\text{Generators}}(t) \tag{4.21}$$

Depending on the state of charge of the battery at every time step, the system operates in different ways. Figure 4.4 summarises the control logic of the system when the SoC of the battery is within limits, this state is defined as state 1. Based on the power of the generator and the power demand at each time step, the battery charges and discharges, carefully managing the amount of power that is received and provided to its maximum capacity. When this limit is exceeded, the battery charges or discharges at its maximum, and the generators compensate for the demand while not adhering to the load smoothing function.
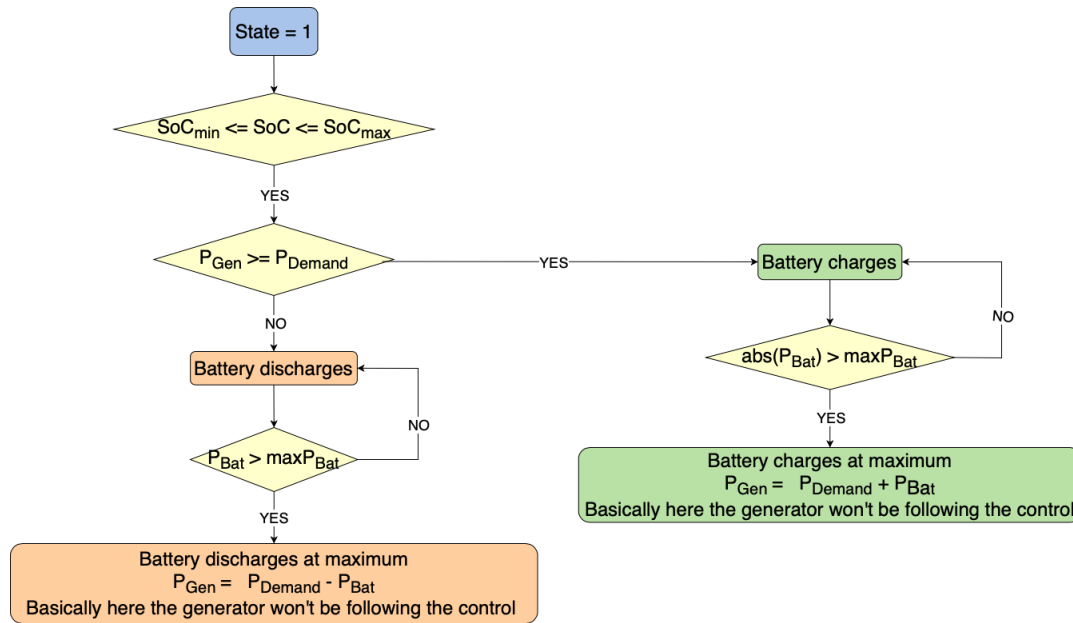
Figure 4.4: Load Smoothing Control Logic State 1

Where in the flowchart:

- P_{Gen} is the total power of the generators in kW,
- P_{Bat} is the power of the battery in kW,
- $maxP_{Bat}$ is the maximum power of the battery in kW,
- SoC_{min} is the minimum allowable state of charge limit,
- SoC_{max} is the maximum allowable state of charge limit.

To ensure the battery maintains sufficient energy at all times, an SoC regulation mechanism has been integrated into the model. The SoC target is set at 0.5, representing the battery's initial state of charge. This target is designed to keep the SoC around 50% consistently. A 10% tolerance has been set, allowing for minor fluctuations around the 50% target, enabling the battery to charge and discharge within this range. If the SoC deviates from the target +/- the tolerance, the regulation system adjusts to steer the SoC back towards 50%, ensuring adequate energy is available for charging and discharging as needed.
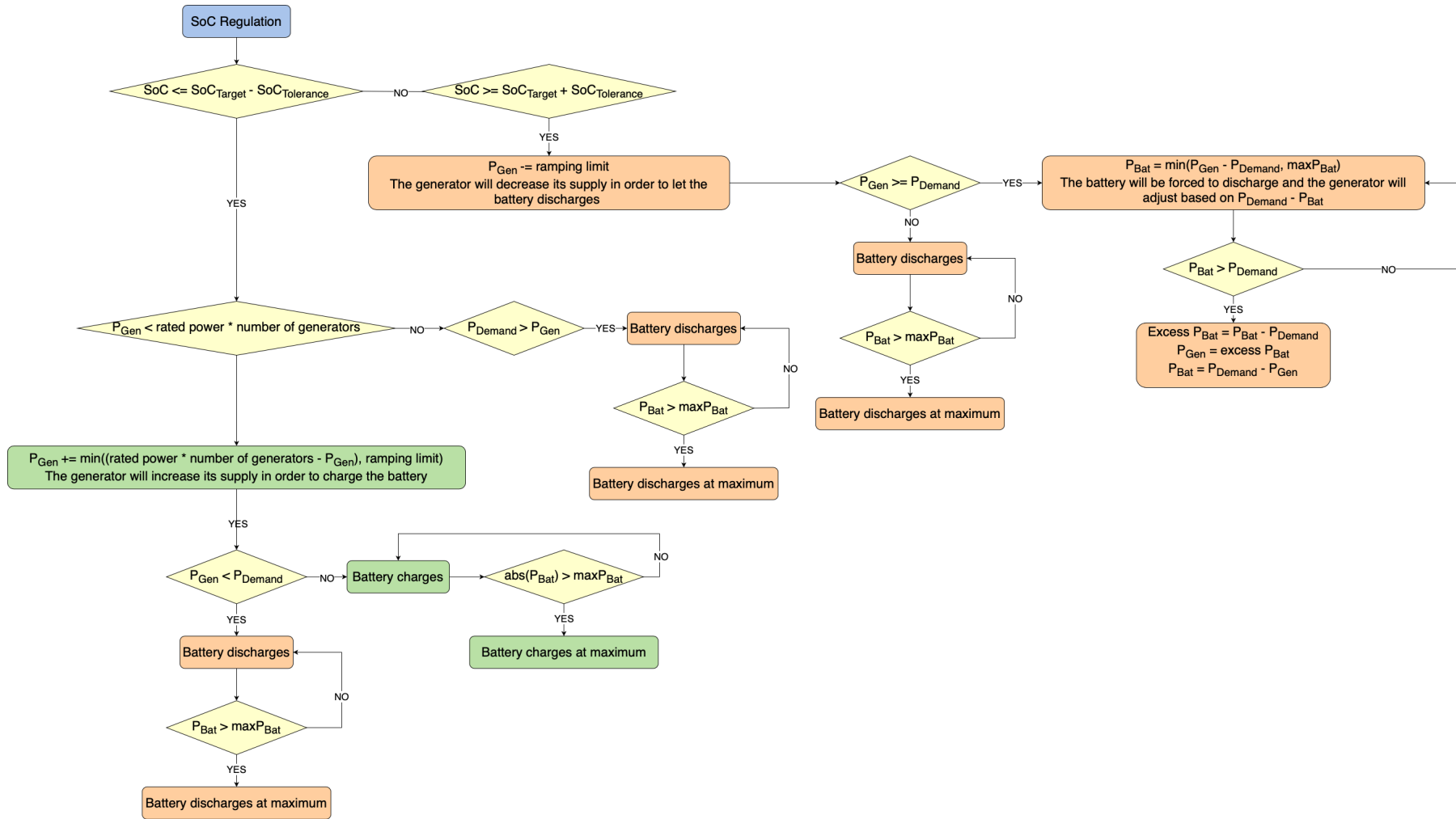
Figure 4.5: State of Charge Regulation

4.2.2. Optimal Range of the Generators

In the optimal range of the generators function, the auto start-stop logic is initially integrated into the system, determining the number of running generators at every time step. The purpose of this function is to let the generators operate within optimal range, where this range is defined as the range where for higher percentage of rated power, smaller fuel consumption can be achieved as per Figure 3.3. Typically, the optimal range for engine performance in such plots is where the SFOC is at its minimum, indicating the most efficient fuel consumption. The SFOC is at its minimum between points C (75%, 174 g/kWh) and D (85%, 175 g/kWh). To have a broader picture of the effect of wider ranges, two optimal ranges are tested, [60%-95%], and [70%-90%].

In Figure 4.6 below, the state of charge control logic is illustrated for the scenario where the SoC remains within acceptable limits. In this state, the battery charges and discharges in response to the load demand and the generator's power output. The battery cannot charge or discharge beyond its maximum capacity; when this limit is reached, the battery operates at its maximum capacity, and the generator(s) adjust their output to meet the remaining power demand. This operational mode is defined as State 1, where in the flowchart:

- The optimal lower bound is the minimum power that the number of generators, as determined by the start-stop logic, must supply to operate optimally.,
- The optimal upper bound is the maximum power that the number of generators, as determined by the start-stop logic, must supply to operate optimally,
- $SoC_{optimal}$ is The optimal state of charge is defined as the average of the minimum and maximum state of charge.
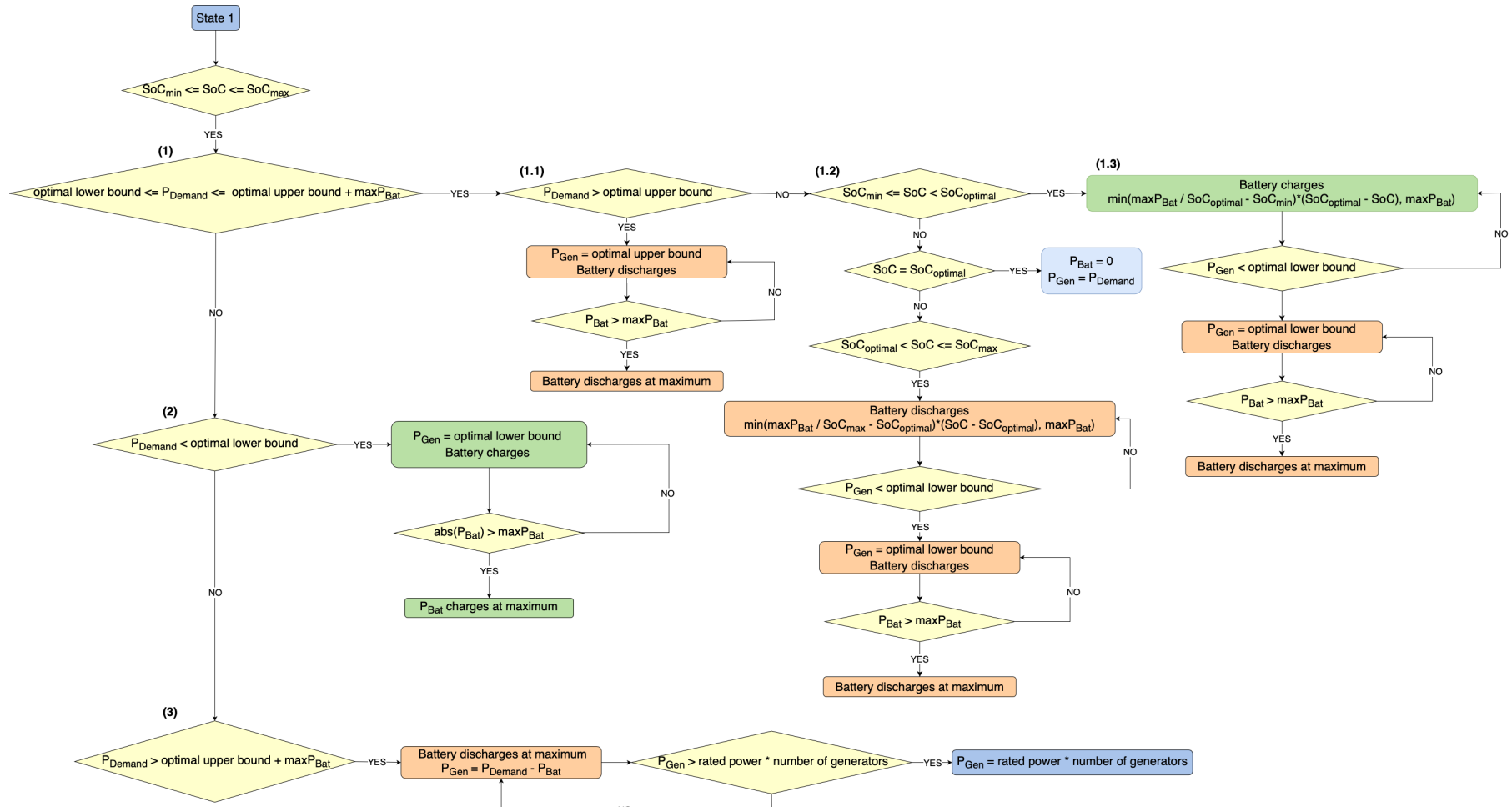
Figure 4.6: Optimal Loading Control Logic State 1

State 2 and State 3, defined as "force charging" and "force discharging" respectively, are illustrated in Figure 4.7. A defined threshold must be reached before transitioning back to State 1, where the SoC operates within its designated limits. In this analysis, the threshold is set at ±10% of the minimum or maximum SoC, depending on whether the battery is charging or discharging. This threshold was chosen to balance the time required for the battery to return to State 1 and to maintain an optimal SoC level.
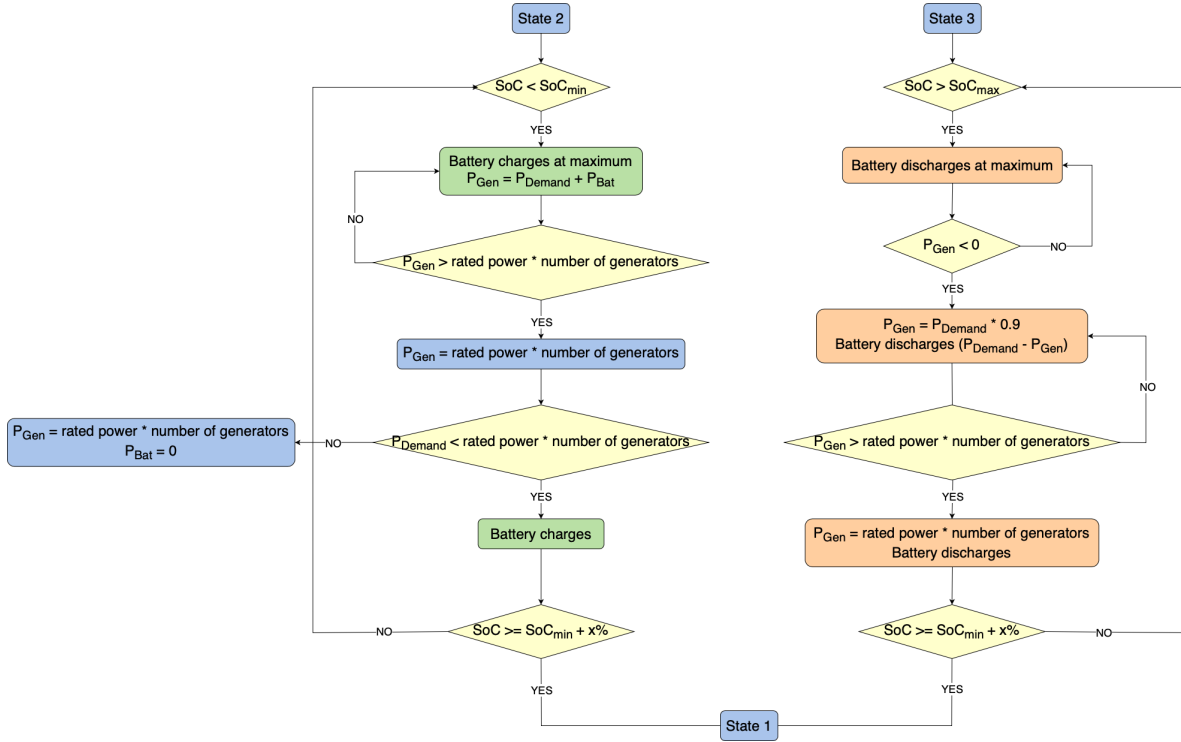
Figure 4.7: Optimal Loading Control Logic State 2 and State 3

4.2.3. Battery Modeling

The dynamic behaviour of the battery can be modeled using various techniques. One such approach is the Rint model, which represents the battery's dynamic behaviour with a simplified electrical circuit. This model includes the open-circuit voltage and accounts for internal resistance to calculate the terminal voltage and associated losses. This study employs the Rint model for battery modeling. The relevant Equations are summarized below:

The open circuit voltage is a function of state of charge represented by:

$$V_{OC,\,cell}(t) = f(SoC(t)) \tag{4.22}$$

To determine the terminal voltage across the battery, whether the battery is charging or discharging, this is calculated by:

$$V_{terminal,\,cell}(t) = \begin{cases} V_{OC,\,charging}(t) - I_{charging}(t) \cdot R_{charging} & \text{if } I_{charging} < 0 \\ V_{OC,\,discharging}(t) - I_{discharging}(t) \cdot R_{discharging} & \text{else} \end{cases} \tag{4.23}$$

where $I_{charging}$ is considered negative since the charging power of the battery is the negative power in this thesis. A battery voltage of 650V is assumed as an input for the boost converter that has an output of 1000V, with a tolerance of +/- 10% [161], determining the number of cells in series:

$$\text{Battery Voltage} \pm \text{tolerance} = V_{terminal} \times \text{number of cells in series} \tag{4.24}$$

The minimum terminal voltage is achieved based on the minimum state of charge limit of the battery:

$$V_{\text{terminal, minimum}} = V_{\text{OC, minimum}} - I_{\text{maximum, discharging}} \cdot R_{\text{discharging}} \quad \text{for SoC}_{\text{min}} \tag{4.25}$$

As such, the maximum terminal voltage is based on the maximum state of charge limit of the battery:

$$V_{\text{terminal, maximum}} = V_{\text{OC, maximum}} - I_{\text{maximum, charging}} \cdot R_{\text{charging}} \quad \text{for SoC}_{\text{max}} \tag{4.26}$$

The minimum and maximum number of cells in series are calculated based on the previous Equations, as the manufacturer's parameters were provided at the cell level, requiring an assessment at the battery level. It is important to use the minimum number of cells as a reference and ensure that it does not exceed the maximum allowable number of cells. This is necessary to stay within voltage limits.

$$\text{Minimum number of cells in series} = \frac{\text{Battery voltage} - \text{tolerance}}{V_{\text{terminal, minimum}}} \tag{4.27}$$

$$\text{Maximum number of cells in series} = \frac{\text{Battery voltage} + \text{tolerance}}{V_{\text{terminal, maximum}}} \tag{4.28}$$

The number of strings in parallel is determined based on the maximum energy capacity of the battery and the cell capacity, with the number of cells in series, represented by:

$$\text{Number of strings in parallel} = \frac{E_{\text{capacity}}}{\text{Number of cells in series} \cdot E_{\text{capacity, cell}}} \tag{4.29}$$

The total number of cells is then computed by the following Equation:

$$\text{Total number of cells} = \text{Number of strings in parallel} \times \text{Number of cells in series} \tag{4.30}$$

The power of the cell at each time step is represented by the power of the battery at that time step over the total number of cells as can be seen below:

$$P_{\text{cell}}(t) = \frac{P_{\text{Battery}}(t)}{\text{Total number of cells}} \tag{4.31}$$

To determine the current at each time step, the follwing formula is described:

$$P_{\text{cell}}(t) = I^2(t) \cdot R_{\text{internal}} + I(t) \cdot V_{\text{OC}}(t) \tag{4.32}$$

Finally, the new energy at every time step is calculated considering battery dynamic losses, where the new state of charge accounting for these losses is recalculated:

$$E(t) = E(t-1) - I(t) \cdot V_{\text{OC}}(t) \cdot \text{Total number of cells} \cdot \Delta t \tag{4.33}$$

$$\text{SoC}(t) = \frac{E(t)}{E_{\text{capacity}}} \tag{4.34}$$

- P is the power in kW,
- E is the energy in kWh,
- I is the current in A,
- V_{OC} is the open-circuit voltage in V,
- V_{terminal} is the terminal voltage in V,
- R is the internal resistance in Ω.

In [45], the open circuit voltage Equations and battery parameters are represented, where in this analysis, this parameters were used to calculate the dynamic behaviour of the battery. NMC, Leclanché Energy Storage Solutions [165], LFP Tesvolt Maritime Solutions [166], and LTO from Toshiba Rechargeable Battery [167], are the manufacturers from which each battery data is sourced. The relation between the open circuit voltage and the state of charge is defined by:

$$V_{\text{OC,cell}}^{\text{charging}} = c_{\text{cha},1} + c_{\text{cha},2} \cdot \text{SoC} + c_{\text{cha},3} \cdot \tanh\left(c_{\text{cha},4} \cdot (\text{SoC} + c_{\text{cha},5})\right) + c_{\text{cha},6} \cdot \exp\left(c_{\text{cha},7} \cdot \text{SoC}\right) \tag{4.35}$$

$$V_{OC,cell}^{discharging} = c_{dis,1} + c_{dis,2} \cdot SoC + c_{dis,3} \cdot \tanh\left(c_{dis,4} \cdot \left(SoC + c_{dis,5}\right)\right) + c_{dis,6} \cdot \exp\left(c_{dis,7} \cdot SoC\right) \quad (4.36)$$

The total number of cells for each chemistry, for every battery power determining the energy capacity, are summarized in Table 4.4.

Battery Chemistry	Battery Power (kW)			
	1800	3600	7200	14400
NMC	2640	5104	10208	20416
LFP	3534	7068	14136	28086
LTO	8092	15895	31501	63002

Table 4.4: Total number of cells

Aging Calculation

Battery lifetime is measured by the number of days it can operate effectively. As discussed in Section 2.4.2, cycle and calendar aging are the two mechanisms that reduce the battery's operational days. This thesis considers three datasets representing different operational scenarios for the vessel: dredging, irregular dredging, and harbour operations. According to the data provided by the company, the vessel is operational for 56% of the year, while for the remaining 44% it is either in transit or idle. It is assumed that during this 44% of the time, the vessel is engaged in harbour operations, where some work is still being performed. To compare the effects of operating a battery during harbour operations, two scenarios are considered:

1. The battery cycles 100% of the time throughout the year, leading to cycling degradation.
2. The battery cycles 56% of the time and remains idle for 44% of the time, resulting in 56% cycling degradation and 44% calendar degradation.

For simplicity, Case 1 assumes continuous battery operation over the course of a year, while Case 2 considers the battery undergoing calendar aging during harbour operations.

(a) **Cycle Aging:** The Rainflow counting algorithm is utilized to assess and analyze the cycle count,

fatigue, and degradation of the battery based on the State of Charge, in order to determine its lifetime. Full and half cycles are calculated determining the equivalent cycles, where the damage due to cycling is found determining the battery lifetime. As previously mentioned, the battery parameters were sourced from a study in literature [45], which was based on specific manufacturers' data. These manufacturers specified the maximum equivalent full cycles that each battery chemistry can perform, along with a defined end-of-life capacity summarized in Appendix A.2. The Equations used for the cycle aging calculation are outlined below:

Full and half cycles are calculated using the rainflow counting method. These cycles have different impacts on battery degradation depending on the depth of discharge range. However, because the manufacturer did not provide detailed information on the number of cycles associated with different DoD ranges, all half cycles are converted into full cycles. This approach allows for the summation of full cycles to determine the total equivalent cycles of the battery. The equivalent cycles that the battery is performing over the course of the number of days the data was recorded is calculated by:

$$\text{Equivalent Cycles} = \text{Full Cycles} + \frac{\text{Half Cycles}}{2} \quad (4.37)$$

The damage per cycle based on the number of days the data is measured is calculated by:

$$\text{Damage per cycle} = \frac{\text{Equivalent Cycles}}{\text{Maximum Equivalent Full Cycles}} \tag{4.38}$$

The Percentage Damage as per the manufacturer data, is calculated as follows:

$$\text{Percentage Damage} = 1 - \text{Defined end-of-life capacity} \tag{4.39}$$

The total damage based on the number of days the data is measured, is calculated by:

$$\text{Total Damage per number of days} = \text{Damage per cycle} \cdot \left(\frac{\text{Percentage Damage}}{100}\right) \tag{4.40}$$

To calculate the annual damage based on the damage incurred over the specific number of days under discussion, the following formula is used:

$$\text{Total Damage per year} = \frac{\text{Total Damage per number of days} \cdot 365 \cdot 56\%}{\text{Number of days}} \tag{4.41}$$

The total damage per year is then converted to percentage described as the percentage damage due to cycling, and the battery's lifetime is then determined using the following Equation:

$$\text{Battery Lifetime} = \frac{\text{Percentage Damage}(\%)}{\text{Percentage Damage per year due to cycling}(\%/\text{year})} \tag{4.42}$$

(b) Calendar Aging: Calendar aging evaluates the capacity fade as a function of temperature,

state-of-charge, and time when the battery is idle, meaning that no current passes through it. Depending upon the chemistry of the battery, the battery ages differently. The trailing suction hopper dredger vessel is assumed to be in harbour operation for 44% of the time, where in Case 2, the battery is considered idle, thus encountering calendar aging. In [105], an analysis on the calendar aging of different chemistries of lithium-ion batteries has been performed, where the fitting parameters for each chemistry are obtained. These parameters are shown in the Table below.

Fitting parameters					
Chemistry	a_1	a_2	b_1	b_2	c_1
NMC	0.03304	0.5036	385.3	-2708	0.51
LFP	0.00157	1.317	142300	-3492	0.48
LTO	0.6129	0.5274	2191	-3970	0.5988

Table 4.5: Fitting parameter values for NMC, LFP, and LTO chemistries [105]

To estimate the capacity loss during storage, [105] uses a semi-empirical model. The Equation is defined as follows:

$$\text{Capacity Degradation} = a_1 e^{a_2 \text{SoC}} \cdot b_1 e^{b_2/T} \cdot t^{c_1} \tag{4.43}$$

where a_1, a_2, b_1, b_2, and c_1 are the fitting parameters, SoC is the state of charge, T is the temperature in Kelvin, and t is the time in days. In this thesis study, it is assumed that the battery is kept at a temperature of 298.15 Kelvin, with a state of charge of 20%, and the battery is considered idle for 161 days per year.

For NMC, LFP, and LTO, the capacity degradation resulting from calendar aging can be computed to be 2.13%, 2.73%, and 5.15% per year, respectively. To determine the lifetime of the battery, the percentage of damage due to calendar aging is added to the percentage of damage due to cycle aging, as represented by the Equation below:

$$\text{Battery Lifetime} = \frac{\text{Percentage Damage}}{\text{\% Damage per year due to cycle aging} + \text{\% Damage per year due to calendar aging}}$$
$$(4.44)$$

Model Limitations

In this thesis analysis, some limitations have an impact on the accuracy of the results. The efficiencies assumed for components during charging and discharging, along with other key assumptions, may lead to varying results under different conditions. Additionally, the calendar aging parameters are derived from a different source than the Rint model parameters, potentially causing discrepancies in the results. In addition, to gain a complete overview of the financial impact of battery installation, it is important to consider the component and installation costs needed for the full investment, as these costs depend on the type of vessel in discussion.

<div style="text-align: right; font-size: 4em;">5</div>

Numerical Results

In Section 5.1, the results of the optimal operation of the current system without battery are discussed. Following this, Section 5.2 presents the various outcomes of the load smoothing function, summarizing the battery solutions in terms of fuel consumption, maintenance costs, and lifetime. Section 5.3 explores the optimal range of the generators' function solutions, highlighting the battery solutions with respect to fuel consumption, maintenance costs, and lifetime. Finally, Section 5.4, answers the research questions.

5.1. Optimal Operation of Current System Results

The different ranges of % load auto start and % load auto stop with the different time delays previously discussed in Section 4.1 have been tested. The percentage of each generator's operating time for the different parameters of auto start-stop logic, for each of the three different data scenarios are shown in Figure 5.1, 5.2, and 5.3. Each data scenario is compared to its normal operation.

Figure 5.1 illustrates the 12-day dredging operations. It is evident that in the current scenario, the three generators were utilized nearly 100% of the time. However, the implementation of the auto start-stop logic resulted in a reduction in the running time of generators 2 and 3, with the extent of the reduction varying across different configurations. When the percentage thresholds for load auto start and auto stop are increased for example from [0.8 - 0.5] to [0.9 - 0.6], the running time of generators 2 and 3 decreases. This is due to the quicker response required to turn off a generator as a bigger power demand is needed, and the longer load demand required to turn one on. For example, within the same load auto start-stop range, increasing the time delay causes the running time of the generators to increase, as it takes longer to turn them off. This effect is clearly observed in the scenarios with a [0.9 - 0.6], and [0.8-0.5] load range and time delays of 60s, 120s, and 300s. On the other hand, it is important to note the decrease in the running time of generator 2 in the [0.6-0.3] load range with a 120s time delay compared to a 60s delay. This reduction can be attributed to the interaction between the load auto start/stop thresholds and the time delay. Depending on the power demand, the cumulative running time of two generators might be sufficient, reducing the need to activate the third generator.

<div style="text-align: center;">56</div>
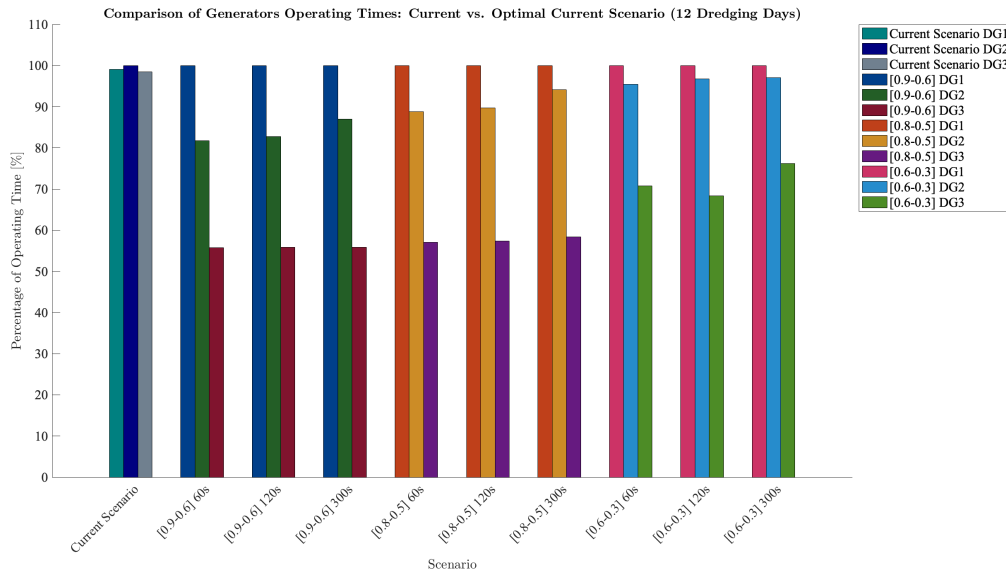
Figure 5.1: Comparison of Generator Operating Time Between Current and Optimal Scenarios for 12 Days of Dredging Operations

Figure 5.2 represents 11 irregular dredging cycles. In this scenario, the three generators are operating nearly 100% of the time. However, with the implementation of the auto start-stop logic, a significant reduction in the running time of the third generator is observed, particularly in the [0.9 - 0.6] and [0.8 - 0.5] load ranges. This indicates that, in the previous configuration, all three generators were running simultaneously, even when the power demand was often within the capacity of one to two generators as can be seen in Figure 3.2 . The increased running time of generator 3 in the [0.6 - 0.3] load range is attributed to the narrower power margin, requiring the activation of an additional generator more frequently.
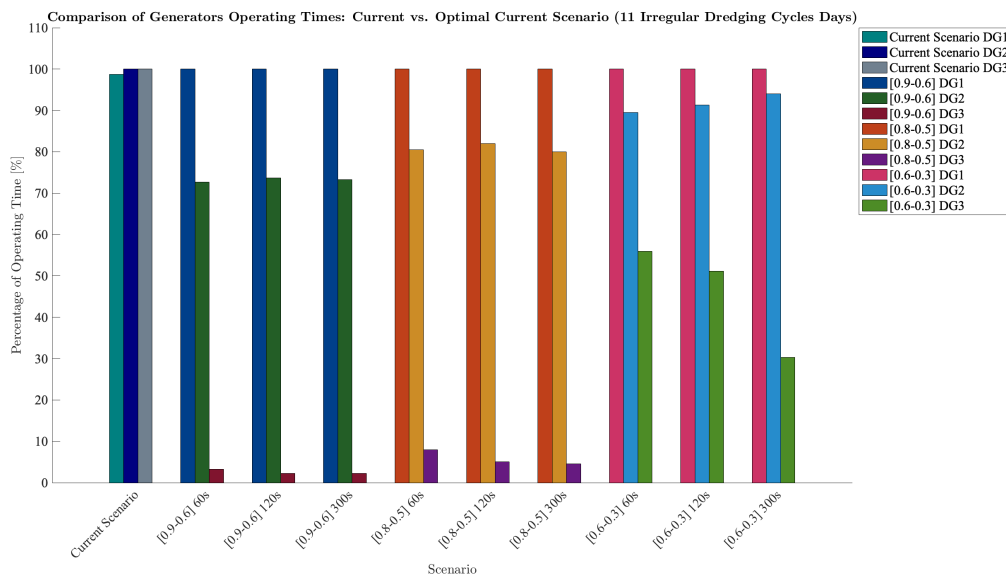
Figure 5.2: Comparison of Generator Operating Time Between Current and Optimal Scenarios for 11 Days of Irregular Dredging Operations

Figure 5.3 shows the operation over three harbour days. In the current scenario, it is evident that one generator was running most of the time. Specifically, generator 2 was active approximately 94% of the time, while generators 1 and 3 were in operation for about 19% and 7% of the time, respectively.

This can be explained by Figure 3.2, which shows that a frequent power demand below 7,200 kW was supplied as the vessel was in the harbour where dredging operations, which require higher power supply, were not taking place. With the implementation of the auto start-stop logic, the running time of one generator increased, leading to a decrease in the running time of the second generator, while the third generator was consistently turned off as the power demand never exceeded 14,400 kW.
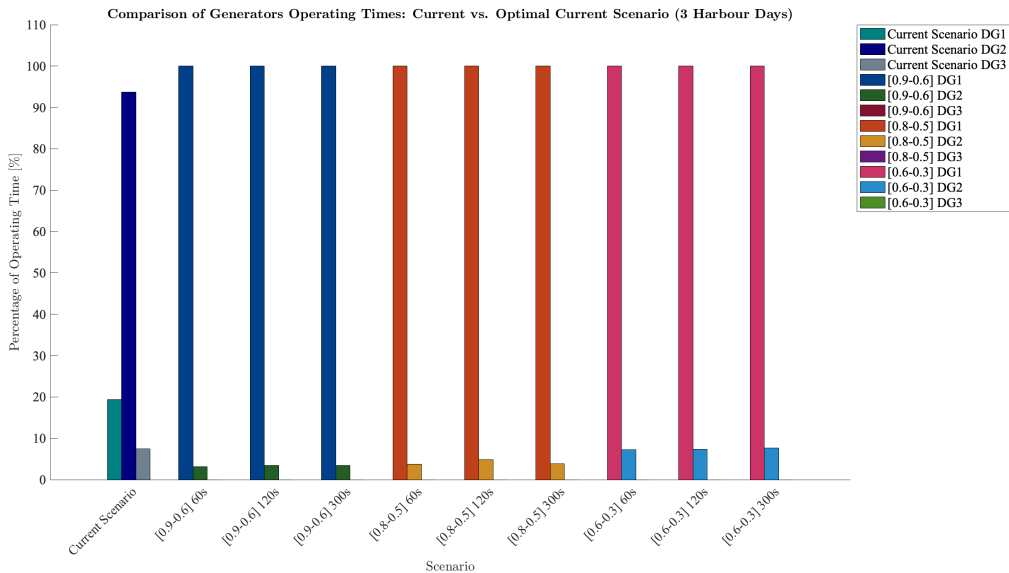
Figure 5.3: Comparison of Generator Operating Time Between Current and Optimal Scenarios for 3 Days of Harbour Operations

For clarity, the scenarios will be labeled sequentially from 0 to 10, corresponding to their order of appearance from left to right in the Figures above.

An example of the power distribution for each generator is illustrated in Figure 5.4. This Figure compares the data from the 12 dredging days in the current scenario with the optimal operation of the same scenario. For each percentage load auto start and stop range, with a consistent 60-second time delay, the power distribution of each generator is depicted. In the current scenario, the power distribution across the generators is nearly identical. However, in the optimal operation, a noticeable shift in power range to the right for each generator brings them closer to their rated capacity, thereby improving fuel efficiency. Additionally, generators 2 and 3 are turned off for significant periods.
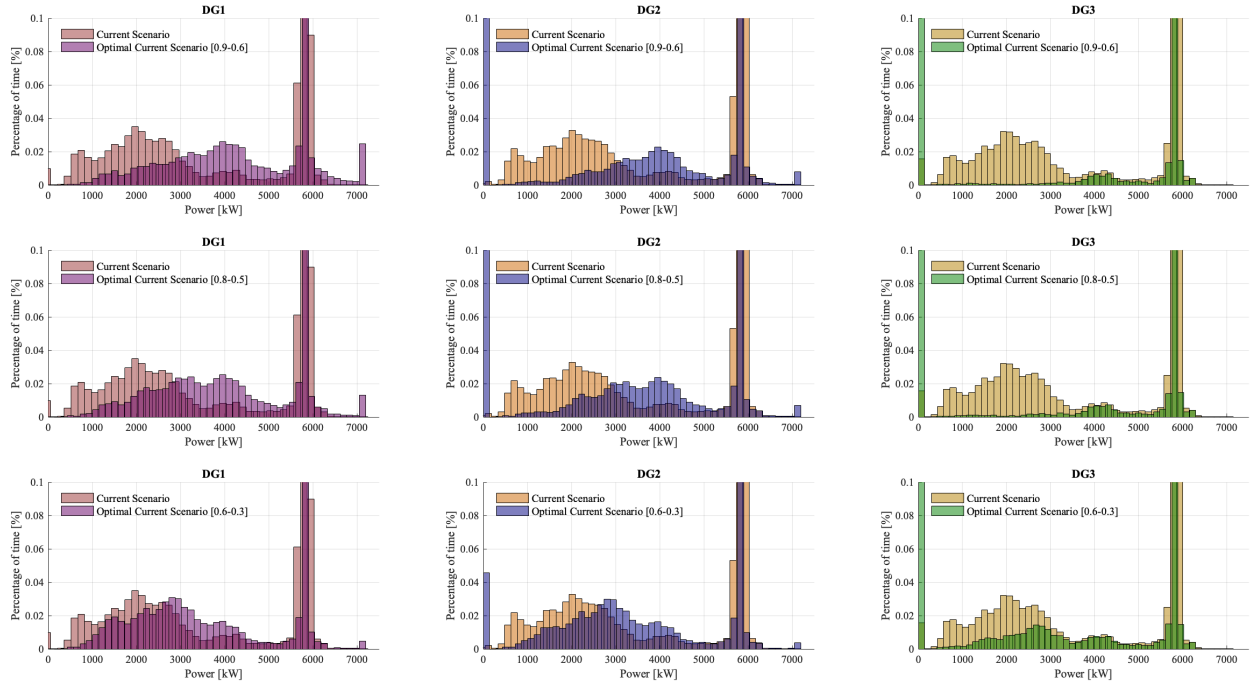
Figure 5.4: Comparison of power distribution among the three generators between the current scenario of the 12 dredging days and the optimal operation of the same scenario for the three different percentage load auto start-stop settings, each with a 60-second time delay.

Fuel Consumption

The fuel consumption (FC) for each scenario was calculated for each dataset by evaluating the power output of each generator at every time step, using the SFOC curve depicted in Figure 3.3. The total fuel consumption over a one-year period was then determined using the following Equation:

$$\text{Total fuel consumption per year} = \frac{(\text{FC}_{12\ \text{dredging days}} + \text{FC}_{11\ \text{irregular dredging days}} + \text{FC}_{3\ \text{harbour days}}) \cdot 365\ \text{days}}{26\ \text{days}}$$

(5.1)

Due to the automatic start-stop logic, a Supply Deficit (SD) may occur when power demand exceeds the capacity of the currently running generators. This is because, in situations where the demand requires the activation of a third generator, the time delay in the start-stop logic might not permit a quick respond, meeting the increased demand. The total SD over a period of one year is calculated using similar approach to the Equation 5.1 above. Table 5.1 summarizes the total FC and supply deficit of each scenario of the auto start-stop logic for each dataset, and the total FC and supply deficit per year per scenario.

Table 5.1: Fuel Consumption and Supply Deficit for Each Scenario

Metric	Scenario									
	0	**1**	**2**	**3**	**4**	**5**	**6**	**7**	**8**	**9**
FC 12 dredging days (tonnes)	626.84	612	611	608.7	615.11	614.3	613.1	621	620	621
FC 11 irregular dredging days (tonnes)	355.1	322.24	322	320.4	326	325.3	323.7	340	338.35	333.21
FC 3 harbour days (tonnes)	21.23	21	21	21	21	21	21	21	21	21
Total FC (tonnes/year)	14,083	13,404	13,377	13,333	13,503	13,482	13,441	13,779	13,748	13,685
SD 12 dredging days (%)	0	2.62	4.02	6.71	1.5	2.51	4.25	0.58	0.95	1.63
SD 11 irregular dredging days (%)	0	3.71	4.28	6.27	1.81	2.24	4.01	0.35	0.49	0.99
SD 3 harbour days (%)	0	0.11	0.16	0.36	0.09	0.15	0.28	0.04	0.1	0.23
Total SD (%/year)	0	90.4	118.76	187.3	47.73	68.78	119.88	13.62	21.62	40

The difference in Fuel Consumption arises from the difference in Supply Deficit, as can be seen in the Table, where for a lower shortage, a higher fuel consumption is achieved.

Maintenance Costs

Based on the percentage of on time of each generator as depicted in Figures 5.1, 5.2, and 5.3, the Maintenance Costs (MC) were calculated based on Equation 3.4. Using the same approach as Equation 5.1, the total maintenance costs over a period of one year is determined. It can be concluded that higher maintenance costs occur for a smaller range of percentage load in auto start and stop settings, as the generators turn on for lower power demand values compared to a larger range, where the generators turn on for higher power demands.

Table 5.2: Maintenance Costs for Each Scenario

Metric	Scenario									
	0	**1**	**2**	**3**	**4**	**5**	**6**	**7**	**8**	**9**
MC 12 dredging days (euros)	34,623	27,637	27,752	28,253.7	28,609	28,744	29,374	30,967	30,852	31,804
MC 11 irregular dredging days (euros)	34,763	20,469	20,480	20,427	21,930	21,761	21,467	28,562	28,217	26,105
MC 3 harbour days (euros)	14,026	11,998	12,035	12,035	12,071	12,203	12,082	12,482	12,490	12,524
Total MC (euros/year)	1,170,967	843,760	846,042	852,345	878,964	880,331	883,330	1,010,921	1,004,576	988,770

5.2. Load Smoothing Results

In this Section, the results of the load smoothing model are discussed. As outlined in Subsection 4.2.3, the analysis considers two distinct scenarios for battery operation: Case 1, where the battery undergoes cycling during harbour operations, and Case 2, where the battery remains idle during harbour operations. To ensure clarity and simplicity, each of the three different datasets was simulated using the Load Smoothing method, and the results were then combined. Key metrics such as Fuel Consumption, Maintenance Costs, and Supply Deficit were evaluated over a period of 12 dredging days, 11 irregular dredging days, and 3 harbour days. These results, representing a total of 26 days, were then used to perform an annual extrapolation to find the metrics values over a year.

For Case 1, where the battery is cycling during harbour operations, the load smoothing model was applied to the 3-day dataset and the relevant metrics were derived. The battery lifetime was then estimated by calculating the equivalent cycles the battery performed in each dataset, summing them, and applying the Equations outlined in Subsection **(a)** to determine the overall lifetime. However, in Case 2 where the battery is considered idle in harbour operations, the analysis was simplified by using the metric values from the current scenario without battery implementation. These values were combined with the metrics from the 12-day and 11-day datasets, and the results were extrapolated to estimate values for a full year. Calendar aging percentage was then combined with the cycle aging percentage of the 23 days extrapolated to one year, to determine the battery's lifetime, using the Equation provided in Subsection **(b)**.

Figure 5.5 below presents a comparison of the results for fuel consumption, maintenance costs, supply deficit, and the lifespan of 648 different parameter combinations. These solutions include 216 parameter combinations for each chemistry type, with distinctions made between Case 1 and Case 2. For details on the simulation parameters, please refer to Table 4.3, where a moving average of 1, 2, and 5 minutes was tested across two ramping rates of 0.5% and 5%. As previously mentioned, these ramping rates are per second, equating to 1.5% and 15% respectively, due to the 3-second time step found in the data.
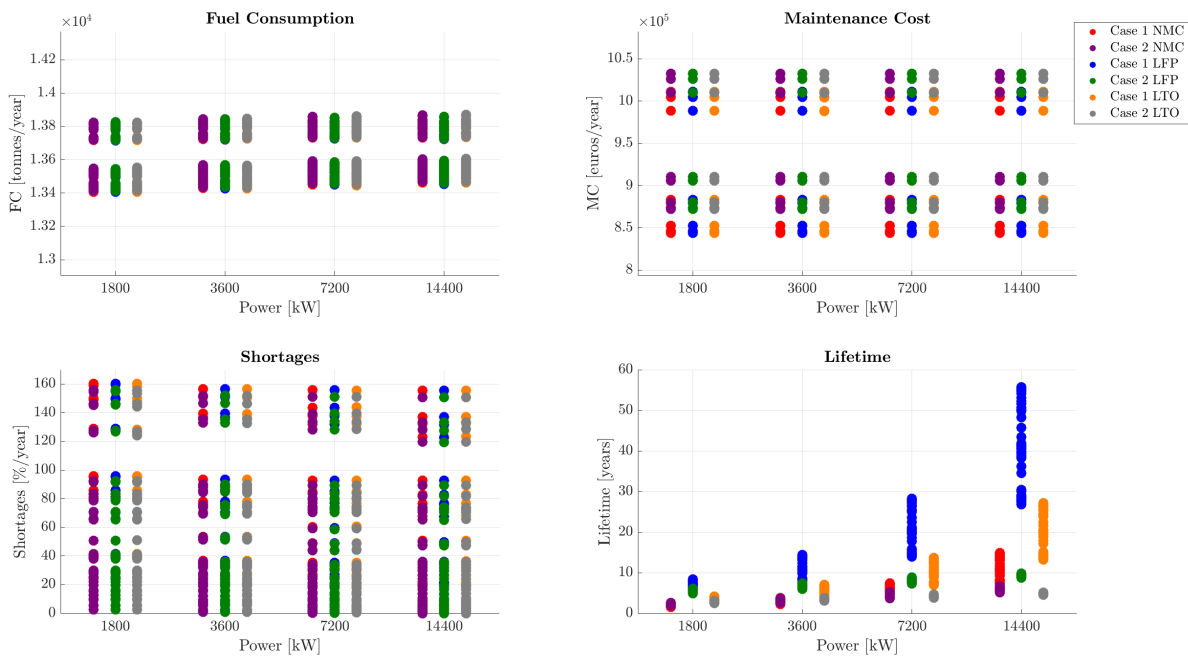

Figure 5.5: Fuel Consumption, Maintenance Costs, Supply Deficit, and Lifetime vs. Battery Power for All Parameters Combinations over the course of one year

As outlined, the automatic start-stop logic is implemented as model initialization, where various percentage load auto start and auto stop thresholds, along with different time delays, were evaluated to determine the impact of battery integration on the optimized operation of generators. Consequently, maintenance expenses for the same scenarios are expected to be similar, as the generators are anticipated to run for the same duration. Any minor differences in maintenance costs between systems with identical auto start-stop settings are attributed to the additional time required for generators to shut down, which depends on the preceding power supply and the ramping down limit. In the top right image of Figure 5.5, higher maintenance costs are associated with a range of [0.6 - 0.3] in percentage load for auto start-stop, where lower maintenance costs are for a range of [0.9 - 0.6].

In the load smoothing function and for scenarios with similar automatic start-stop boundaries and identical control to follow, the fuel consumption remains nearly identical, with only small variations. This consistency is due to the similar optimal range set for the generators to turn ON, ramping up and down in response to the control given. The battery charges and discharges to compensate for the difference between load demand and generator output, thereby balancing the power system and reducing supply deficits, which ultimately enhances the system's reliability. A decrease in fuel consumption and maintenance costs are achieved in all batteries compared to the current scenario where a fuel consumption of 14,083 tonnes/year was found.

In Case 2, which examines the calendar aging of the battery when idle during harbour operations, there is a slight increase in fuel consumption and maintenance costs compared to Case 1. This is because the generators, supplying the entire power demand, consume more fuel. Conversely, when the battery is not in use at the harbour, supply deficit are zero since the generators operate similarly to the current scenario. As a result, these supply deficit slightly decrease. On the other hand, Case 1 demonstrates a longer battery lifetime compared to Case 2, as highlighted by the bottom right Figure. This is attributed to the reduced damage per cycle when the battery is actively used, as opposed to being kept idle.

Based on specific criteria established by the author, the selection of parameter combinations was narrowed down. The criteria are outlined as follows:

1. Supply Deficit of less than 5% are deemed acceptable,
2. A battery lifetime of 10 to 15 years, as set by manufacturer,
3. The cycle cost must be lower than the fuel savings achieved per year,
4. The payback period must be shorter than the battery's expected lifetime.

As of 8 August 2024, the fuel price amounted to 717.4 euros/tonne [168]. This price will be considered as a reference for this analysis. Compared to the current scenario, fuel and maintenance savings were calculated for each battery combination based on the following Equations:

$$\text{Fuel Savings} \left(\frac{\text{tonnes}}{\text{year}} \right) = \text{FC Current Scenario} - \text{FC Load Smoothing Scenario} \tag{5.2}$$

$$\text{Fuel Savings} \left(\frac{\text{euros}}{\text{year}} \right) = \text{Fuel Savings} \left(\frac{\text{tonnes}}{\text{year}} \right) \cdot \text{Fuel Price} \left(\frac{\text{euros}}{\text{tonne}} \right) \tag{5.3}$$

$$\text{Maintenance Savings} \left(\frac{\text{euros}}{\text{year}} \right) = \text{MC Current Scenario} - \text{MC Load Smoothing Scenario} \tag{5.4}$$

The total savings per year were determined by Equation 4.8. In this thesis study, the analysis focused solely on the costs associated with the battery investment. However, for a more complete financial assessment in future studies, it will be essential to also include the costs associated with additional components such as the DC-DC converter and the Active Front End (AFE), as well as the installation costs. The battery cost in euro/kWh as set by the manufacturers in [45], determine the capital expenditure associated with each battery chemistry and power. These are summed up in Table 5.3.

Chemistry	NMC	LFP	LTO
Battery Cost (euro/kWh)	500	460	700
Power (kW)	Battery Cost (euros)		
1800	321,428.6	1,182,857	290,322.6
3600	642,857	2,365,714.3	580,645.2
7200	1,285,714.3	4,731,428.6	1,161,290.3
14400	2,571,428.6	9,462,857	2,322,581

Table 5.3: Battery Investment Cost

The Return on Investment was calculated using Equation 4.7. Then the annual cycle cost of the battery was calculated by:

$$\text{Cycle Cost} = \frac{\text{Equivalent Cycles per year}}{\text{Maximum Equivalent Full Cycles}} \cdot \text{Battery Investment Cost} \tag{5.5}$$

It was compared to the yearly fuel savings, as achieving higher fuel savings is essential to ensuring the profitability of battery integration. Based on these criteria, the parameter combinations for the two case scenarios were assessed and will be analyzed separately.

Case 1: Figure 5.6 illustrates the 27 solutions that meet the established criteria in Case 1, where 100% cycling over the year is achieved. Among these, 7 NMC, 5 LFP, and 15 LTO batteries are identified across various battery power levels. Appendix A.3 summarizes the 27 best solutions, including their specific metric calculations.
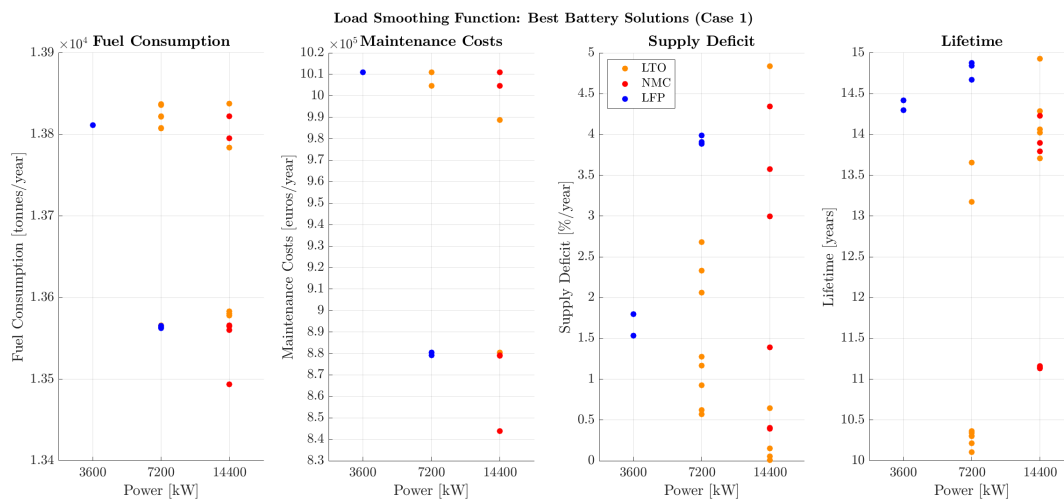
Figure 5.6: Solutions with a 100% cycling behaviour over a period of one year

When choosing between the different solutions and since all incur a positive return on investment, the decision hinges on balancing between profitability and longevity. For that case scenario, an LTO battery with a power capacity of 7,200kW, an auto start stop boundaries of [0.8 - 0.5] and 60 seconds, with a ramping rate of 0.5% and a moving average of 2 minutes offers a highest return on investment of 5 times the investment cost for a lifetime of 10.4 years. On the other hand, an LTO battery with 14,400 kW battery power, an auto start-stop boundaries of [0.8 - 0.5] and 60 seconds, with a ramping rate of

0.5% and a moving average of 5 minutes, offer the highest lifetime of 15 years but with a return on investment of 3.2 times the initial investment cost. The higher ROI option is ideal for maximizing short-term profitability, especially in scenarios where replacements are manageable. However, the longer cycle life might be more attractive in applications where minimizing maintenance and replacement disruptions is crucial. Ultimately, the best choice depends on whether the priority is immediate financial returns or sustainable, long-term operational efficiency.

Case 2: In this scenario, when the battery undergoes calendar aging during harbour operations, the variation in achieved battery lifetime becomes evident. Notably, the discrepancies between the data used for battery modeling and the calendar aging calculations may contribute to the significant reduction in battery lifespan. This reduction prevents the battery from achieving the minimum 10-year lifespan. Consequently, Criterion 2 is not considered in this case. Figure 5.7 illustrates the 69 solutions identified, comprising 17 NMC, 12 LFP, and 40 LTO batteries across various battery power levels found in Appendix A.3.
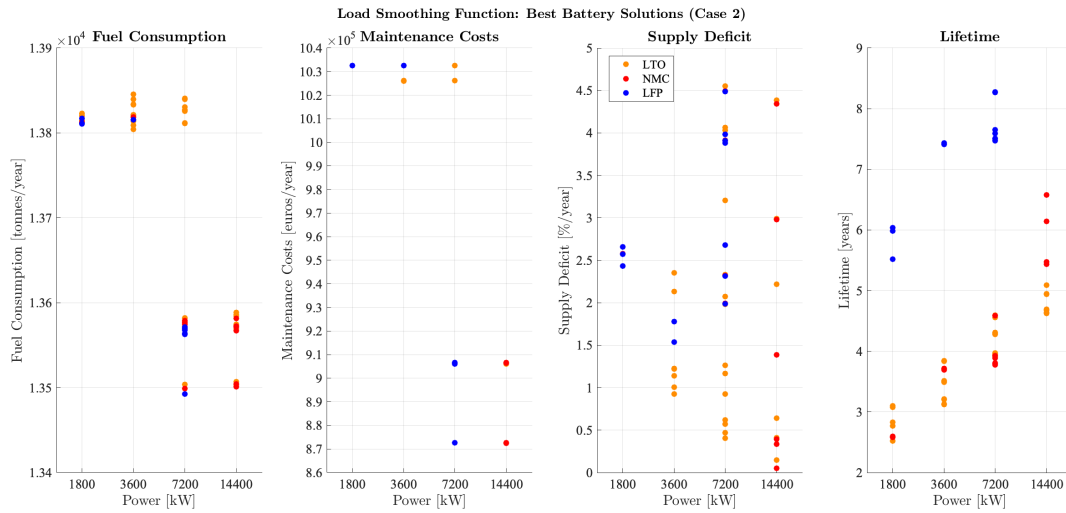
Figure 5.7: Solutions with a calendar aging behaviour in harbour operations over a period of one year

The ROI was calculated, showing that the LTO battery with a power capacity of 1,800, an auto start-stop boundaries of [0.6 - 0.3] and 60 seconds, a ramping rate of 0.5%, and a moving average of 1 minute achieved the highest ROI of 2.5 times the initial investment over a 3 year lifespan. On the other side, an LFP battery with a power capacity of 7,200, an auto start-stop boundaries of [0.8 - 0.5] and 60 seconds, a ramping rate of 0.5%, and a moving average of 2 minutes achieved a longer lifetime of 8.3 years but a lower ROI of 0.11. It is important to note that the initial investment varies depending on the battery technology and size. Therefore, to accurately assess and choose between these batteries, it is more appropriate to compare the return on investment over the entire project duration, taking into account the variations in battery price and technology.

The battery with the highest lifetime in Case 1 was selected to illustrate the battery's behaviour using the load smoothing function. The Figure 5.8 illustrates the rate of change in power output ($\frac{dP}{dt}$) for the three diesel generators over the 12-day dredging period under two scenarios: the current scenario (top row) and the load smoothing scenario (bottom row). The top row shows significant fluctuations and sharp spikes in the rate of change, especially around the date of March 5th, indicating highly variable generator loads. In contrast, the bottom row demonstrates the effects of load smoothing, with visibly reduced amplitude and frequency of extreme changes in $\frac{dP}{dt}$. The smoothed data results in a narrower range of values and fewer sudden transitions, showing a more stable and controlled generator performance under the load smoothing strategy. This can be seen in Figure 5.9 illustrating the power distribution of the rate of change in generators.
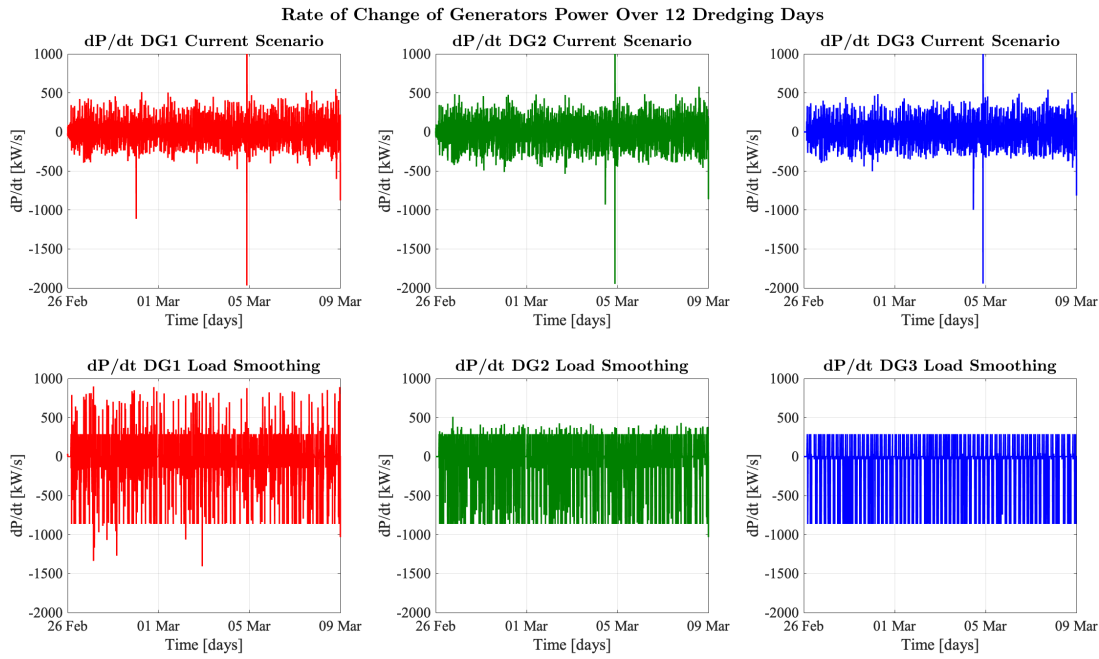
Figure 5.8: Comparison of the rate of change of generators power between the current scenario and the load smoothing scenario over 12 dredging days
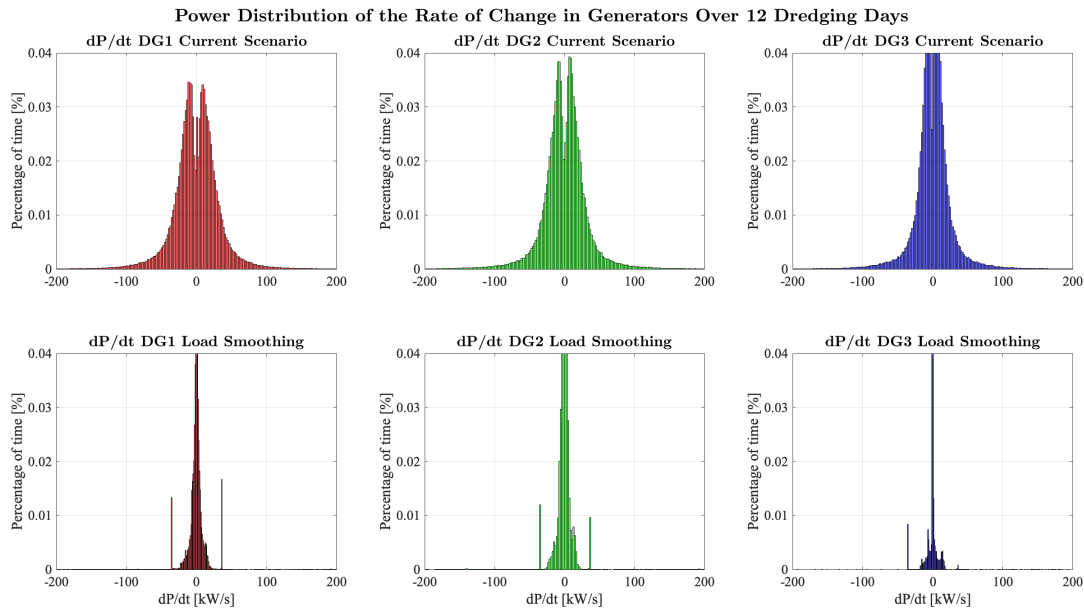
Figure 5.9: Power Distribution of the Rate of Change in Generators Over 12 Dredging Days

Figure 5.10, shows the power distribution of the generators across each of the three datasets in the load smoothing scenario, with each dataset compared to its current scenario. The load smoothing scenario demonstrates a more evenly distributed power usage across a wider range of outputs, particularly seen in DG1 and DG2. This smoothing effect spreads the load more uniformly and lessens the likelihood of high-power peaks, which may improve operation efficiency and minimize stress on the generators and operational expenses. As can be seen from Figure 3.2, in harbour operations a power

less than 14,400kW is required. With the auto start-stop logic, generator 3 is turned off. This can be seen from Figure 5.10 below in the bottom right image.
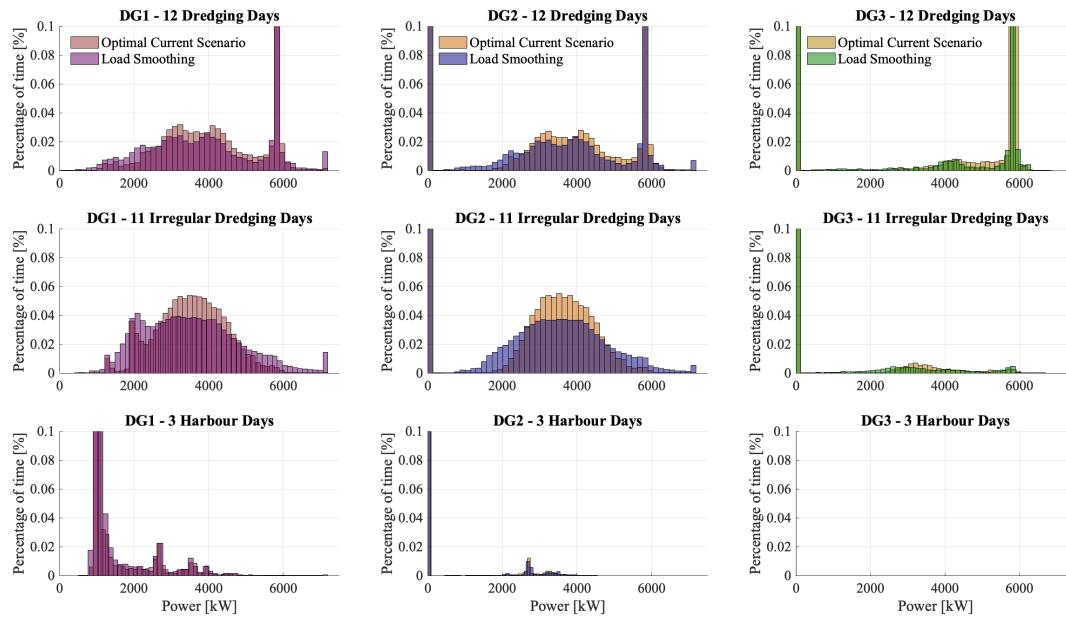
Figure 5.10: Comparative power distribution between current optimal and load smoothing scenarios across the three generators with consistent auto start-stop boundaries for the three datasets

Battery power and state of charge over time for the three datasets are shown in Figure 5.11. Over the 12 dredging days, the battery power exhibited significant fluctuations with frequent spikes and drops, reflecting the regular charging and discharging cycles typical of the variable energy demands in dredging operations as illustrated by the state of charge image in the top right corner. While power variability occurred over the course of 11 irregular dredging days, there were more frequent instances of lower power outputs from the battery. In contrast, during the 3 harbour days, the battery power was much smoother and less variable, with occasional spikes, representative of the more consistent and lower energy demand found in harbour activities. The state of charge (SoC) regulation shown in Figure 4.5 is reflected in the SoC plots, where the charging and discharging processes are kept within the range of 0.4 to 0.6, maintaining the battery close to a 50% state of charge. This regulation ensures that the battery consistently has sufficient energy available for sudden demands or the next operational day.
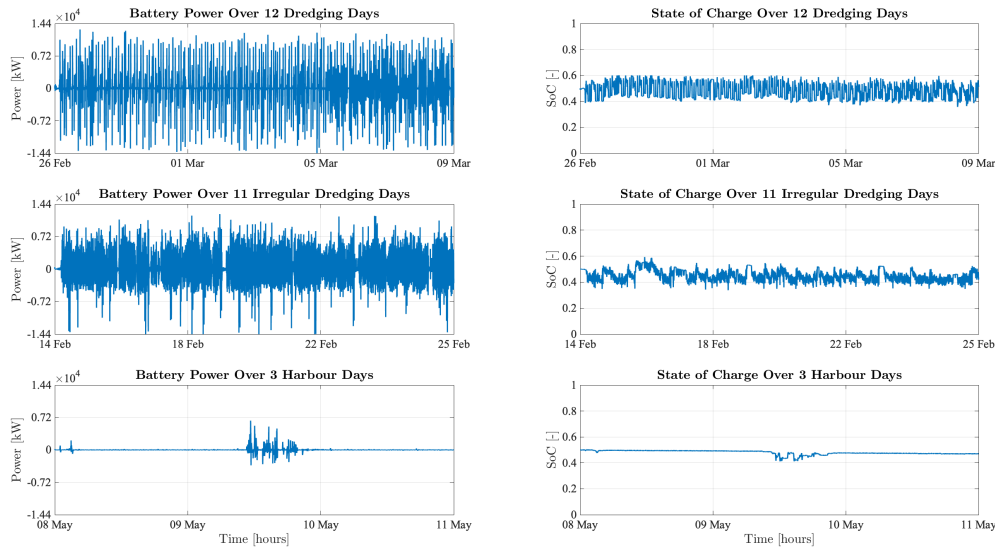
Figure 5.11: Battery power over time for the load smoothing model of the three datasets

5.3. Optimal Range of the Generators Results

In this Section, the results of the optimal loading of the generators function are discussed. 216 different parameter combinations have been generated, 72 for each chemistry type. Refer to Table 4.3 for more details on the parameters used in the combinations, while having two different optimal ranges of 60% to 95%, and 70% to 90%. The fuel consumption, maintenance costs, supply deficit, and lifetime of each of these parameter combinations are represented in Figure 5.12. The maintenance cost is influenced by the parameters set in the auto-start/stop logic. As noted earlier, when the same boundaries are applied, the maintenance cost remains consistent, as the generators operate for the same duration. In scenarios of optimal loading, fuel consumption is reduced compared to the current scenario. By comparing Figure 5.12 and 5.5, it is evident that in the optimal range scenario the fuel consumption decreases compared to the load smoothing scenario . The optimal operating range of the generator is designed to keep the generators between their optimal range thereby reducing fuel consumption. A difference in supply deficit is observed among the three different battery types at the same power level. NMC batteries show a higher supply deficit, while LTO batteries have the lowest. This variation is due to the number of cells each battery type contains. An increase in the number of cells leads to a higher state of charge, allowing the battery to supply more power.
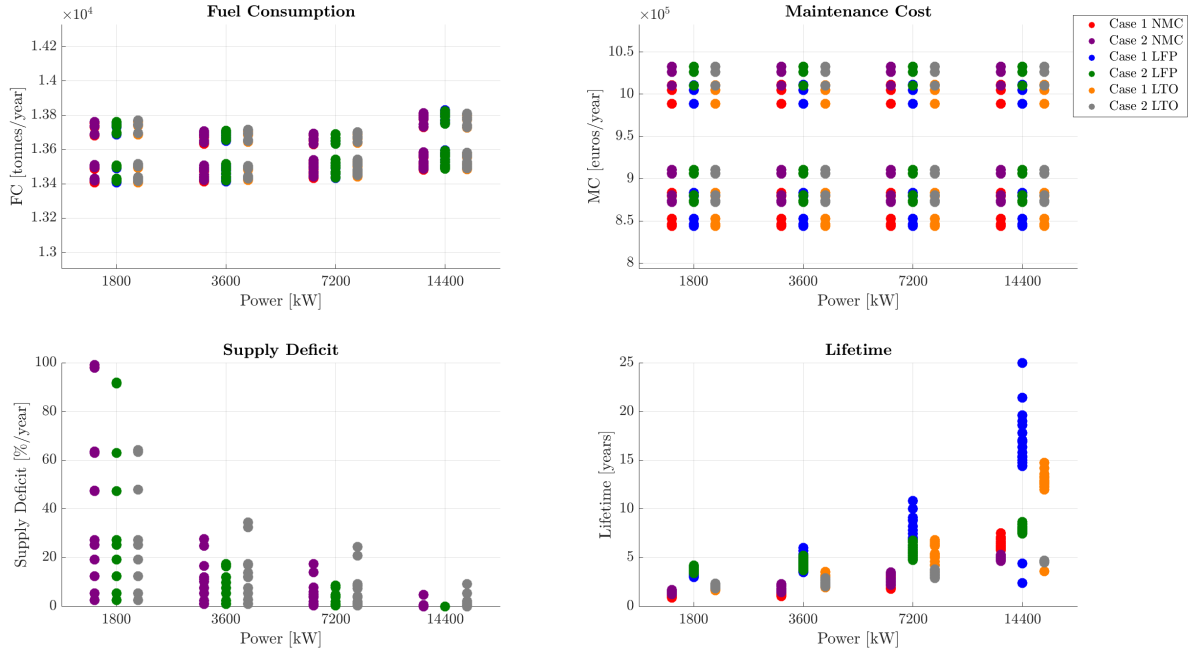
Figure 5.12: Fuel Consumption, Maintenance Costs, Supply Deficit, and Lifetime vs. Battery Power for All Parameter Combinations over the course of one year

Similar criteria and calculations set and performed in the load smoothing function have been applied to the optimal range function. Two case scenarios were evaluated, and based on these criteria, the best solutions were identified.

Case 1: Figure 5.13 illustrates the 17 solutions that meet the established criteria in Case 1, where 100% cycling over the year is achieved. Among these, 1 LFP battery and 16 LTO batteries are identified across two power levels. The LFP battery is specified for a power of 7,200 kW, while the 16 LTO batteries are specified for a power of 14,400 kW. Appendix A.3.2 summarizes the metrics for the different best solutions.
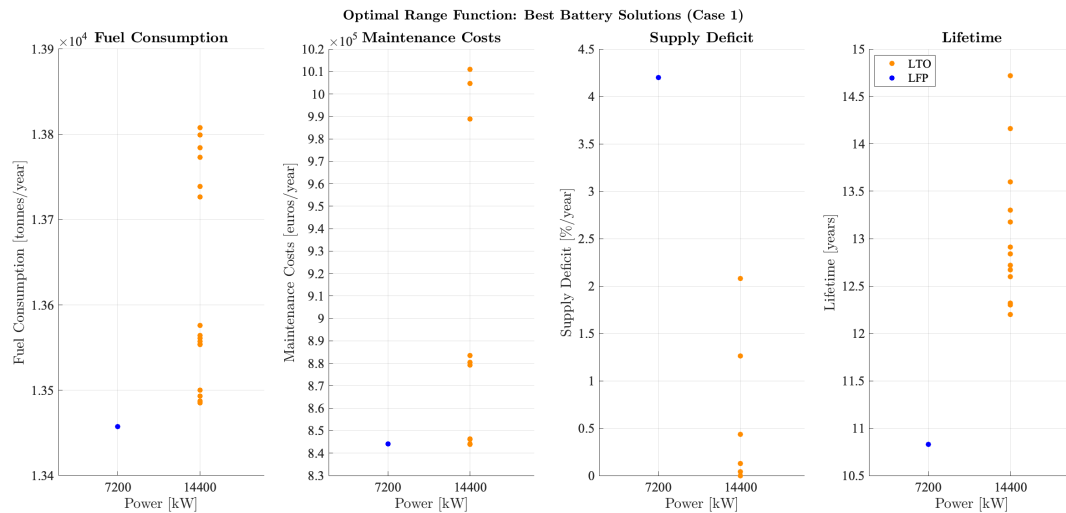
Figure 5.13: Solutions with a 100% cycling behaviour over a period of one year

The LTO battery with a power capacity of 14,400 kW demonstrated the highest lifetime among the

batteries, operating within auto start-stop boundaries of 0.9 to 0.6 and with a cycle duration of 60 seconds. It also had an optimal operating range between 0.6 and 0.95. This broader optimal range allows generators to operate more efficiently, reducing the frequency of battery cycling. As a result, this battery achieved the highest return on investment, largely due to its extended lifespan and reduced fuel consumption. When comparing this LTO battery to other LTO solutions with the same power capacity, the investment cost remains consistent. However, the high savings and extended lifetime of this particular battery result in a superior ROI. In comparison to the LFP battery with a power capacity of 7,200 kW, the LTO battery offers a greater ROI due to its longer lifespan and higher savings. Conversely, the higher investment cost of the LFP battery, coupled with its shorter lifespan, results in a lower ROI compared to the discussed LTO battery and all other LTO batteries.

Case 2: As previously outlined, in this scenario, the battery experiences calendar aging during harbour operations, highlighting the variation in battery lifetime compared to Case 1. Since the battery is subject to both cycling and calendar aging, representing a more realistic scenario, this case will be analyzed while Criterion 2 is not taken into account since none of the battery achieves a lifetime of 10 years or more. Figure 5.14 illustrates the 26 solutions, where 4 NMC batteries and 22 LTO batteries are identified across all battery power levels. Appendix A.3.2 summarizes the best solutions pertinent to this specific scenario. The battery with the highest lifetime of 5.3 years is found for an NMC battery with a power rated of 14,400 kW, an automatic start-stop boundaries of [0.9 - 0.6] with a time delay of 60 seconds, and an optimal range of [0.6 - 0.95], with a ROI of 0.49 times the investment cost. However, the battery with the highest ROI is found to be an LTO battery with a rated power of 7,200 kW, an automatic start-stop boundaries of [0.9 - 0.6], with a time delay of 60 seconds and an optimal range of [0.6 - 0.95] for a lifetime of 3.8 years. If one would compare NMC and LTO batteries to make a choice, the net gain would be compared. The initial investment cost of the NMC battery is 2,571,428.50 euros with an ROI of 0.49, resulting in a profit of 1,260,000 euros. This leads to a net loss of 1,311,428.5 euros. In contrast, the LTO battery, with an investment cost of 1,161,290 euros and an ROI of 1.43, generates a profit of 1,660,645 euros resulting in a net gain of 499,355 euros. Therefore, if profitability is the priority, the LTO battery is the better option due to its higher return on investment and positive net gain, making it a financially good investment despite its shorter lifetime. However, if long-term stability and a longer operational life are more crucial, the NMC battery would be a better choice.
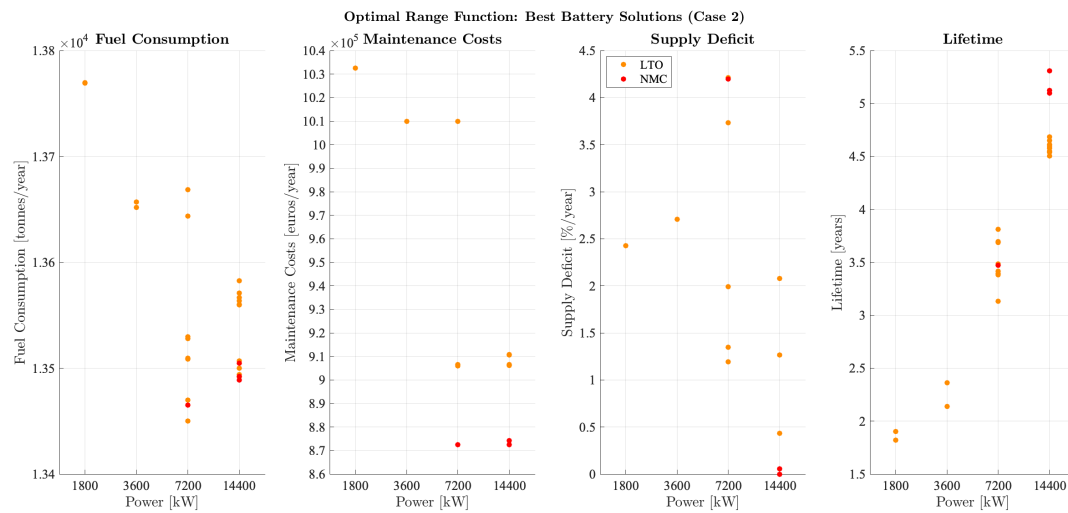
Figure 5.14: Solutions with a calendar aging behaviour in harbour operations over a period of one year

The battery with the highest lifetime in Case 1 was selected to illustrate the battery's behaviour using the optimal range function. The power distribution among the three generators over time for the three datasets is shown in Figure 5.15. The generators operate within an optimal range of [0.6 - 0.95], corresponding to a power between 4,320 kW and 6,840 kW. During harbour operations, where power demand is typically low, diesel generator 1 consistently supplies 4,320 kW, with only minor deviations, as shown in the bottom left image. According to the strategy, when power demand is less than the

lower optimal bound, the generators supply the lower bound, and the battery charges.
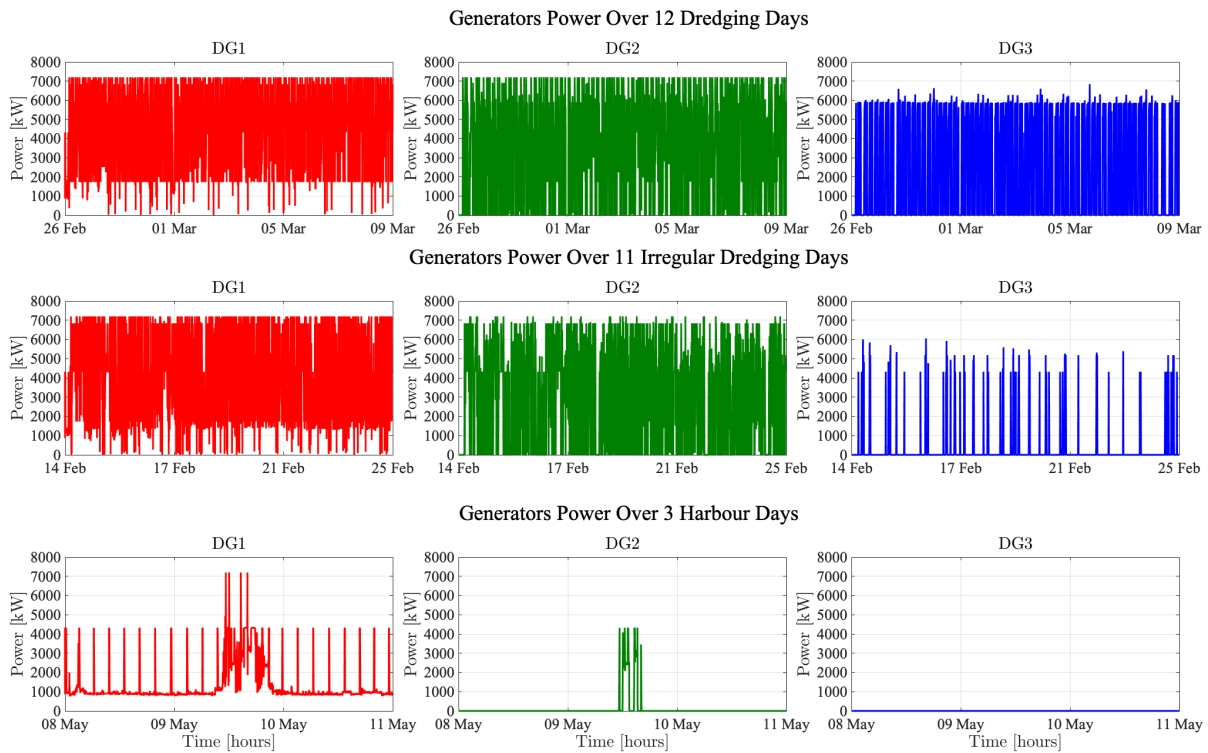
Figure 5.15: Generators power over time for the optimal range model of the three datasets

Figure 5.16, compares the power distribution of each generator under the optimal range function with their optimal operation in the current scenario, using the same auto start-stop boundaries. With a shift in power supply to the right, closer to the rated power, the power distribution clearly illustrates that the generators are operating with improved fuel efficiency.
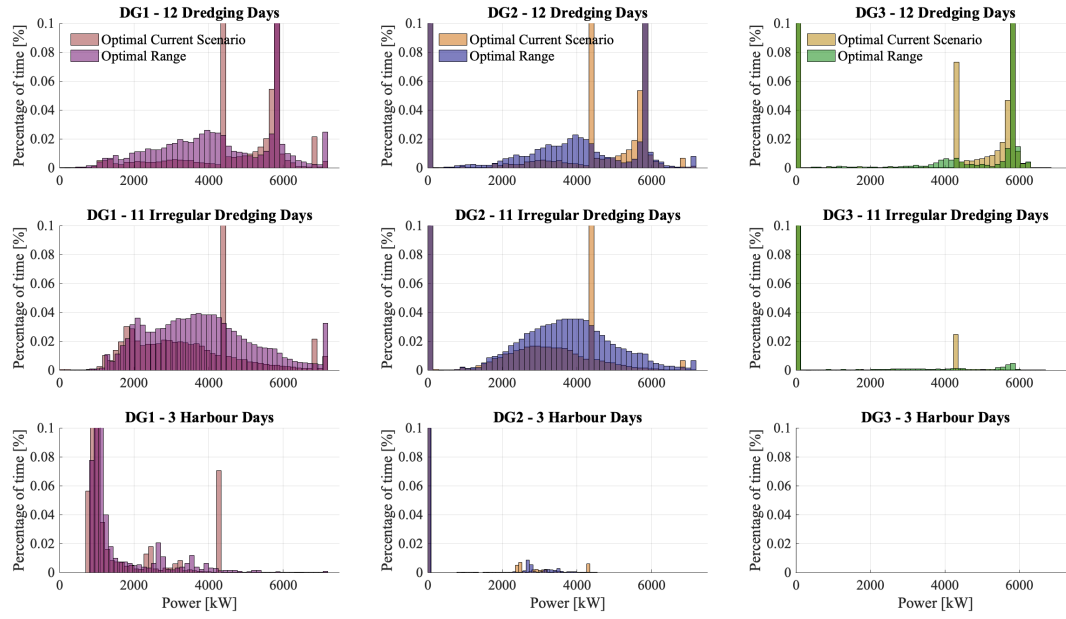
Figure 5.16: Comparative power distribution between current optimal and optimal range scenarios across the three generators with consistent auto start-stop boundaries for the three datasets

Below is the battery power distribution and state of charge over time for the three datasets. The SoC behaviour indicates that the battery underwent cycles of forced discharge followed by normal charging. This pattern is driven by the generators' power demand distribution. When the power demand is below the generators' optimal lower bound, the generators maintain operation at this minimum level, resulting in battery charging. After extended charging, the battery reached its maximum SoC of 0.8, leading a forced discharge mode. This mode forces the battery to discharge to a specific threshold before returning to normal operation. On the other hand, a positive remaining energy at the end of the period is seen from the SoC plots, meaning that the battery is more charged compared to its initial state of charge. Consequently, the battery contains excess energy that can be used the next day. This surplus energy implies that less fuel will be needed, as the battery already has more energy stored and requires less input from the generators to meet the energy demands. Thus, having a more charged battery results in reduced fuel consumption.
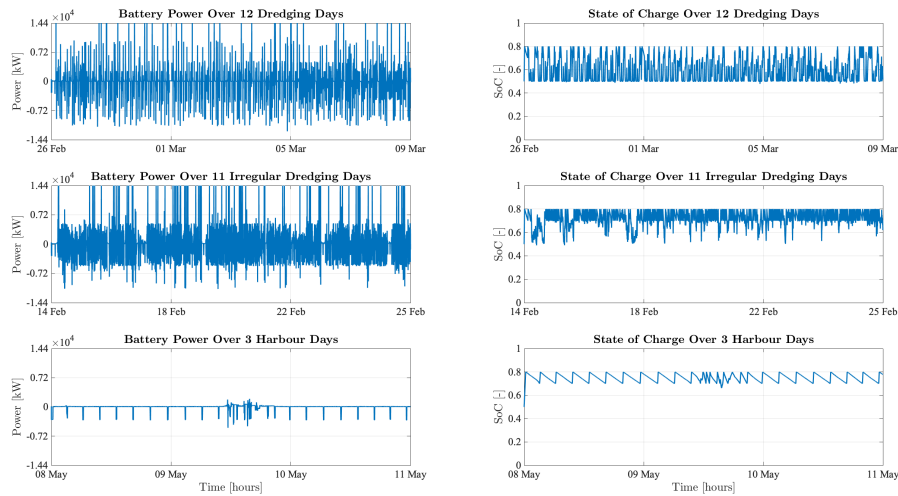
Figure 5.17: Battery power over time for the optimal range model of the three datasets

5.4. Research questions

The goal of this master's thesis is to figure out what battery size and type best aligns with well-defined operational requirements of hybrid vessels, and which methodology is most suitable for determining this. This includes determining the ideal battery size, selecting the appropriate technology, and accurately calculating the return on investment while considering battery degradation. To answer this, the primary research question with 4 sub-questions were defined in Section 1.2. Sections 5.4.1, 5.4.2, 5.4.3, and 5.4.4, answer these questions.

5.4.1. Sub question 1

What are the different battery technologies used in hybrid vessels, and what are the most suitable battery types for ocean going hybrid vessels?

Based on the literature review in Chapter 2, the study addressed battery systems' flexibility in storing and generating electrical energy to optimize vessel operation. While batteries can power a vessel for short distances, their primary goal is to enhance overall performance and efficiency. Different battery functions influence system characteristics, with rechargeable batteries being most suitable for hybrid vessels. The literature review evaluates various rechargeable batteries for hybrid vessels, including lithium-based, nickel-based, sodium-based, lead-acid, and flow batteries. It examines multiple types within each category, providing insights into widely used technologies and emerging solutions that could enhance efficiency and sustainability. The analysis outlines the fundamental aspects, performance variations, and characteristics of these batteries, enabling a comparative assessment on their suitability in ocean-going hybrid vessels. Lithium-ion batteries are preferred for their superior cell voltage (3.6 V) delivering more power within less space, high energy density, efficiency, and reliability. Among the six lithium-ion sub-types, NMC, LFP, and LTO are favored. NMC offers the highest specific energy and balanced properties, LFP provides good safety features and long lifespan, and LTO is suitable for applications requiring fast charging or high cycling.

5.4.2. Sub question 2

What methodologies are commonly utilized in the maritime industry to assess the efficiency, performance, and sizing of batteries, considering variables like energy density, lifespan, and environmental impact?

The existing methods for evaluating the efficiency, performance, and sizing of batteries have been summarized based on a review of the literature. Among the techniques used for battery sizing and selection is the optimization model, which includes various approaches, each with its own specific strengths and weaknesses. For a summary of these techniques, please refer to Table 2.9. Another approach is the numerical modeling that simulate and evaluate various battery configurations under a range of operational conditions. By using this method, the performance and lifespan of different battery chemistries can be predicted and assessed. A popular method to select battery for a hybrid vessel is the multi-criteria decision making, which evaluates various battery characteristics in relation to the operational needs of the particular vessel. This technique takes into account the technical demands, environmental implications, and the economic viability of applying these battery systems on board of the vessel, complying with the focus on optimizing the vessel performance and minimizing the environmental impact. Another method is the TOPSIS technique, intended to determine the best option from a range of choices based on the degree of closeness to the ideal solution by choosing the solution that is the closest to the positive ideal solution and furthest from the negative ideal solution. Another approach based on a full electric vessel for example, required careful analysis of the operational performance, safety, costs, and dimensions. The parameters assessed where the capacity, power, longevity, costs, weight and dimensions.

In addition, The Analytic Hierarchy Process and the Analytic Network Process are two different se-

lection criteria methods that can be used to select batteries. AHP offers a direct approach, making it easier to prioritize and rank alternatives when criteria are independent, while ANP provides a more comprehensive analysis by accounting for interdependencies between criteria, making it ideal for more complex decision-making scenarios. On the other hand, life cycle assessment and life cycle cost assessment are battery selection methods applied in maritime applications, where LCA evaluates the environmental impact of battery technologies over their entire life cycle, ensuring alignment with sustainability goals. LCCA complements this by analyzing the total cost of ownership, including initial costs, maintenance, and disposal, to ensure economic viability. When combined, these techniques offer a fair method for choosing battery technologies that satisfy maritime environments' financial and environmental needs. Research on battery selection process in hybrid vessels is limited. In this thesis, a numerical modeling approach was undertaken to balance battery sizing and technology selection, considering key criteria such as energy density, cycle life, cost, and operational performance.

5.4.3. Sub question 3

What specific cost factors influence the selection of batteries for maritime vessels, and how do these factors impact the overall cost-effectiveness?

In maritime settings, several key cost factors influence the selection of batteries, including battery cost, maintenance costs associated with keeping the battery system operational and in good condition over its lifespan, installation costs, monitoring costs, and component costs as discussed in Section 2.4.3. However, in this thesis, only the battery cost is considered to assess the financial impact of the battery itself, as the analysis focuses on comparing three different battery technologies. The three lithium-ion batteries evaluated are NMC, LFP, and LTO, with investment costs of 500, 460, and 700 euros per kWh, respectively. based on [45]. To assess the cost-effectiveness of each of these battery solutions, the yearly savings, and return on investment were calculated based on Equations 4.8, and 4.7 respectively. The yearly savings include fuel savings, calculated based on a fixed fuel price of 717.4 euros per tonne [168], and maintenance savings resulting from the reduced operating time of the generators. Battery lifetime plays a crucial role in the return on investment, where the interplay between yearly savings, battery lifetime, and initial investment can have diverse impacts on the ROI, ultimately influencing the decision-making process. While a lower initial battery cost might suggest a higher return on investment, this is not always the case. Some batteries with lower initial costs may still offer a lower ROI due to their limited savings potential over time. Conversely, batteries with higher initial costs might provide higher long-term returns due to the higher yearly savings, making them more cost-effective despite the greater initial investment. Therefore, when evaluating battery solutions, it is crucial to consider not just the initial investment but also the long-term financial performance and savings potential of each technology.

5.4.4. Sub question 4

As an example, what methodology will be employed to select the optimal battery technology for Jan de Nul's existing trailing suction hopper dredger vessel, comparing the impact of two different control strategies on the BESS requirements, taking sub-question 1-3 into account?

The overview of the methodology used in this analysis is described in Section 1.1. A comprehensive load analysis is first conducted to assess the current fuel consumption and maintenance costs. To optimize generator operation, an automatic start-stop logic is implemented, regulating the number of active generators at each time step. Three control strategies are then simulated and compared: optimal operation of the current scenario without batteries, load smoothing of the generators with batteries, and optimal range of the generators with batteries. The analysis of the optimal operation without batteries highlights the need for battery integration to address the supply deficits that arise when running the optimal number of generators. The load smoothing and optimal range strategies identify the necessary battery power to compensate for these deficits. Battery power is controlled using state-of-charge control logics, as illustrated in Figures 4.4, 4.5, 4.6, and 4.7. Battery modeling is then performed to simulate the dynamic behaviour of the battery system, accounting for static losses associated with the various components integration such as DC-DC converter and Active Front-End converter. Once the

power profiles of both the generators and the battery are determined, fuel savings are calculated based on current fuel price. Maintenance savings are achieved from the automatic start-stop logic. The total savings, encompassing both fuel and maintenance reductions, are then determined. The battery's aging process, including both calendar and cycle aging, is calculated to estimate its lifespan. A cost analysis is performed determining the return on investment. In conclusion, battery selection is driven by the specific goals of the project, whether the focus is on achieving immediate financial returns or on ensuring long-term operational efficiency and sustainability.

6

Conclusion and Recommendations

This Chapter presents the conclusion and recommendations for future research based on the findings of this master's thesis.

The primary objective of this study was to develop a strategic approach for sizing and selecting batteries for maritime applications, using a Trailing Suction Hopper Dredger vessel as a case study for retrofitting and integrating a Battery Energy Storage System. Two battery control strategies were simulated and compared across two scenarios: one accounting for the full cycling of the battery, and the other considering calendar aging during harbour operations. Given the model limitations inherent in this research, the findings indicate that when a battery is primarily subjected to calendar aging, a significant reduction in battery lifetime occurs, leading to the conclusion that a cycling behaviour is preferable for achieving greater longevity and return on investment. In comparing the two strategies, the optimal range for the generators model demonstrated a reduction in fuel consumption compared to the load smoothing model, highlighting the efficiency of optimized generator operation. On the other hand, the load smoothing function resulted in a longer battery lifetime in both calendar and cycling scenarios, resulting from the fewer equivalent cycles performed over the course of a year. This result is directly related to the control strategy implemented determining the battery cycling behaviour.

Batteries serve various functions aboard vessels, and this thesis has focused on analyzing two specific functions: load smoothing using the moving average approach, and the optimal range of the generators. It is recommended to evaluate various battery functions comprehensively, taking into account all investment costs as this will help to determine the most effective ways in which batteries can enhance vessel performance and be cost-effective. The analysis presented in this thesis is based on three distinct datasets that represent different operational behaviours of the vessel, with these behaviours extrapolated over the course of a year. However, for a more accurate understanding of battery performance and its impact on the electric hybrid system, it is preferred to analyze data covering the full year and to verify the model and assumptions with data from other vessels. This will allow for a detailed evaluation of battery behaviour across various operational contexts. While cycle aging of batteries is a well-studied area, calendar aging is less explored. To ensure an accurate evaluation of battery lifespan in hybrid vessels, it is vital to prioritize an in-depth estimation of calendar aging, as this factor significantly influences the overall lifetime and performance of the batteries, as shown in this analysis. For newly constructed vessels, there are distinct opportunities to optimize system design, including potentially reducing the size of generators and designing the entire system with battery integration. By extrapolating load profiles from existing data on previous vessel operations, a more comprehensive understanding of system sizing can be achieved, leading to greater fuel efficiency. Finally, this study utilized numerical modeling for the analysis. It is recommended that future research incorporates optimization techniques to compare the results with those obtained from numerical simulations.

References

[1] European Commission. *Reducing emissions from the shipping sector*. `https://climate.ec.europa.eu/eu-action/transport/reducing-emissions-shipping-sector_en`. [Accessed: day-month-year]. 2024.

[2] European Commission. *Proposal for a Council Decision on the signing, on behalf of the European Union, of the Amendment to the Montreal Protocol on Substances that Deplete the Ozone Layer*. Accessed: Aug. 18, 2024. 2021. URL: `https://climate.ec.europa.eu/system/files/2021-08/c_2021_6022_en.pdf`.

[3] Anthony F. Molland, Stephen R. Turnock, and Dominic A. Hudson. *Ship Resistance and Propulsion: Practical Estimation of Ship Propulsive Power*. Cambridge University Press, 2011. URL: `https://app.knovel.com/hotlink/toc/id:kpSRPPESP1/ship-resistance-propulsion/ship-resistance-propulsion`.

[4] A. Ul-Haq A. K. Khan A. R. Anwar and T. S. Ustun. "Integration of Renewable Energy Resources in Microgrid and Challenges". In: *IEEE Access* 7 (2019), pp. 169774–169779. URL: `https://ieeexplore.ieee.org/stamp/stamp.jsp?tp=%5C&arnumber=8715773`.

[5] M. Saad Alam A. M. Muhammad and M. Rizwan. "Electric Vehicle Charging Using Renewable Energy: A Review". In: *IEEE Access* 9 (2021), pp. 148791–148812. URL: `https://ieeexplore.ieee.org/stamp/stamp.jsp?tp=%5C&arnumber=9606740`.

[6] ABB. *Onboard DC Grid Brochure*. Accessed: Aug. 5, 2024. 2014. URL: `https://new.abb.com/docs/librariesprovider91/articles/lm00614-onboard-dc-grid-brochure_june2014_1.pdf?sfvrsn=2`.

[7] Srinivasa Rao K. P. J. Chauhan Sanjib K. Panda Gary Wilson Xiong Liu Amit K. Gupta. "An Exercise to Qualify LVAC and LVDC Power System Architectures for a Platform Supply Vessel". In: *2016 IEEE Transportation Electrification Conference and Expo, Asia-Pacific (ITEC)*. Busan, Korea, 2016, pp. 332–337. URL: `https://ieeexplore.ieee.org/stamp/stamp.jsp?tp=%5C&arnumber=8715773`.

[8] R.D. Geertsma et al. "Design and control of hybrid power and propulsion systems for smart ships: A review of developments". In: *Applied Energy* 194 (2017), pp. 30–54. ISSN: 0306-2619. URL: `https://www.sciencedirect.com/science/article/pii/S0306261917301940`.

[9] MAN Energy Solutions. *Basic Principles of Ship Propulsion*. Accessed: August 5, 2024. 2018. URL: `https://www.man-es.com/docs/default-source/marine/5510-0004-04_18-1021-basic-principles-of-ship-propulsion_web.pdf`.

[10] Omer Berkehan Inal, Jean-Frédéric Charpentier, and Cengiz Deniz. "Hybrid power and propulsion systems for ships: Current status and future challenges". In: *Renewable and Sustainable Energy Reviews* 156 (2022), p. 111965. ISSN: 1364-0321. URL: `https://www.sciencedirect.com/science/article/pii/S1364032121012302`.

[11] K. Nanthagopal et al. "Experimental investigation on performance, combustion and emission characteristics of diesel engine fueled with higher alcohol blends of n-propanol and n-butanol". In: *Energy* 80 (Feb. 2015), pp. 391–406. URL: `https://www.sciencedirect.com/science/article/pii/S0360544214011694`.

[12] Ying Lu. "Optimal Scheduling and Loadsharing of a Hybrid Power Plant with Gensets and Battery Banks". MSc. thesis. Trondheim, Norway: Norwegian University of Science and Technology, Department of Marine Technology, 2019. URL: `https://ntnuopen.ntnu.no/ntnu-xmlui/handle/11250/2622976`.

[13] I. Boldea. *Synchronous Generators*. 1st. CRC Press, 2005. DOI: `10.1201/9781420037258`.

[14] Electrical Engineering Toolbox et al. *Permanent Magnet Synchronous Motors (PMSM)*. https://www.electricalengineeringtoolbox.com/2016/02/how-to-calculate-synchronous-speed-and.html. Accessed: 23-Jul-2024. 2024.

[15] Electrical Engineering Toolbox. *How to Calculate Synchronous Speed and Slip of AC Induction Motors*. Accessed: 23-Jul-2024. 2016. URL: https://www.electricalengineeringtoolbox.com/2016/02/how-to-calculate-synchronous-speed-and.html.

[16] M.T. Ameli, S. Moslehpour, and A. Mirzaie. "Feasibility study for replacing asynchronous generators with synchronous generators in wind farm power stations". In: *Proc. IAJC–IJME, Int. Conf. Eng. Technol.* Music City Sheraton, Nashville, TN, US, Nov. 2008, pp. 17–19. URL: https://www.ijme.us/cd_08/PDF/129-%20ENT%20204.pdf.

[17] WB Power Services Ltd. *An Overview of Diesel Generators*. Accessed: 2024-08-06. URL: https://www.wbpsltd.co.uk/news/an-overview-of-diesel-generators/.

[18] O. L. Osen. "Optimizing electric energy production on-board offshore vessels: Vessel power consumption profile and production strategies using genetic algorithms". In: *OCEANS 2016 - Shanghai*. 2016, pp. 1–10. DOI: 10.1109/OCEANSAP.2016.7485614.

[19] J. Gao X. Zhang Y. Li X. Wang and X. Liu. "Investigation on the Role of Battery Storage Systems in Renewable Energy Integration". In: *Energy* 258 (2022), p. 124302. URL: https://www.sciencedirect.com/science/article/pii/S0360544222015900.

[20] A. S. Abdo H. Saleh M. H. Albakri and A. B. Albduljabbar. "Enhancing the Reliability of Power Systems Using Redundancy". In: *IEEE Access* 7 (2019). Accessed: 2024-08-06, pp. 42084–42090. URL: https://ieeexplore.ieee.org/stamp/stamp.jsp?tp=&arnumber=8715773.

[21] ABB. *Switchboards*. Accessed: August 5, 2024. 2024. URL: https://electrification.us.abb.com/products/switchboards.

[22] ABB. *Busbars*. Accessed: August 5, 2024. 2024. URL: https://new.abb.com/low-voltage/products/system-pro-m/modular-din-rail-components/protection-device/busbars.

[23] ABB. *Hardware Manual ACS880-1604LC*. Accessed: 2024-08-06. 2024. URL: https://library.e.abb.com/public/eaeed051221c4d1aa2f54a34709c6087/EN_ACS880-1604LC_HW_C_A4.pdf?x-sign=u4uEDujeKRde2c3wu2tqQlnZIIy0+RFQcZmuI7pDcFqqad9O95G8ADKQMCsJgVum.

[24] Ho-Sung Kim et al. "High Efficiency Isolated Bidirectional AC-DC Power Converter". In: *Intelligent Robotics and Applications*. Ed. by Jangmyung Lee et al. Vol. 8103. Lecture Notes in Computer Science. Springer, Berlin, Heidelberg, 2013, pp. 399–407. URL: https://link.springer.com/chapter/10.1007/978-3-642-40849-6_30.

[25] Brusa Technology. *DMC544 DC/AC Inverter*. Accessed: 2024-08-06. URL: https://www.brusatechnology.com/portfolio/dmc544/.

[26] R. W. Alexander and C. T. L. Lu. "High efficiency transformers: a cost-effective solution for energy management". In: *IEEE Transactions on Industry Applications* 27.2 (1991). Accessed: 2024-08-06, pp. 233–238. URL: https://ieeexplore.ieee.org/stamp/stamp.jsp?tp=&arnumber=730768.

[27] M. Mittermaier and H. Lange. "A review on electrical motors energy use and energy savings". In: *Renewable and Sustainable Energy Reviews* 14.1 (Jan. 2010), pp. 177–186. URL: https://www.sciencedirect.com/science/article/abs/pii/S1364032109002494.

[28] Ming Cheng et al. "Overview of stator-permanent magnet brushless machines". In: *IEEE Transactions on Industrial Electronics* 58.11 (Nov. 2011), pp. 5087–5101. URL: https://ieeexplore.ieee.org/stamp/stamp.jsp?tp=%5C&arnumber=7317729.

[29] Peng Wu et al. "Energy-Efficient and Fault-Tolerant Autonomic Resource Provisioning for Hybrid IoT Systems". In: *IEEE Transactions on Sustainable Computing* 4.1 (Jan. 2019), pp. 49–61. URL: https://ieeexplore.ieee.org/stamp/stamp.jsp?tp=&arnumber=8715773.

[30] A. J. Forsyth R. T. Naayagi and R. Shuttleworth. "High-power bidirectional DC-DC converter for aerospace applications". In: *2008 13th International Power Electronics and Motion Control Conference*. 2008, pp. 1688–1695. URL: https://ieeexplore.ieee.org/document/4592198.

[31] Saša Sladić, Damir Kolić, and Marko Šuljić. "Bidirectional DC/DC Power Converter for Hybrid Yacht Propulsion System". In: *Pomorski Zbornik* Special Issue (2020). Accessed: 2024-08-06, pp. 133–142. URL: https://www.mdpi.com/1996-1073/15/3/898.

[32] Zhibin Zhou et al. "A review of energy storage technologies for marine current energy systems". In: *Renewable and Sustainable Energy Reviews* 18 (2013), pp. 390–400. ISSN: 1364-0321. URL: https://www.sciencedirect.com/science/article/pii/S1364032112005485.

[33] Abraham Alem Kebede et al. "A comprehensive review of stationary energy storage devices for large scale renewable energy sources grid integration". In: *Renewable and Sustainable Energy Reviews* 159 (2022), p. 112213. ISSN: 1364-0321. URL: https://www.sciencedirect.com/science/article/pii/S1364032122001368.

[34] Muhammad Umair Mutarraf et al. "Energy Storage Systems for Shipboard Microgrids—A Review". In: *Energies* 11.12 (2018), p. 3492. URL: https://doi.org/10.3390/en11123492.

[35] Jaya Verma and Deepak Kumar. "Recent developments in energy storage systems for marine environment". In: *Centre for Automotive Research and Tribology, Indian Institute of Technology Delhi* (2021). First published on 29th September 2021. URL: https://pubs.rsc.org/en/content/articlehtml/2021/ma/d1ma00746g.

[36] Reza Hemmati and Hedayat Saboori. "Emergence of hybrid energy storage systems in renewable energy and transport applications – A review". In: *Renewable and Sustainable Energy Reviews* 65 (2016), pp. 11–23. ISSN: 1364-0321. URL: https://www.sciencedirect.com/science/article/pii/S1364032116302374.

[37] Chalermkiat Nuchturee, Tie Li, and Hongpu Xia. "Energy efficiency of integrated electric propulsion for ships – A review". In: *Renewable and Sustainable Energy Reviews* 134 (2020), p. 110145. ISSN: 1364-0321. URL: https://www.sciencedirect.com/science/article/pii/S1364032120304366.

[38] C. Dall'Armi D. Pivetta and R. Taccani. "Multi-objective optimization of hybrid PEMFC/Li-ion battery propulsion systems for small and medium size ferries". In: *International Journal of Hydrogen Energy* 46.72 (2021), pp. 35949–35960. URL: https://www.researchgate.net/publication/350136648_Multi-objective_optimization_of_hybrid_PEMFCLi-ion_battery_propulsion_systems_for_small_and_medium_size_ferries.

[39] Y. Wu et al. "Research progress in battery thermal management system under vessel working conditions". In: *Journal of Energy Storage* 96 (2024), p. 112761. DOI: 10.1016/j.est.2024.112761.

[40] J. Marco C. Watts and P. Faithfull. *Safe energy storage systems for hybrid electric marine vessels*. 2017. URL: https://wrap.warwick.ac.uk/id/eprint/95438/.

[41] R. Peng et al. "Numerical investigation on explosion hazards of lithium-ion battery vented gases and deflagration venting design in containerized energy storage system". In: *Fuel* 351 (2023), p. 128782. URL: https://www.sciencedirect.com/science/article/pii/S0016236123013959.

[42] P. Andersson et al. *Safe introduction of battery propulsion at sea*. https://example.com/safe-introduction-of-battery-propulsion-at-sea. Institution Name, 2017.

[43] Ben Gully et al. *Technical Reference for Li-ion Battery Explosion Risk and Fire Suppression*. Technical Report 2019-1025, Rev. 4. Høvik, Norway: DNV GL, Nov. 2019. URL: https://www.dnvgl.com.

[44] Crisley de Souza Peixoto. "Title of the Master's Dissertation". Available: https://www.teses.usp.br/teses/disponiveis/3/3150/tde-30112022-081832/publico/CrisleydeSouzaPeixotoCorr22.pdf. Master's Dissertation. Escola Politécnica, 2022.

[45] Lukas Kistner, Astrid Bensmann, and Richard Hanke-Rauschenbach. "Potentials and limitations of battery-electric container ship propulsion systems". In: *Energy Conversion and Management: X* 21 (2024), p. 100507. URL: https://doi.org/10.1016/j.ecmx.2023.100507.

[46] DNV GL. *Handbook for Maritime and Offshore Battery Systems*. Tech. rep. DNV GL, 2016. URL: https://www.dnv.com.

[47] A. R. Dehghani-Sanij et al. "Study of energy storage systems and environmental challenges of batteries". In: *Renewable and Sustainable Energy Reviews* 104 (2019), pp. 192–208. ISSN: 1364-0321. URL: https://www.sciencedirect.com/science/article/pii/S1364032119300334.

[48] Z. Lyu. "Concept Design of Hybrid Crane Vessel". Embargo date: 2016-04-19. MA thesis. Delft University of Technology, 2016. URL: http://resolver.tudelft.nl/uuid:444bc057-6100-4f62-a02d-d85faadf928c.

[49] Nolann G. Williams et al. *A Comparative Analysis of Lithium-Ion Battery Chemistries for Cold-Climate Maritime Applications*. Tech. rep. United States, 2021. URL: https://www.osti.gov/biblio/1844295.

[50] M. A. Abdelkareem et al. "Environmental aspects of batteries". In: *Sustainable Horizons* 8 (2023), p. 100074. ISSN: 2772-7378. URL: https://www.sciencedirect.com/science/article/pii/S2772737823000287.

[51] S. Thangalakshmi and V. Ganeshram. "Energy Storage Systems - Possible Impacts on Maritime Sector". In: *International Journal of Innovative Research in Electrical, Electronics, Instrumentation and Control Engineering* 10 (6 2022). ISO 3297:2007 Certified, Impact Factor 7.047. URL: https://www.researchgate.net/publication/361500416_Energy_Storage_Systems_-Possible_Impacts_on_Maritime_Sector.

[52] Davut Solyali et al. "A comprehensive state-of-the-art review of electrochemical battery storage systems for power grids". In: *Energy Reviews* Not Provided.Not Provided (2022). First published: 10 August 2022, Not Provided. URL: https://doi.org/10.1002/er.8451.

[53] Peter Kurzweil. "Chapter 16 - Lithium Battery Energy Storage: State of the Art Including Lithium–Air and Lithium–Sulfur Systems". In: *Electrochemical Energy Storage for Renewable Sources and Grid Balancing*. Ed. by Patrick T. Moseley and Jürgen Garche. Elsevier, 2015, pp. 269–307. ISBN: 9780444626165. URL: https://www.sciencedirect.com/science/article/pii/B9780444626165000164.

[54] K Mongird et al. *Energy Storage Technology and Cost Characterization Report*. Tech. rep. PNNL-28866. Pacific Northwest National Laboratory (PNNL), 2019. URL: https://www.osti.gov/servlets/purl/1573487.

[55] Sayem M. Abu et al. "State of the art of lithium-ion battery material potentials: An analytical evaluations, issues and future research directions". In: *Journal of Cleaner Production* 394 (2023), p. 136246. ISSN: 0959-6526. URL: https://www.sciencedirect.com/science/article/pii/S0959652623004043.

[56] X. Chen et al. "An overview of lithium-ion batteries for electric vehicles". In: *2012 10th International Power & Energy Conference (IPEC)*. Ho Chi Minh City, Vietnam, 2012, pp. 230–235. URL: https://ieeexplore.ieee.org/document/6523269.

[57] Bao Zhang et al. "Spinel LiMn2O4 with Remarkable Electrochemical Performances by Synergistic Enhancement of Double-Cation (Sm3+, Mo6+) Doping for Li-Ion Batteries". In: *JOM* 74.12 (2022), pp. 4672–4681. URL: https://link.springer.com/article/10.1007/s11837-022-05429-3.

[58] European Maritime Safety Agency. *Study on Electrical Energy Storage for Ships: Battery Systems for Maritime Applications – Technology, Sustainability and Safety*. Tech. rep. [Online]. Available: itsflowingtothesoul/Shutterstock.com. European Maritime Safety Agency, 2020. URL: https://www.emsa.europa.eu/publications/item/3895-study-on-electrical-energy-storage-for-ships.html.

[59] Christian M. Julien and Alain Mauger. "NCA, NCM811, and the Route to Ni-Richer Lithium-Ion Batteries". In: *Energies* 13.23 (2020), p. 6363. URL: https://www.mdpi.com/1996-1073/13/23/6363.

[60] S. F. J. van Kleef. "A techno-economic analysis of the implementation of grid-connected battery energy storage systems into shore power installations in the port of Rotterdam". MSc. thesis. Delft, Netherlands: Delft University of Technology, 2023. URL: https://repository.tudelft.nl/record/uuid:84d12dc7-e621-40fc-a464-cbb035d552af.

[61] TYCORUN ENERGY. *NCA Battery Characteristics and Comparison - NCA vs NCM*. `https://www.takomabattery.com/nca-battery/`. Accessed: Aug. 18, 2024. 2023.

[62] Thomas Nemeth et al. "Lithium titanate oxide battery cells for high-power automotive applications – Electro-thermal properties, aging behavior and cost considerations". In: *Journal of Energy Storage* 31 (2020), p. 101656. ISSN: 2352-152X. URL: `https://www.sciencedirect.com/science/article/pii/S2352152X20314936`.

[63] L. Wang, J. Wang, L. Wang, et al. "A critical review on nickel-based cathodes in rechargeable batteries". In: *International Journal of Minerals, Metallurgy, and Materials* 29 (2022). Issue Date: May 2022, pp. 925–941. URL: `https://doi.org/10.1007/s12613-022-2446-z`.

[64] C. Chakkaravarthy et al. "The nickel/iron battery". In: *Journal of Power Sources* 35 (1 1991), pp. 21–35. ISSN: 0378-7753. URL: `https://www.sciencedirect.com/science/article/pii/037877539180002F`.

[65] Author's Name. *Nickel-Iron Batteries: Properties and Applications*. Accessed: Aug. 18, 2024. Elsevier, 2024. Chap. 11. URL: `https://www.sciencedirect.com/science/article/pii/B9781845697846500111`.

[66] M. Fetcenko, J. Koch, and M. Zelinsky. "Nickel–metal hydride and nickel–zinc batteries for hybrid electric vehicles and battery electric vehicles". In: *Advances in Battery Technologies for Electric Vehicles*. Ed. by Bruno Scrosati, Jürgen Garche, and Werner Tillmetz. Woodhead Publishing Series in Energy. Woodhead Publishing, 2015. Chap. 6, pp. 103–126. ISBN: 9781782423775. URL: `https://www.sciencedirect.com/science/article/pii/B9781782423775000066`.

[67] Constantine Spanos, Damon E. Turney, and Vasilis Fthenakis. "Life-cycle analysis of flow-assisted nickel zinc-, manganese dioxide-, and valve-regulated lead-acid batteries designed for demand-charge reduction". In: *Renewable and Sustainable Energy Reviews* 43 (2015), pp. 478–494. ISSN: 1364-0321. URL: `https://www.sciencedirect.com/science/article/pii/S1364032114008971`.

[68] Wei Chen et al. "Nickel-hydrogen batteries for large-scale energy storage". In: *Proceedings of the National Academy of Sciences* Not Provided.Not Provided (2018). Edited by Peidong Yang, University of California, Berkeley, and approved September 26, 2018 (received for review June 1, 2018), Not Provided. URL: `https://www.pnas.org/doi/epdf/10.1073/pnas.1809344115`.

[69] Chenglong Zhao et al. "Rational design of layered oxide materials for sodium-ion batteries". In: *Science* 370 (2020), pp. 708–711. URL: `https://doi.org/10.1126/science.aay9970`.

[70] Abraham Alem Kebede et al. "A comprehensive review of stationary energy storage devices for large scale renewable energy sources grid integration". In: *Renewable and Sustainable Energy Reviews* 159 (2022), p. 112213. ISSN: 1364-0321. URL: `https://www.sciencedirect.com/science/article/pii/S1364032122001368`.

[71] Deepak Kumar et al. "Progress and prospects of sodium-sulfur batteries: A review". In: *Solid State Ionics* 312 (2017), pp. 8–16. ISSN: 0167-2738. URL: `https://www.sciencedirect.com/science/article/pii/S0167273817306501`.

[72] Author's Name. "Title of the Article". In: *Journal Name* Volume Number.Issue Number (2024), Page Range. URL: `https://www.sciencedirect.com/science/article/pii/S0378775312008750`.

[73] Geoffrey J. May, Alistair Davidson, and Boris Monahov. "Lead batteries for utility energy storage: A review". In: *Journal of Energy Storage* 15 (2018), pp. 145–157. ISSN: 2352-152X. URL: `https://www.sciencedirect.com/science/article/pii/S2352152X17304437`.

[74] Anne Sorflakne and Marco Ottiker. "Electric & hybrid marine technology international". In: *Solid-state batteries* (2024), pp. 62–63.

[75] J. Ming et al. "Zinc-ion batteries: Materials, mechanisms, and applications". In: *Materials Science and Engineering: R: Reports* 135 (2019), pp. 58–84. ISSN: 0927-796X. URL: `https://www.sciencedirect.com/science/article/pii/S0927796X18301955`.

[76] A. M. Skundin, T. L. Kulova, and A. B. Yaroslavtsev. "Sodium-Ion Batteries (a Review)". In: *Russ. J. Electrochem.* 54.Not Provided (2018), pp. 113–152. DOI: `10.1134/S1023193518020076`.

[77] Xue Li, Hua Zhang, and Jie Sun. "Advanced Sodium-Ion Battery Materials and Their Electro-chemical Properties". In: *ACS Central Science* 6.10 (2020), pp. 1830–1838. URL: https://pubs.acs.org/doi/epdf/10.1021/acscentsci.0c00449.

[78] *Lead-acid characteristics*. https://www.researchgate.net/figure/Lead-acid-characteristics-4-5-7-8-19_tbl1_351220012. Accessed: 2024-07-23. 2021.

[79] Y. V. Frolov, A. G. Surin, and V. E. Fortunov. "Prospects for the development of polymeric materials with special properties". In: *Russian Chemical Reviews* (2017). URL: https://russchemrev.org/RCR4987pdf.

[80] G. L. Soloveichik. "Flow Batteries: Current Status and Trends". In: *Chemical Reviews* 115.20 (2015), pp. 11533–11558. DOI: 10.1021/cr500720t.

[81] Author's Name. "Title of the Article". In: *Journal Name* Volume Number.Issue Number (2024), Page Range. URL: https://pdf.sciencedirectassets.com/277423/1-s2.0-S0973082610X00059/1-s2.0-S0973082610000566/main.pdf.

[82] D. J. L. Brett, N. P. Brandon, and J. D. Van de Ven. "Electrochemical hydrogen compressors: Efficiency analysis and thermodynamic limitations". In: *Journal of Power Sources* 293 (2015), pp. 127–136. URL: https://ui.adsabs.harvard.edu/abs/2015JPS...293..127B/abstract.

[83] European Association for Storage of Energy (EASE). *Technical Document on Electrochemical Storage: Sodium-Nickel Chloride (NaNiCl2)*. Accessed: August 9, 2024. 2016. URL: https://ease-storage.eu/wp-content/uploads/2016/07/EASE_TD_Electrochemical_NaNiCl2.pdf.

[84] Andrea Coraddu et al. "Chapter 5 - Energy storage on ships". In: *Sustainable Energy Systems on Ships*. Ed. by Francesco Baldi, Andrea Coraddu, and Maria E. Mondejar. Elsevier, 2022, pp. 197–232. ISBN: 9780128244715. URL: https://www.sciencedirect.com/science/article/pii/B9780128244715000128.

[85] M. M. Kabir and Dervis Emre Demirocak. "Degradation mechanisms in Li-ion batteries: a state-of-the-art review". In: *Energy Reviews* (2017). First published: 26 April 2017. URL: https://onlinelibrary.wiley.com/doi/full/10.1002/er.3762.

[86] Maritime CleanTech. "Viking Lady". In: *Maritime CleanTech* (2024). Accessed: Aug. 7, 2024. URL: https://maritimecleantech.no/project/viking-lady/.

[87] Offshore Energy. *World's First Electric Car Ferry Enters Service*. Accessed: Aug. 7, 2024. 2024. URL: https://www.offshore-energy.biz/worlds-first-electric-car-ferry-enters-service/.

[88] Aspin Kemp & Associates (AKA). *Introducing Europe's First Hybrid Tugboat – The "e-KOTUG"*. Accessed: Aug. 7, 2024. 2012. URL: https://www.aka-group.com/introducing-europes-first-hybrid-tugboat-e-kotug/.

[89] Marcin Kolodziejski and Iwona Michalska-Pozoga. "Battery Energy Storage Systems in Ships' Hybrid/Electric Propulsion Systems". In: *Energies* 16.3 (2023), p. 1122. DOI: 10.3390/en16031122. URL: https://doi.org/10.3390/en16031122.

[90] G. Lucà Trombetta et al. "Lithium-ion batteries on board: A review on their integration for enabling the energy transition in shipping industry". In: *Energies* 17.5 (2024), p. 1019. URL: https://www.mdpi.com/1996-1073/17/5/1019.

[91] L. Wang et al. "Reviving lithium cobalt oxide-based lithium secondary batteries-toward a higher energy density". In: *Chemical Society Reviews* 47.17 (2018), pp. 6505–6602. URL: https://www.researchgate.net/publication/326062532_Reviving_lithium_cobalt_oxide-based_lithium_secondary_batteries-toward_a_higher_energy_density.

[92] X. Lin et al. "State of charge and lithium manganate batteries internal resistance estimation at low charge/discharge rates". In: *International Journal of Electrochemical Science* 16.1 (2021), p. 151024. URL: https://www.sciencedirect.com/science/article/pii/S1452398123008428.

[93] Y. Ding et al. "Automotive Li-ion batteries: current status and future perspectives". In: *Electrochemical Energy Reviews* 2 (2019), pp. 1–28. URL: https://link.springer.com/article/10.1007/s41918-018-0022-z.

[94] P. Hou et al. "Stabilizing the electrode/electrolyte interface of $LiNi_{0.8}Co_{0.15}Al_{0.05}O_2$ through tailoring aluminum distribution in microspheres as long-life, high-rate, and safe cathode for lithium-ion batteries". In: *ACS Applied Materials & Interfaces* 9.35 (2017), pp. 29643–29653. URL: https://pubs.acs.org/doi/10.1021/acsami.7b05986.

[95] N. Takami et al. "High-power and long-life lithium-ion batteries using lithium titanium oxide anode for automotive and stationary power applications". In: *Journal of Power Sources* 244 (2013), pp. 469–475. URL: https://www.sciencedirect.com/science/article/pii/S0378775312017296.

[96] Lukas Kistner, Astrid Bensmann, and Richard Hanke-Rauschenbach. "Potentials and limitations of battery-electric container ship propulsion systems". In: *Energy Conversion and Management: X* 21 (2024), p. 100507. ISSN: 2590-1745. URL: https://www.sciencedirect.com/science/article/pii/S2590174523001630.

[97] Climatebiz. *Lithium-Titanate Batteries: Everything You Need To Know*. Accessed: Aug. 09, 2024. 2023. URL: https://climatebiz.com/lithium-titanate-batteries/.

[98] *The Six Main Types of Lithium-ion Batteries*. Tritek Battery. URL: https://tritekbattery.com/the-six-main-types-of-lithium-ion-batteries/.

[99] T.-F. Yi J. Shu Y.-R. Zhu H. Zhu and R.-S. Zhu. "Li4Ti5O12: A promising anode material for high power lithium-ion batteries". In: *Ionics* 21.5 (2014), pp. 1113–1126. URL: https://link.springer.com/article/10.1007/s11581-014-1113-4.

[100] *Lithium Titanate Batteries Market Size, Share, Growth, Trends Analysis by 2032*. Accessed: Aug. 09, 2024. Precedence Research. 2024. URL: https://www.precedenceresearch.com/lithium-titanate-batteries-market.

[101] Jacqueline S. Edge et al. "Lithium Ion Battery Degradation: What You Need to Know". In: *Phys. Chem. Chem. Phys.* 23 (2021), pp. 8200–8221. URL: https://pubs.rsc.org/en/content/articlehtml/2021/cp/d1cp00359c.

[102] J. Jaguemont, L. Boulon, and Y. Dubé. "A comprehensive review of lithium-ion batteries used in hybrid and electric vehicles at cold temperatures". In: *Applied Energy* 164 (2016), pp. 99–114. ISSN: 0306-2619. URL: https://www.sciencedirect.com/science/article/pii/S0306261915014841.

[103] Mohamed Ben-Marzouk et al. "Experimental Protocols and First Results of Calendar and/or Cycling Aging Study of Lithium-Ion Batteries – the MOBICUS Project". In: *World Electric Vehicle Journal* 8.2 (2016), pp. 388–397. URL: https://doi.org/10.3390/wevj8020388.

[104] S. ten Cate Hoedemaker. *How to select a battery system for your ship?* https://www.maritimebatteryforum.com/news/maritime-batteries. Accessed: 2024-02-19. 2023.

[105] H. Ali et al. "Assessment of the Calendar Aging of Lithium-Ion Batteries for Long-Term Space Missions". In: *Frontiers in Energy Research* 11 (2023), p. 1108269. URL: https://www.frontiersin.org/journals/energy-research/articles/10.3389/fenrg.2023.1108269/full.

[106] S. Barcellona and L. Piegari. "Effect of current on cycle aging of lithium ion batteries". In: *Journal of Energy Storage* 29 (2020), p. 101310. ISSN: 2352-152X. URL: https://www.sciencedirect.com/science/article/pii/S2352152X19314574.

[107] L. Somerville et al. "The effect of charging rate on the graphite electrode of commercial lithium-ion cells: A post-mortem study". In: *Journal of Power Sources* 335 (2016), pp. 189–196. ISSN: 0378-7753. URL: https://www.sciencedirect.com/science/article/pii/S0378775316313842.

[108] K. Jalkanen et al. "Cycle aging of commercial NMC/graphite pouch cells at different temperatures". In: *Applied Energy* 154 (2015), pp. 160–172. ISSN: 0306-2619. URL: https://www.sciencedirect.com/science/article/pii/S0306261915005735.

[109] D. Anseán et al. "Fast charging technique for high power lithium iron phosphate batteries: A cycle life analysis". In: *Journal of Power Sources* 239 (2013), pp. 9–15. ISSN: 0378-7753. URL: https://www.sciencedirect.com/science/article/pii/S0378775313004357.

[110] John Wang et al. "Cycle-life model for graphite-LiFePO4 cells". In: *Journal of Power Sources* 196 (8 2011), pp. 3942–3948. ISSN: 0378-7753. URL: https://www.sciencedirect.com/science/article/pii/S0378775310021269.

[111] Xuebing Han et al. "Cycle Life of Commercial Lithium-Ion Batteries with Lithium Titanium Oxide Anodes in Electric Vehicles". In: *Energies* 7.8 (2014), pp. 4895–4909. URL: https://doi.org/10.3390/en7084895.

[112] Sijia Liu et al. "Analysis of cyclic aging performance of commercial Li4Ti5O12-based batteries at room temperature". In: *Energy* 173 (2019), pp. 1041–1053. ISSN: 0360-5442. URL: https://www.sciencedirect.com/science/article/pii/S0360544219303494.

[113] S. Barcellona et al. "Analysis of Ageing Effect on Li-Polymer Batteries". In: *The Scientific World Journal* 2015 (2015), pp. 1–8. DOI: 10.1155/2015/979321.

[114] *Praxis Automation Technology*. https://www.praxis-automation.eu. Accessed: 2024-07-23. 2024.

[115] L. Chen, Y. Tong, and Z. Dong. "Li-Ion Battery Performance Degradation Modeling for the Optimal Design and Energy Management of Electrified Propulsion Systems". In: *Energies* 13 (2020), p. 1629. URL: https://doi.org/10.3390/en13071629.

[116] D. Anseán et al. "Fast charging technique for high power lithium iron phosphate batteries: A cycle life analysis". In: *Journal of Power Sources* 239 (2013), pp. 9–15. ISSN: 0378-7753. URL: https://www.sciencedirect.com/science/article/pii/S0378775313004357.

[117] D. Anseán et al. "Fast charging technique for high power LiFePO4 batteries: A mechanistic analysis of aging". In: *Journal of Power Sources* 321 (2016), pp. 201–209. ISSN: 0378-7753. URL: https://www.sciencedirect.com/science/article/pii/S0378775316305249.

[118] L. Somerville et al. "The effect of charging rate on the graphite electrode of commercial lithium-ion cells: A post-mortem study". In: *Journal of Power Sources* 335 (2016), pp. 189–196. ISSN: 0378-7753. URL: https://www.sciencedirect.com/science/article/pii/S0378775316313842.

[119] J. Nájera et al. "Semi-empirical ageing model for LFP and NMC Li-ion battery chemistries". In: *Journal of Energy Storage* 72.Part A (2023), p. 108016. ISSN: 2352-152X. URL: https://www.sciencedirect.com/science/article/pii/S2352152X23014135.

[120] Ahmed Chahbaz et al. "Non-invasive identification of calendar and cyclic ageing mechanisms for lithium-titanate-oxide batteries". In: *Energy Storage Materials* 42 (2021), pp. 794–805. ISSN: 2405-8297. URL: https://www.sciencedirect.com/science/article/pii/S2405829721003950.

[121] W. Vermeer, G. R. Chandra Mouli, and P. Bauer. "A Comprehensive Review on the Characteristics and Modeling of Lithium-Ion Battery Aging". In: *IEEE Transactions on Transportation Electrification* 8.2 (2022), pp. 2205–2232. URL: https://ieeexplore.ieee.org/abstract/document/9662298.

[122] Yifan Zhang et al. "Energy storage system: Current studies on batteries and power condition system". In: *Applied Energy* 180 (2016), pp. 463–475. URL: https://www.sciencedirect.com/science/article/pii/S0306261916304500.

[123] Ankur Jain et al. "A review on Li-ion battery safety mechanisms and concerns: The issues, strategies, and testing standards". In: *Electrochimica Acta* 388 (2021), p. 138134. URL: https://www.sciencedirect.com/science/article/pii/S0013468621014237.

[124] Yiyang Li and Mengdi Wang. "Understanding Reinforcement Learning via Dissection and Unified Perspectives". In: *arXiv preprint arXiv:2308.07824* (2023). URL: https://arxiv.org/pdf/2308.07824.

[125] Jaeshin Yi et al. "Modeling the effect of aging on the electrical and thermal behaviors of a lithium-ion battery during constant current charge and discharge cycling". In: *Computers & Chemical Engineering* 99 (2017), pp. 31–39. URL: https://www.sciencedirect.com/science/article/pii/S0098135417300066.

[126] Junhan Huang et al. "A Novel Autoregressive Rainflow—Integrated Moving Average Modeling Method for the Accurate State of Health Prediction of Lithium-Ion Batteries". In: *Processes* 9.5 (2021), p. 795. URL: https://www.mdpi.com/2227-9717/9/5/795.

[127] Pablo A. Gonzalez et al. "Energy resilience assessment framework for multi-energy systems in hospitals: A case study". In: *Sustainable Cities and Society* 110 (2024), p. 104353. URL: https://www.sciencedirect.com/science/article/pii/S2352152X24004353.

[128] Yao Yang et al. "Real-time monitoring and ageing detection algorithm design with application on SiC-based automotive power drive system". In: *Automotive Power Electronics* (2023). URL: https://www.researchgate.net/publication/379000522_Real-time_monitoring_and_ageing_detection_algorithm_design_with_application_on_SiC-based_automotive_power_drive_system.

[129] Kailong Liu et al. "An evaluation study of different modelling techniques for calendar ageing prediction of lithium-ion batteries". In: *Renewable and Sustainable Energy Reviews* 131 (2020), p. 110017. ISSN: 1364-0321. DOI: 10.1016/j.rser.2020.110017.

[130] X. Wang et al. "Sizing and Control of a Hybrid Ship Propulsion System Using Multi-Objective Double-Layer Optimization". In: *IEEE Access* 9 (2021), pp. 72587–72601. DOI: 10.1109/ACCESS.2021.3080195.

[131] S. Mashayekh et al. "Optimum sizing of energy storage for an electric ferry ship". In: *2012 IEEE Power and Energy Society General Meeting*. San Diego, CA, USA, 2012, pp. 1–8. DOI: 10.1109/PESGM.2012.6345228.

[132] Mohammad Amini et al. "Optimal sizing of battery energy storage in a microgrid considering capacity degradation and replacement year". In: *Electric Power Systems Research* 195 (2021), p. 107170. ISSN: 0378-7796. URL: https://www.sciencedirect.com/science/article/pii/S0378779621001516.

[133] A. Anvari-Moghaddam et al. "Optimal planning and operation management of a ship electrical power system with energy storage system". In: *IECON 2016 - 42nd Annual Conference of the IEEE Industrial Electronics Society*. Florence, Italy, 2016, pp. 2095–2099. DOI: 10.1109/IECON.2016.7793272.

[134] C. Yan, G. K. Venayagamoorthy, and K. A. Corzine. "Optimal location and sizing of energy storage modules for a smart electric ship power system". In: *2011 IEEE Symposium on Computational Intelligence Applications In Smart Grid (CIASG)*. Paris, French Guiana, 2011, pp. 1–8. DOI: 10.1109/CIASG.2011.5953336.

[135] J. J. Valera-García and I. Atutxa-Lekue. "On the Optimal Design of Hybrid-Electric Power Systems for Offshore Vessels". In: *IEEE Transactions on Transportation Electrification* 5.1 (2019), pp. 324–334. DOI: 10.1109/TTE.2018.2883870.

[136] Onur Yuksel and Burak Koseoglu. "Numerical simulation of the hybrid ship power distribution system and an analysis of its emission reduction potential". In: *Ships and Offshore Structures* 18.1 (2023), pp. 78–94. DOI: 10.1080/17445302.2022.2028435.

[137] R. Tjandra et al. "Design consideration on size of hybrid electric marine vessel's battery energy storage-Ferry Case Study". In: *2017 Asian Conference on Energy, Power and Transportation Electrification (ACEPT)*. Singapore, 2017, pp. 1–5. DOI: 10.1109/ACEPT.2017.8168608.

[138] E. Ovrum and T.F. Bergh. "Modelling lithium-ion battery hybrid ship crane operation". In: *Applied Energy* 152 (2015), pp. 162–172. DOI: 10.1016/j.apenergy.2015.01.066.

[139] O. Yuksel and B. Koseoglu. "Numerical Simulation of the Hybrid Ship Power Distribution System and an Analysis of Its Emission Reduction Potential". In: *Ships and Offshore Structures* 18.1 (2023), pp. 78–94. DOI: 10.1080/17445302.2022.2028435.

[140] F. Balsamo et al. "Optimal Design and Energy Management of Hybrid Storage Systems for Marine Propulsion Applications". In: *Applied Energy* 278 (2020), p. 115629. DOI: 10.1016/j.apenergy.2020.115629.

[141] O. Mo R. Barrera-Cardenas and G. Guidi. "Optimal Sizing of Battery Energy Storage Systems for Hybrid Marine Power Systems". In: *IEEE* (2019), pp. 293–302. URL: https://ieeexplore-ieee-org.tudelft.idm.oclc.org/stamp/stamp.jsp?tp=&arnumber=8847932.

[142] I. A. Shkrob et al. "Fast charging of Li-ion cells: Part II. nonlinear contributions to cell and electrode polarization". In: *Journal of The Electrochemical Society* 166.14 (2019), A3305–A3313. URL: https://iopscience.iop.org/article/10.1149/2.0561914jes.

[143] W. Zhou et al. "Review on the Battery Model and SOC Estimation Method". In: *Processes* 9.9 (2021), p. 1685. URL: https://doi.org/10.3390/pr9091685.

[144] P. Gaikwad. "Online State Estimators for Lithium Ion Batteries". To obtain the degree of Master of Science in Sustainable Energy Technology. MA thesis. Delft, Netherlands: Delft University of Technology, 2023. URL: http://resolver.tudelft.nl/uuid:3308b4f1-3206-4cae-96ad-da908625c362.

[145] J. Meng et al. "Overview of Lithium-Ion Battery Modeling Methods for State-of-Charge Estimation in Electrical Vehicles". In: *Applied Sciences* 8.5 (2018), p. 659. ISSN: 2076-3417. URL: https://doi.org/10.3390/app8050659.

[146] E. Ovrum and T.F. Bergh. "Modelling lithium-ion battery hybrid ship crane operation". In: *Applied Energy* 152 (2015), pp. 162–172. ISSN: 0306-2619. URL: https://doi.org/10.1016/j.apenergy.2015.01.066.

[147] Shuzhi Zhang, Xu Guo, and Xiongwen Zhang. "Multi-objective decision analysis for data-driven based estimation of battery states: A case study of remaining useful life estimation". In: *International Journal of Hydrogen Energy* 45.27 (2020), pp. 14156–14173. ISSN: 0360-3199. URL: https://www.sciencedirect.com/science/article/pii/S0360319920310375.

[148] Javad Gholami and Mohammad Fallah Barzoki. "Electrochemical modeling and parameter sensitivity of lithium-ion battery at low temperature". In: *Journal of Energy Storage* 43 (2021), p. 103189. ISSN: 2352-152X. URL: https://www.sciencedirect.com/science/article/pii/S2352152X21008884.

[149] Saehong Park et al. "Optimal Experimental Design for Parameterization of an Electrochemical Lithium-Ion Battery Model". In: *Journal of The Electrochemical Society* 165.7 (2018), A1309. URL: https://iopscience.iop.org/article/10.1149/2.0421807jes/pdf.

[150] L. Zhang et al. "Comparative research on RC equivalent circuit models for lithium-ion batteries of electric vehicles". In: *Applied Sciences* 7.10 (2017), p. 1002. URL: https://www.mdpi.com/2076-3417/7/10/1002.

[151] M. Hossain et al. "A Parameter Extraction Method for the Thevenin Equivalent Circuit Model of Li-ion Batteries". In: *2019 IEEE Industry Applications Society Annual Meeting*. Baltimore, MD, USA, 2019, pp. 1–7. DOI: 10.1109/IAS.2019.8912326.

[152] B. Chen et al. "An approach for state of charge estimation of Li-ion battery based on Thevenin equivalent circuit model". In: *2014 Prognostics and System Health Management Conference (PHM-2014 Hunan)*. Zhangjiajie, China, 2014, pp. 647–652. DOI: 10.1109/PHM.2014.6988253.

[153] Byongug Jeong et al. "An effective framework for life cycle and cost assessment for marine vessels aiming to select optimal propulsion systems". In: *Journal of Cleaner Production* 187 (2018), pp. 111–130. ISSN: 0959-6526. URL: https://www.sciencedirect.com/science/article/pii/S0959652618308552.

[154] M. Bayraktar and M. Nuran. "Multi-Criteria Decision Making using TOPSIS Method for Battery Type Selection in Hybrid Propulsion System". In: *Transactions on Maritime Science* 11.1 (2022), pp. 45–53. DOI: 10.7225/toms.v11.n01.w02.

[155] H. Xuan et al. "Decision-Making on the Selection of Clean Energy Technology for Green Ships Based on the Rough Set and TOPSIS Method". In: *J. Mar. Sci. Eng.* 10 (2022), p. 579. URL: https://doi.org/10.3390/jmse10050579.

[156] S. ten Cate Hoedemaker. "Battery Aging in Full Electric Ships". Publicly defended on Tuesday September 12, 2017 at 10:00 AM. MSc Thesis. Delft, Netherlands: Delft University of Technology, Sept. 2017.

[157] Cristian Morales. *A Methodology to Select the Electric Propulsion System for Platform Supply Vessels (PSV)*. Accessed: date. 2014. URL: https://www.teses.usp.br/teses/disponiveis/3/3135/tde-26122014-164655/publico/Dissertacao_Cristian_Morales.pdf.

[158] T. L. Saaty. "Decision making — the Analytic Hierarchy and Network Processes (AHP/ANP)". In: *Journal of Systems Science and Systems Engineering* 13 (2004), pp. 1–35. URL: https://doi.org/10.1007/s11518-006-0151-5.

[159] Maja Perčić et al. "Life-cycle assessment and life-cycle cost assessment of power batteries for all-electric vessels for short-sea navigation". In: *Energy* 251 (2022), p. 123895. ISSN: 0360-5442. URL: https://www.sciencedirect.com/science/article/pii/S0360544222007988.

[160] Jaroslaw Krzywanski et al. "Advanced Computational Methods for Modeling, Prediction and Optimization—A Review". In: *Materials* 17.14 (2024), p. 3521. URL: https://www.mdpi.com/1996-1944/17/14/3521.

[161] ABB. *ABB Industrial Drives: ACS880, Drive Modules, 0.55 to 3200 kW*. Available: https://library.e.abb.com/public/a8d78c07a8c14df692f81896524a6f1f/ACS880_drive_modules_catalog_3AUA0000115038_RevO_EN_lowres.pdf. ABB. 2024.

[162] ABB Industrial Drives. *ACS880-1604LC DC/DC-converter modules Hardware Manual*. 3AXD50000371631 Rev C. 2024. URL: https://library.e.abb.com/public/eaeed051221c4d1aa2f54a34709c6087/EN_ACS880-1604LC_HW_C_A4.pdf.

[163] I. Georgescu, M. Godjevac, and K. Visser. "Efficiency Constraints of Energy Storage for On-Board Power Systems". In: *Ocean Engineering* 162 (2018), pp. 239–247. DOI: 10.1016/j.oceaneng.2018.05.004. URL: https://www.sciencedirect.com/science/article/pii/S0029801818307030.

[164] Q. Wang, Q. Wo, and W. Qi. "Adaptive Optimal Charge Strategy for Lithium-ion Power Battery Based on Multi-Objective Algorithm". In: *Journal of Control, Automation and Electrical Systems* 32.6 (2021), pp. 1408–1416. DOI: 10.1007/s40313-021-00759-0.

[165] Leclanché Energy Storage Solutions. *Navius MRS-3 Marine Battery System*. https://www.leclanche.com/leclanche-announces-development-of-third-generation-marine-battery-system-for-electrification-of-broad-range-of-vessels/. Accessed: 2023-02-01.

[166] Tesvolt. *Tesvolt Maritime Solutions, System specifications*. Accessed: 2023-02-01. 2020. URL: https://www.tesvolt-maritime.com/en/.

[167] Toshiba. *Toshiba Rechargeable Battery SCiB*. https://www.global.toshiba/ww/products-solutions/battery/scib/product/cell/high-energy.html. Accessed: 2023-02-01.

[168] Ship & Bunker. *Global Average Bunker Price*. https://shipandbunker.com/prices/av/global/av-glb-global-average-bunker-price#MGO. Accessed: 2024-07-20. 2024.

[169] Martin Winter and Ralph J. Brodd. "What Are Batteries, Fuel Cells, and Supercapacitors?" In: *Chemical Reviews* 104.10 (2004), pp. 4245–4270. URL: https://pubs.acs.org/doi/abs/10.1021/cr020730k.

[170] Ronald Dell and David Anthony James Rand. *Understanding Batteries*. Accessed on: February 13, 2024. The Royal Society of Chemistry, 2001. ISBN: 0-85404-605-4. URL: https://books.google.nl/books?id=-VJg6gLmy2UC.

A
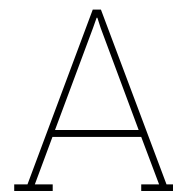
Appendix

A.1. Classification of Batteries

There are two types of batteries: primary and secondary. A primary cell is designed for a single use, unlike a secondary cell that can be recharged for repeated usage. Generally, the chemical process within a primary cell is irreversible, making it non-rechargeable [51]. On the other hand, the chemical process of secondary cells can be reversed. The later are difficult to use and have higher initial costs than primary cells. Because they are rechargeable, these batteries typically have less of an adverse effect on the environment [50], [47].

A.1.1. Traditional Rechargeable Batteries

Batteries store electrical energy by acting as chemical reservoirs. They are made up of one or more electrochemical cells with electrodes, an electrolyte, and an external circuit that are connected in parallel or series. Chemical energy is transformed into electrical energy at these electrodes through processes known as reduction-oxidation (redox) reactions [169]. Within these cells, the electrodes, separated by the electrolyte, facilitate the transfer of electrons through an external circuit and the movement of ions through the electrolyte. The atoms at the reaction electrodes undergo a change in oxidation state as a result of this process. One electrode undergoes oxidation, losing electrons and positive ions (cations) that are then transported to the other electrode, leading to a gain of electrons and cations, thus undergoing reduction. In contrast to how cations move, negative ions, or anions, move in the opposite direction. The electrode undergoing oxidation is often referred to as the negative electrode, anode, or reducing agent, on the other hand, the electrode that is reducing is known as the cathode, oxidizing agent, or positive electrode. During discharge, the negative electrode functions as the anode, but during charging, the roles reverse due to the change in the redox reaction. The negative/positive electrode designation does not change over the course of the battery's operation, in contrast to the anode/cathode labels. The battery's discharge and charge reactions are reversible, with discharge occurring naturally due to a built-in driving force, while charging requires additional work against this natural driving force. This driving force is produced by the potential difference between the half-reactions at the electrodes [170].
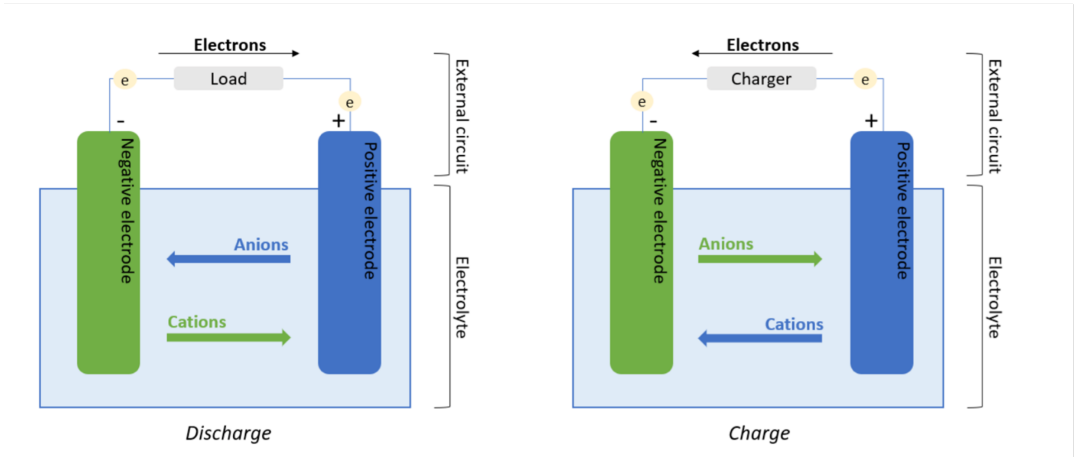
Figure A.1: Diagram Illustrating a Typical Battery Configuration
[60]

A.2. Rint Model Parameters

Parameter		NMC	LFP	LTO	unit
Physical parameter					
Charge capacity (cell)		65	230	23	[Ah]
Energy capacity (cell)		0.252	0.733	0.0528	[kWh]
Operating parameter					
Max. charging C-rate		1	0.7	4.34	[A/Ah]
Max. discharging C-rate		-2.8	-0.7	-4.34	[A/Ah]
Economic parameter					
Specific investment costs		500	460	700	[euros/kWh]
Defined end-of-life capacity		80	70	70	[%]
Max. equivalent full cycles		7,000	6,500	20,000	[-]
Fit parameter					
Open circuit voltage charging	$c_{\mathrm{cha},1}$	-314.48	-284.96	-535.885	[V]
	$c_{\mathrm{cha},2}$	0.308	0.125	0.4269	[V]
	$c_{\mathrm{cha},3}$	317.99	288.231	537.95	[V]
	$c_{\mathrm{cha},4}$	13.931	18.42	-10.119	[V]
	$c_{\mathrm{cha},5}$	0.273	0.199	-1.1799	[V]
	$c_{\mathrm{cha},6}$	8.15E-03	2.90E-78	6.34E-08	[V]
	$c_{\mathrm{cha},7}$	3.674	177.178	19.896	[V]
Open circuit voltage discharging	$c_{\mathrm{dis},1}$	-180.9	-1201.59	0.0685	[V]
	$c_{\mathrm{dis},2}$	-3.796	0.154	0.339	[V]
	$c_{\mathrm{dis},3}$	172.524	1204.77	2	[V]
	$c_{\mathrm{dis},4}$	6.499	24.608	14.326	[V]
	$c_{\mathrm{dis},5}$	0.5347	0.1689	0.18249	[V]
	$c_{\mathrm{dis},6}$	11.921	3.78E-110	1.24E-03	[V]
	$c_{\mathrm{dis},7}$	0.3129	250.4175	5.081	[V]

Parameter	NMC	LFP	LTO	unit
Inner charge resistance	0.000934	0.0003237	0.001315	[ohm]
Inner discharge resistance	0.001093	0.0003797	0.001098	[ohm]

A.3. Functions Battery Solutions Metrics

A.3.1. Load Smoothing Function

No.	Combination	FC [tonnes/year]	MC [euros/year]	SD [%]	Lifetime [years]	Total Savings [euros/year]	ROI
1	LFP, 3600kW, [0.6-0.3]60s, rr=0.005	13,812	1,010,956	1.54	14.42	355,447	1.17
2	LFP, 3600kW, [0.6-0.3]60s, rr=0.05	13,812	1,010,945	1.80	14.30	355,358	1.15
3	LFP, 7200kW, [0.8-0.5]60s, rr=0.05	13,565	879,232	3.99	14.88	663,910	1.09
4	LFP, 7200kW, [0.8-0.5]120s, rr=0.005	13,562	880,472	3.88	14.84	664,739	1.09
5	LFP, 7200kW, [0.8-0.5]120s, rr=0.05	13,564	880,472	3.91	14.67	663,526	1.06
6	LTO, 7200kW, [0.8-0.5]60s, rr=0.005	13,564	879,079	2.33	10.37	664,578	4.93
7	LTO, 7200kW, [0.8-0.5]60s, rr=0.05	13,566	879,075	2.68	10.34	663,539	4.91
8	LTO, 7200kW, [0.6-0.3]60s, rr=0.005	13,823	1,010,966	0.93	13.17	347,539	2.94
9	LTO, 7200kW, [0.6-0.3]60s, rr=0.005	13,836	1,010,979	0.57	10.30	337,643	2.00

Table A.2: Load Smoothing Best Solutions Case 1 Metrics

No.	Combination	FC [tonnes/year]	MC [euros/year]	SD [%]	Lifetime [years]	Total Savings [euros/year]	ROI
10	LTO, 7200kW, [0.6-0.3]60s, rr=0.05	13,822	1,010,945	1.28	13.66	347,999	3.09
11	LTO, 7200kW, [0.6-0.3]60s, rr=0.05	13,837	1,010,974	0.62	10.31	336,985	1.99
12	LTO, 7200kW, [0.6-0.3]120s, rr=0.005	13,807	1,004,631	1.17	10.11	364,684	2.17
13	LTO, 7200kW, [0.6-0.3]120s, rr=0.05	13,808	1,004,628	2.06	10.22	364,300	2.20
14	NMC, 14400kW, [0.8-0.5]60s, rr=0.005	13,560	879,012	3.00	13.80	667,497	2.58
15	NMC, 14400kW, [0.8-0.5]60s, rr=0.005	13,565	879,081	0.40	11.16	664,312	1.88
16	NMC, 14400kW, [0.8-0.5]60s, rr=0.05	13,566	879,075	1.39	11.13	663,497	1.87
17	NMC, 14400kW, [0.6-0.3]60s, rr=0.005	13,823	1,010,955	0.41	14.23	347,543	0.92
18	NMC, 14400kW, [0.6-0.3]60s, rr=0.05	13,821	1,010,945	1.17	14.84	348,533	1.01
19	NMC, 14400kW, [0.9-0.6]60s, rr=0.005	13,494	843,940	4.34	11.15	750,514	2.25
20	NMC, 14400kW, [0.6-0.3]120s, rr=0.005	13,795	1,004,631	3.58	13.89	373,495	1.02

Table A.2: Load Smoothing Best Solutions Case 1 Metrics

No.	Combination	FC [tonnes/year]	MC [euros/year]	SD [%]	Lifetime [years]	Total Savings [euros/year]	ROI
21	LTO, 14400kW, [0.8-0.5]60s, rr=0.005, MAW5	13,578	879,231	0.05	14.93	654,535	3.21
22	LTO, 14400kW, [0.8-0.5]60s, rr=0.05	13,582	879,237	2.22	14.27	651,736	3
23	LTO, 14400kW, [0.8-0.5]120s, rr=0.005	13,580	880,472	0.15	14.29	651,877	3.01
24	LTO, 14400kW, [0.8-0.5]120s, rr=0.05	13,583	880,472	0.64	14.06	649,817	2.93
25	LTO, 14400kW, [0.6-0.3]120s, rr=0.005	13,835	1,004,655	0	14.09	344,612	1.09
26	LTO, 14400kW, [0.6-0.3]120s, rr=0.05	13,838	1,004,655	0.01	14.02	342,866	1.07
27	LTO, 14400kW, [0.6-0.3]300s, rr=0.005	13,784	988,827	4.84	13.71	397,487	1.35

Table A.2: Load Smoothing Best Solutions Case 1 Metrics

No.	Combination	FC [tonnes/year]	MC [euros/year]	SD [%]	Lifetime [years]	Total Savings [euros/year]	ROI
1	NMC, 1,800kW, [0.6-0.3]60s, rr=0.005	13,812	1,032,622	2.576	2.600	333,249	1.696
2	NMC, 1,800kW, [0.6-0.3]60s, rr=0.05	13,813	1,032,611	2.659	2.579	333,024	1.672
3	LFP, 1,800kW, [0.6-0.3]60s, rr=0.005	13,811	1,032,622	2.572	6.035	334,170	0.705
4	LFP, 1,800kW, [0.6-0.3]60s, rr=0.005	13,817	1,032,637	2.432	5.518	329,770	0.538
5	LFP, 1,800kW, [0.6-0.3]60s, rr=0.05	13,811	1,032,613	2.659	5.988	334,457	0.693
6	LTO, 1,800kW, [0.6-0.3]60s, rr=0.005	13,815	1,032,622	2.580	3.100	331,625	2.541
7	LTO, 1,800kW, [0.6-0.3]60s, rr=0.005	13,820	1,032,637	2.432	2.833	327,928	2.200
8	LTO, 1,800kW, [0.6-0.3]60s, rr=0.005	13,823	1,032,637	2.432	2.598	325,387	1.912
9	LTO, 1,800kW, [0.6-0.3]60s, rr=0.05	13,815	1,032,599	2.659	3.078	331,290	2.512
10	LTO, 1,800kW, [0.6-0.3]60s, rr=0.05	13,821	1,032,618	2.432	2.773	327,318	2.126
11	LTO, 1,800kW, [0.6-0.3]60s, rr=0.05	13,822	1,032,632	2.432	2.520	326,071	1.831
12	NMC, 3,600kW, [0.6-0.3]60s, rr=0.005	13,819	1,032,626	1.537	3.693	328,660	0.888

Table A.3: Load Smoothing Best Solutions Case 2 Metrics

No.	Combination	FC [tonnes/year]	MC [euros/year]	SD [%]	Lifetime [years]	Total Savings [euros/year]	ROI
13	NMC, 3,600kW, [0.6-0.3]60s, rr=0.05	13,819	1,032,615	1.780	3.714	328,545	0.898
14	LFP, 3,600kW, [0.6-0.3]60s, rr=0.005	13,815	1,032,626	1.537	7.431	331,114	0.040
15	LFP, 3,600kW, [0.6-0.3]60s, rr=0.05	13,815	1,032,615	1.780	7.412	331,069	0.037
16	LTO, 3,600kW, [0.6-0.3]60s, rr=0.005	13,821	1,032,626	1.537	3.837	326,894	1.160
17	LTO, 3,600kW, [0.6-0.3]60s, rr=0.005	13,833	1,032,640	1.219	3.514	318,391	0.927
18	LTO, 3,600kW, [0.6-0.3]60s, rr=0.005	13,845	1,032,649	1.221	3.124	309,410	0.665
19	LTO, 3,600kW, [0.6-0.3]60s, rr=0.05	13,821	1,032,615	1.780	3.843	326,756	1.163
20	LTO, 3,600kW, [0.6-0.3]60s, rr=0.05	13,834	1,032,620	1.228	3.502	317,850	0.917
21	LTO, 3,600kW, [0.6-0.3]60s, rr=0.05	13,840	1,032,637	1.139	3.215	313,465	0.736
22	LTO, 3,600kW, [0.6-0.3]120s, rr=0.005	13,804	1,026,186	2.130	3.497	345,516	1.081
23	LTO, 3,600kW, [0.6-0.3]120s, rr=0.005	13,814	1,026,187	1.008	3.127	338,558	0.823
24	LTO, 3,600kW, [0.6-0.3]120s, rr=0.05	13,804	1,026,016	2.354	3.492	345,473	1.078

Table A.3: Load Smoothing Best Solutions Case 2 Metrics

No.	Combination	FC [tonnes/year]	MC [euros/year]	SD [%]	Lifetime [years]	Total Savings [euros/year]	ROI
25	LTO, 3,600kW, [0.6-0.3]120s, rr=0.05	13,809	1,026,103	0.926	3.206	341,985	0.888
26	NMC, 7,200kW, [0.8-0.5]60s, rr=0.005	13,568	906,512	2.320	4.591	634,442	1.265
27	NMC, 7,200kW, [0.8-0.5]60s, rr=0.005	13,577	906,660	1.990	3.890	628,271	0.901
28	NMC, 7,200kW, [0.8-0.5]60s, rr=0.05	13,570	906,508	2.680	4.585	633,535	1.259
29	NMC, 7,200kW, [0.8-0.5]60s, rr=0.05	13,579	906,659	3.985	3.803	626,471	0.853
30	NMC, 7,200kW, [0.9-0.6]60s, rr=0.005	13,499	872,590	4.493	3.928	718,148	1.194
31	NMC, 7,200kW, [0.8-0.5]120s, rr=0.005	13,574	906,058	3.911	3.802	630,435	0.864
32	NMC, 7,200kW, [0.8-0.5]120s, rr=0.05	13,576	906,060	3.912	3.777	628,972	0.848
33	LFP, 7,200kW, [0.8-0.5]60s, rr=0.005	13,563	906,512	2.312	8.274	638,357	0.116
34	LFP, 7,200kW, [0.8-0.5]60s, rr=0.005	13,570	906,662	1.986	7.595	632,990	0.016
35	LFP, 7,200kW, [0.8-0.5]60s, rr=0.05	13,564	906,508	2.680	8.270	637,709	0.115
36	LFP, 7,200kW, [0.8-0.5]60s, rr=0.05	13,572	906,663	3.985	7.508	631,902	0.003

Table A.3: Load Smoothing Best Solutions Case 2 Metrics

No.	Combination	FC [tonnes/year]	MC [euros/year]	SD [%]	Lifetime [years]	Total Savings [euros/year]	ROI
37	LFP, 7,200kW, [0.9-0.6]60s, rr=0.005	13,492	872,592	4.485	7.649	722,850	0.169
38	LFP, 7,200kW, [0.8-0.5]120s, rr=0.005	13,568	906,061	3.883	7.505	635,235	0.008
39	LFP, 7,200kW, [0.8-0.5]120s, rr=0.05	13,569	906,061	3.908	7.475	633,986	0.002
40	LTO, 7,200kW, [0.8-0.5]60s, rr=0.005	13,571	906,512	2.329	4.307	632,480	1.346
41	LTO, 7,200kW, [0.8-0.5]60s, rr=0.005	13,582	906,637	2.076	3.947	624,729	1.123
42	LTO, 7,200kW, [0.8-0.5]60s, rr=0.05	13,572	906,508	2.680	4.304	631,442	1.340
43	LTO, 7,200kW, [0.8-0.5]60s, rr=0.05	13,582	906,628	3.205	3.955	624,188	1.126
44	LTO, 7,200kW, [0.6-0.3]60s, rr=0.005	13,826	1,032,637	0.926	4.559	323,177	0.269
45	LTO, 7,200kW, [0.6-0.3]60s, rr=0.005	13,840	1,032,649	0.572	4.300	313,473	0.161
46	LTO, 7,200kW, [0.6-0.3]60s, rr=0.05	13,826	1,032,615	1.261	4.595	323,708	0.281
47	LTO, 7,200kW, [0.6-0.3]60s, rr=0.05	13,841	1,032,644	0.621	4.300	312,790	0.158
48	LTO, 7,200kW, [0.9-0.6]60s, rr=0.005	13,504	872,571	4.555	3.972	714,547	1.444

Table A.3: Load Smoothing Best Solutions Case 2 Metrics

No.	Combination	FC [tonnes/year]	MC [euros/year]	SD [%]	Lifetime [years]	Total Savings [euros/year]	ROI
49	LTO, 7,200kW, [0.8-0.5]120s, rr=0.005	13,578	906,034	4.066	3.913	628,187	1.117
50	LTO, 7,200kW, [0.8-0.5]120s, rr=0.05	13,579	906,029	4.032	3.939	627,111	1.127
51	LTO, 7,200kW, [0.6-0.3]120s, rr=0.005	13,811	1,026,186	1.168	4.278	340,568	0.255
52	LTO, 7,200kW, [0.6-0.3]120s, rr=0.005	13,830	1,026,201	0.469	3.888	326,627	0.093
53	LTO, 7,200kW, [0.6-0.3]120s, rr=0.05	13,812	1,026,183	1.980	4.290	340,192	0.257
54	LTO, 7,200kW, [0.6-0.3]120s, rr=0.05	13,827	1,026,154	0.404	3.932	328,874	0.114
55	NMC, 14,400kW, [0.8-0.5]60s, rr=0.005	13,567	906,445	2.979	6.576	635,234	0.624
56	NMC, 14,400kW, [0.8-0.5]60s, rr=0.005	13,571	906,514	0.395	6.146	632,209	0.511
57	NMC, 14,400kW, [0.8-0.5]60s, rr=0.005	13,582	906,663	0.049	5.436	624,715	0.321
58	NMC, 14,400kW, [0.8-0.5]60s, rr=0.05	13,572	906,509	1.388	6.140	631,389	0.508
59	NMC, 14,400kW, [0.9-0.6]60s, rr=0.005	13,501	872,401	4.344	6.142	716,880	0.712
60	NMC, 14,400kW, [0.9-0.6]60s, rr=0.005	13,504	872,600	0.334	5.471	714,329	0.520

Table A.3: Load Smoothing Best Solutions Case 2 Metrics

No.	Combination	FC [tonnes/year]	MC [euros/year]	SD [%]	Lifetime [years]	Total Savings [euros/year]	ROI
61	LTO, 14,400kW, [0.8-0.5]60s, rr=0.005	13,569	906,445	2.993	5.090	633,879	0.389
62	LTO, 14,400kW, [0.8-0.5]60s, rr=0.005	13,574	906,514	0.411	4.946	630,640	0.343
63	LTO, 14,400kW, [0.8-0.5]60s, rr=0.005	13,584	906,663	0.053	4.680	622,621	0.255
64	LTO, 14,400kW, [0.8-0.5]60s, rr=0.05	13,575	906,509	1.388	4.943	629,780	0.340
65	LTO, 14,400kW, [0.8-0.5]60s, rr=0.05	13,589	906,668	2.218	4.637	619,733	0.237
66	LTO, 14,400kW, [0.9-0.6]60s, rr=0.005	13,503	872,401	4.386	4.943	715,261	0.522
67	LTO, 14,400kW, [0.9-0.6]60s, rr=0.005	13,507	872,599	0.334	4.692	712,202	0.439
68	LTO, 14,400kW, [0.8-0.5]120s, rr=0.005	13,586	906,061	0.150	4.639	622,373	0.243
69	LTO, 14,400kW, [0.8-0.5]120s, rr=0.05	13,589	906,061	0.644	4.623	620,293	0.235

Table A.3: Load Smoothing Best Solutions Case 2 Metrics

A.3.2. Optimal Range Function

No.	Combination	FC [tonnes/year]	MC [euros/year]	SD [%]	Lifetime [years]	Total Savings [euros/year]	ROI
1	LFP, 7200kW, [0.7-0.2]60s, OR=[0.6-0.95]	13,457.63	844,133.83	4.20	10.83	776,161.82	0.78
2	LTO, 14400kW, [0.8-0.5]60s, OR=[0.6-0.95]	13,557.24	879,202.19	0	14.16	669,638.35	3.08
3	LTO, 14400kW, [0.8-0.5]60s, OR=[0.7-0.9]	13,553.64	879,158.96	0	13.18	672,259.80	2.81
4	LTO, 14400kW, [0.6-0.3]60s, OR=[0.6-0.95]	13,808.01	1,011,058.41	0	12.91	357,880.42	0.99
5	LTO, 14400kW, [0.6-0.3]60s, OR=[0.7-0.9]	13,799.27	1,011,029.93	0	12.21	364,173.19	0.91
6	LTO, 14400kW, [0.9-0.6]60s, OR=[0.6-0.95]	13,487.24	844,075.28	0	14.72	754,980.22	3.79
7	LTO, 14400kW, [0.9-0.6]60s, OR=[0.7-0.9]	13,485.04	844,000.97	0	13.60	756,635.71	3.43
8	LTO, 14400kW, [0.8-0.5]120s, OR=[0.6-0.95]	13,561.13	880,515.61	0	13.33	665,535.21	2.82
9	LTO, 14400kW, [0.8-0.5]120s, OR=[0.7-0.9]	13,553.95	880,477.38	0	12.72	670,719.81	2.67
10	LTO, 14400kW, [0.6-0.3]120s, OR=[0.6-0.95]	13,784.15	1,004,673.18	0	12.72	381,376.60	1.09

Table A.4: Optimal Range Best Solutions Case 1 Metrics

No.	Combination	FC [tonnes/year]	MC [euros/year]	SD [%]	Lifetime [years]	Total Savings [euros/year]	ROI
11	LTO, 14400kW, [0.6-0.3]120s, OR=[0.7-0.9]	13,773.22	1,004,657.26	0	12.20	389,237.98	1.04
12	LTO, 14400kW, [0.9-0.6]120s, OR=[0.6-0.95]	13,500.38	846,261.09	0.44	13.58	743,367.77	3.35
13	LTO, 14400kW, [0.9-0.6]120s, OR=[0.7-0.9]	13,493.38	846,216.67	0	12.84	748,437.72	3.14
14	LTO, 14400kW, [0.8-0.5]300s, OR=[0.6-0.95]	13,576.03	883,428.63	2.08	12.67	651,926.57	2.56
15	LTO, 14400kW, [0.8-0.5]300s, OR=[0.7-0.9]	13,564.31	883,402.94	1.26	12.26	660,361.71	2.49
16	LTO, 14400kW, [0.6-0.3]300s, OR=[0.6-0.95]	13,738.82	988,832.28	0.04	12.59	429,737.38	1.33
17	LTO, 14400kW, [0.6-0.3]300s, OR=[0.7-0.9]	13,726.68	988,828.07	0.13	12.32	438,453.17	1.33

Table A.4: Optimal Range Best Solutions Case 1 Metrics

No.	Combination	FC [tonnes/year]	MC [euros/year]	SD [%]	Lifetime [years]	Total Savings [euros/year]	ROI
1	LTO, 1800kW, [0.6-0.3]60s, OR=[0.6-0.95]	13,769.26	1,032,636.76	2.43	1.90	364,098.56	1.38
2	LTO, 1800kW, [0.6-0.3]60s, OR=[0.7-0.9]	13,769.81	1,032,636.76	2.43	1.82	363,705.78	1.28
3	LTO, 3600kW, [0.6-0.3]300s, OR=[0.6-0.95]	13,657.00	1,009,903.55	2.71	2.36	467,371.10	0.90
4	LTO, 3600kW, [0.6-0.3]300s, OR=[0.7-0.9]	13,651.84	1,009,904.49	2.71	2.14	471,066.28	0.73
5	NMC, 7200kW, [0.9-0.6]60s, OR=[0.6-0.95]	13,464.96	872,553.46	4.20	3.47	742,485.03	1.00
6	LTO, 7200kW, [0.8-0.5]60s, OR=[0.6-0.95]	13,528.05	906,608.98	1.99	3.69	663,169.56	1.11
7	LTO, 7200kW, [0.8-0.5]60s, OR=[0.7-0.9]	13,508.55	906,555.58	1.99	3.38	677,211.85	0.97
8	LTO, 7200kW, [0.9-0.6]60s, OR=[0.6-0.95]	13,469.78	872,523.46	4.21	3.81	739,060.61	1.43
9	LTO, 7200kW, [0.9-0.6]60s, OR=[0.7-0.9]	13,450.07	872,418.86	4.21	3.49	753,305.16	1.26
10	LTO, 7200kW, [0.8-0.5]120s, OR=[0.6-0.95]	13,529.78	906,060.75	3.73	3.70	662,479.04	1.11

Table A.5: Optimal Range Best Solutions Case 2 Metrics

No.	Combination	FC [tonnes/year]	MC [euros/year]	SD [%]	Lifetime [years]	Total Savings [euros/year]	ROI
11	LTO, 7200kW, [0.8-0.5]120s, OR=[0.7-0.9]	13,509.53	906,033.39	3.73	3.42	677,029.06	0.99
12	LTO, 7200kW, [0.6-0.3]300s, OR=[0.6-0.95]	13,668.67	1,009,904.03	1.19	3.40	458,991.39	0.34
13	LTO, 7200kW, [0.6-0.3]300s, OR=[0.7-0.9]	13,643.52	1,009,904.49	1.35	3.13	477,038.50	0.29
14	NMC, 14400kW, [0.9-0.6]60s, OR=[0.6-0.95]	13,492.07	872,539.87	0	5.31	723,051.14	0.49
15	NMC, 14400kW, [0.9-0.6]60s, OR=[0.7-0.9]	13,488.62	872,480.35	0	5.10	725,588.18	0.44
16	NMC, 14400kW, [0.9-0.6]120s, OR=[0.6-0.95]	13,504.65	874,212.52	0.06	5.12	712,354.70	0.42
17	LTO, 14400kW, [0.8-0.5]60s, OR=[0.6-0.95]	13,563.50	906,633.78	0	4.65	637,715.01	0.28
18	LTO, 14400kW, [0.8-0.5]60s, OR=[0.7-0.9]	13,560.16	906,590.55	0	4.58	640,155.18	0.26

Table A.5: Optimal Range Best Solutions Case 2 Metrics

No.	Combination	FC [tonnes/year]	MC [euros/year]	SD [%]	Lifetime [years]	Total Savings [euros/year]	ROI
19	LTO, 14400kW, [0.9-0.6]60s, OR=[0.6-0.95]	13,494.18	872,538.89	0	4.69	721,541.45	0.46
20	LTO, 14400kW, [0.9-0.6]60s, OR=[0.7-0.9]	13,492.04	872,466.46	0	4.61	723,144.69	0.44
21	LTO, 14400kW, [0.8-0.5]120s, OR=[0.6-0.95]	13,566.60	906,104.32	0	4.59	636,018.74	0.26
22	LTO, 14400kW, [0.8-0.5]120s, OR=[0.7-0.9]	13,559.81	906,066.09	0	4.54	640,931.42	0.25
23	LTO, 14400kW, [0.9-0.6]120s, OR=[0.6-0.95]	13,506.88	874,210.59	0.44	4.61	710,755.32	0.41
24	LTO, 14400kW, [0.9-0.6]120s, OR=[0.7-0.9]	13,500.10	874,164.27	0	4.55	715,666.02	0.40
25	LTO, 14400kW, [0.8-0.5]300s, OR=[0.6-0.95]	13,582.38	910,710.91	2.08	4.54	620,092.12	0.21
26	LTO, 14400kW, [0.8-0.5]300s, OR=[0.7-0.9]	13,570.78	910,685.22	1.26	4.51	628,436.62	0.22

Table A.5: Optimal Range Best Solutions Case 2 Metrics